Pyrotechnic Literature Series No. 12

Selected Pyrotechnic Publications of K. L. and B. J. Kosanke, Part 8 (2005 through 2007)

Table of Contents — Part 8

An earlier version appeared in: *Fireworks Business*, No. 280, 2005.

Typical Aerial Shell Firing Time Sequence

K. L. and B. J. Kosanke

As part of a continuing study of the nature and causes of aerial shell malfunctions, it was useful to produce a detailed time sequence for the events occurring during the firing of typical (properly functioning) aerial shells. In particular, this information was needed to facilitate the investigation and analysis of those types of malfunctioning aerial shells that explode within or just above their firing mortar. The in-mortar malfunctions are so-called "flowerpots" and "aerial shell detonations" (which are sometimes more accurately referred to as "violent in mortar explosions" or VIMEs). The just-above-the-mortar malfunctions are so-called "muzzle bursts". While it is recognized that few if any non-researchers will find much practical information in this article, it was written in the thought that such information might be of general interest to those wishing to better understand the shell firing process.

The information used in preparing this time sequence of shell firing events comes from several sources, some of which has been published previously. The sources of information include normal and high frame rate video recording of aerial shell firings, mortar pressure profiles (internal mortar pressure as a function of time) during actual shell firings, and simple calculations based Newton's second law of motion (Force = Mass × Acceleration).

The basic configuration of the aerial shell and mortar before firing is shown in Figure 1. In this study it is assumed that the shell is fired using a quick match shell leader with black match as the delay element. When ignited on its very tip, the black match takes an average of 2.6 seconds to burn and reach the quickmatch portion of the shell leader.[1] After reaching the quick match portion of the shell leader, on average another 0.3 second is required for the fire to reach the lift charge.[2]

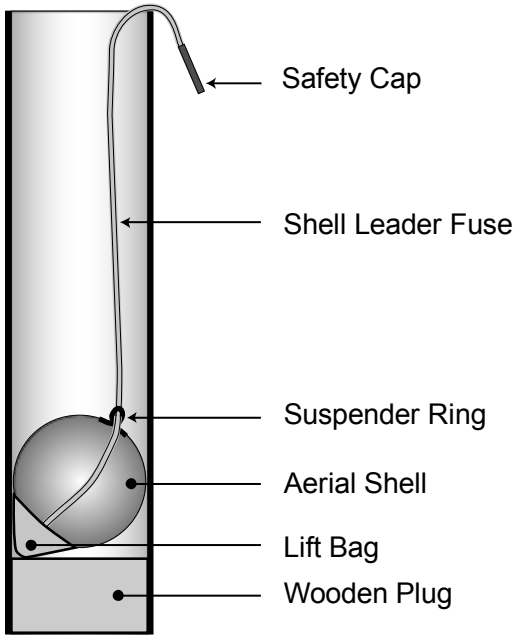

Figure 1. A sketch of an aerial shell in its mortar before firing.

Once the lift charge ignites, the fire propagates through it as substantial amounts of flame begin to be produced. The first (left-most) image of Figure 2 depicts the mortar when the flame has filled the area below the aerial shell and it has advanced around the sides of the shell to just past its top. Based on high frame rate video recordings, this occurs in approximately 7 milliseconds (0.007 second) after the fire from the shell leader first reached the lift charge. (For an electrically fired aerial shell, this would also be the time after the firing of an electric match inserted into the lift charge.) Next in the process, the second image in Figure 2, the flame has advanced up the length of the mortar and just begins to emerge from its top. This requires approximately another 10 milliseconds. However, at this time the pressure under the shell is still insufficient to overcome the force of gravity and cause the shell to begin to move. In the third

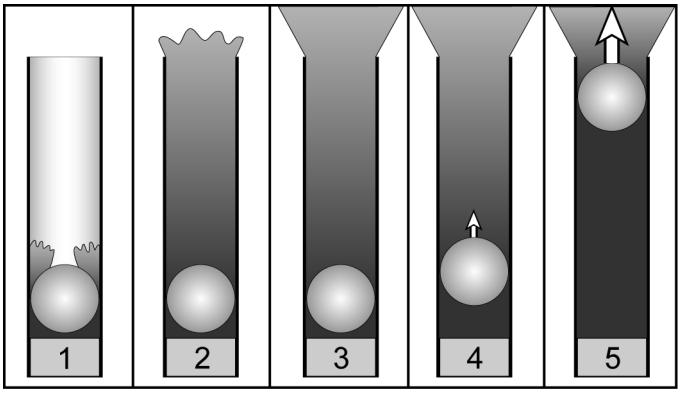

Figure 2. A series of drawings illustrating the sequence of events during a normal aerial shell firing.

image, the flame has reached well above the top of the mortar, the mortar pressure below the shell is starting to rise significantly and the upward force on the aerial shell has just reached the point of equaling the downward force of gravity. Time has now advanced approximately another 2 milliseconds. In the fourth image the shell has risen approximately 12 percent of the length of the mortar, and the pressure under the shell has just reached its maximum. This has required approximately another 5 milliseconds. In the fifth image of Figure 2, after another approximately 7 milliseconds, the aerial shell is about to exit the mortar and the pressure under the shell has already decreased substantially. At this point the total time elapsed since the ignition of the lift charge is approximately 31 milliseconds. The now quite rapidly moving aerial shell (traveling at a rate of approximately 500 feet per second) exits the mortar approximately 2 milliseconds later. The total time elapsing since the lift charge was ignited is approximately 33 milliseconds (i.e., 0.033 second). This compares well with previously published results of a series of measurements of aerial shell exit times. In that study, it was found the average exit time for an 8-inch spherical aerial shell was 35 milliseconds.[3]

Details of the mortar pressures developed and the upward progress of the aerial shell is presented in Figure 3, where time zero corresponds to the start of ignition of the lift charge. The solid line in the graph is the mortar pressure developed during the firing of a typical 8-inch spherical aerial shell. The dashed line is the displacement of the aerial shell as it travels up the mortar. This was calculated from the measured mortar pressure as a function of time, and the actual diameter and the mass of the shell. (That

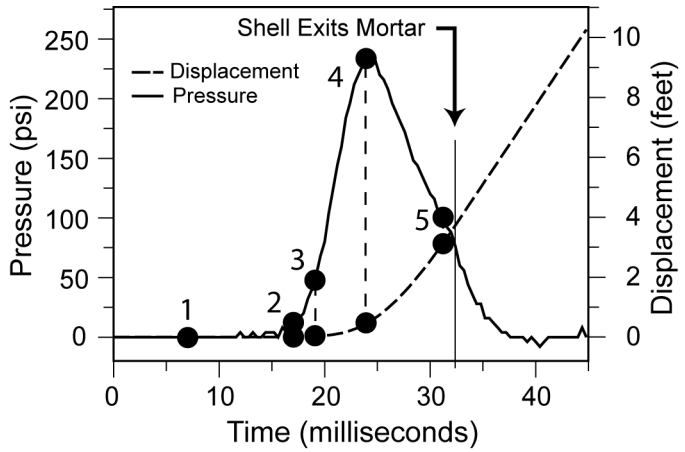

Figure 3. Graphs of mortar pressure and aerial shell displacement as functions of time.

the calculation of displacement was correct is confirmed by the fact that the calculated exit time exactly matches the time of shell exit documented by a slight discontinuity in the derivative of the mortar pressure curve.) The numbered pairs of points in Figure 3 correspond to the series of images in Figure 2.

Note that the sequence of events after igniting the lift charge spans a time interval short enough to be perceived by a human observer as occurring instantaneously. While the detailed information about the timing of a normal shell firing presented in this article might be of general interest, its principal usefulness lies in support of studies attempting to discover more about the cause and course of various within-mortar and near-above-mortar aerial shell malfunctions.

References

1) "Manual Firing Delay Times for Aerial Shells", K. L. and B. J. Kosanke, *Fireworks Business*, No. 243 ,2004; *Selected Pyrotechnic Publications of K. L. and B. J. Kosanke, Part 7 (2003 and 2004),* 2006.

2) "Firing Precision for Choreographed Displays", K. L. and B. J. Kosanke, *Fireworks Business*, No. 194, 2000; *Selected Pyrotechnic Publications of K. L. and B. J. Kosanke, Part 5 (1998 to 2000),* 2002.

3) "Hypothesis Explaining Muzzle Breaks", K. L. and B. J. Kosanke, *Proceedings of the Second International Symposium on Fireworks*, Vancouver, BC, Canada, 1994; *Selected Pyrotechnic Publications of K. L. and B. J. Kosanke, Part 3 (1993 and 1994),* 1996.

An earlier version appeared in: *Fireworks Business*, No. 253, 2005.

Confirmation of Mortar Recoil Information

K. L. and B. J. Kosanke

About a year ago an article appeared in which information about the magnitude of firework mortar recoil forces was presented.[1] As a starting point, that article used the averages of 136 measurements of the peak internal mortar pressure produced upon firing 3- to 12-inch spherical aerial shells. These peak pressures were then converted to recoil forces using basic principles of physics. However, while the average peak recoil force results are thought to be highly reliable for typical shells, those results were not confirmed by physical measurements of peak recoil forces.

During the period of the 1990s, the Canadian Explosives Research Laboratory (CERL) conducted a large number of measurements of firework mortar recoil forces. Some of the results from the testing of 205-, 255- and 305-millimeter (8-, 10-, and 12-inch) aerial shells have been published.[2] Approximately half of these test shells were produced in the Orient and half were from Europe. The purpose of this short article is to compare the CERL results with the results from Reference 1 and to draw some conclusions from those comparisons.

Columns 1 through 5 of Table 1 summarize CERL's measured recoil force results for those large diameter aerial shells. Column 6 presents the results previously published in reference 1 using measured peak internal mortar pressure values.

Two things about the data in Table 1 are worth further comment. The first is that the range of values measured by CERL is quite large, with the largest values being from approximately 2.5 to 5 times larger than the smallest values for the same size shell. This should serve to emphasize the need to use mortar support structures that are substantially stronger than might be concluded based solely on the average recoil force values in Table 1 (and those in reference 1 for smaller caliber aerial shells). The second thing worth mentioning from Table 1 is that for each size shell, the average of the field test results are in very close agreement with the calculated results from Reference 1. This tends to suggest that the Reference 1 results for smaller-sized shells can reasonably be expected to be confirmed by actual field measurements of recoil force.

References

1) "Typical Mortar Recoil Forces for Spherical Aerial Shell Firings", K. L. and B. J. Kosanke, *Fireworks Business*, No. 242, 2004; *Selected Pyrotechnic Publications of K. L. and B. J. Kosanke, Part 7 (2003 and 2004),* 2006.

2) "Loads Resulting from the Recoil of Fireworks Mortars", E. Contestabile, R. Guibeault and D. Wilson, *Proceedings of the 4th International Symposium on Fireworks*, 1998.

Table 1. A Comparison of Recoil Force Results between CERL and Reference 1.

Shell Size (in.)	Number of Tests	CERL Recoil Force Results			Reference 1 Results (lbf)	Difference
		Least (lbf)	Greatest (lbf)	Average (lbf)		
8	23	2,200	10,240	5,320	5,300	–0.4 %
10	12	5,600	13,600	10,585	11,000	+3.9 %
12	12	11,400	26,000	18,920	18,000	–4.9 %

An earlier version appeared in: *Fireworks Business*, No. 253, 2005.

Angel Fire Brand of Indoor Pyrotechnics

K. L. and B. J. Kosanke

Recently, a supply of indoor (proximate audience) pyrotechnic items was supplied for our casual (non-quantitative) evaluation. The claim to fame for this product line is reputed to be its low smoke output and its high purity flame colors. The principals of the company (DMD Systems, LLC) are some of the same researchers that previously developed and wrote about similarly performing pyrotechnics in the *Journal of Pyrotechnics*.[1,2] We were willing to provide such a cursory evaluation (without cost) because of our general curiosity regarding these products.

The Angel Fire products were definitely found to perform exceptionally well. Although side-by-side comparisons with other manufacturers' products were not performed, it was estimated that the Angel Fire products generated no more than approximately half of the smoke of typical items with similar performance characteristics. The colors appeared to have higher purity (and in some cases much higher purity) than typical items on the market. Also, the colors seemed significantly brighter than those from typical items on the market.

The authors have no information about how the price of Angel Fire products compare with those of other producers. However, if the costs are roughly comparable, being able to produce items that have a distinct performance advantage aesthetically (better color and lower smoke), as well as presumably having lower potential health impacts (less smoke), should prove to provide a major competitive advantage for DMD Systems' products.

Below, in response to our request, is some information provided by DMD Systems, about their company and products.

Two explosives chemists, seeing a need for low-smoke theatrical pyrotechnics, formed DMD Systems LLC. DMD specializes in the manufacture of Angel Fire brand indoor pyrotechnic special effects (see www.angelfirepyro.com, or call 505-583-2278 for more details). Our products burn with vivid colors and large flame envelopes, yet produce little smoke.

The formulations are mainly composed of stabilized nitrocellulose with patented burn rate modifiers. Our gerbs and line rockets utilize a patented "core burn" geometry to produce sufficient gas pressure without a traditional-style clay nozzle. This "nozzleless" configuration enhances the size of the flame envelope and reduces the need for smoke producing colorants. Currently DMD Systems is only distributing through both Luna Tech and RES Specialty Pyrotechnics in the US. We currently offer red, orange, yellow, green, blue, purple and white 3s x 20', 10s x 10' gerbs and 3s wire rockets with or without Ti flitter as well as 10 s flares with or without Ti. Special order items with custom spark heights are available on request. In addition, star mines in all the above colors plus hot pink and lime-green are available in two different heights, either 15-20' range or 35'. All mines contain approximately 40 to 50 stars and are available in any combination of colors as well as with or without Ti flitter. In the near future DMD will introduce a line of low-smoke colored waterfalls, larger colored gerbs, and uncolored end-burning gerbs in a variety of sizes, durations and heights.

References

1) D. E. Chavez and M. A. Hiskey, "High-Nitrogen Pyrotechnic Compositions", *Journal of Pyrotechnics*, No. 7, 1998.

2) D. E. Chavez, M. A. Hiskey and D. L. Naud, "High-Nitrogen Fuels for Low-Smoke Pyrotechnics", *Journal of Pyrotechnics*, No. 10, 1999.

An earlier version appeared in: *IABTI Detonator*, Vol. 32, No. 1, 2005.

Black Powder Stability and Aging Example

K. L. and B. J. Kosanke

The stability and aging characteristics of Black Powder are occasional topics of discussion. Having been given a research sample of Black Powder that had been recovered from the explosive charge in cannon balls dating to the time of the US Civil War (ca. 1863), the author was able to investigate these issues for that powder sample.

The physical appearance of the Civil War Black Powder is consistent with its still being of high quality. The powder is unglazed (or minimally glazed); the grains are hard and show no visible signs of physical deterioration. The powder is free flowing with minimal dust present. There is possibly a very subtle difference in color when compared with current production powder (Goex, Inc.); the Civil War powder is ever so slightly lighter in color. Based on its overall physical appearance, it would not be possible to detect that the Civil War powder was not of current production.

The granulation of the Civil War powder fits well within the range reported for Musket powder of that era. The grain density for the Civil War powder is 1.67 g/cm^3. This is close to that of current production powder and to the current US military specification (1.69 to 1.76 g/cm^3); however, the density is slightly lower than the reported standard of that time (>1.75 g/cm^3). It is uncertain whether there has been a slight change in the powder's density over time, if the powder had been manufactured to a somewhat different standard, or if the current measurement is slightly in error. (Note that the powder used in cannon balls is reputed to have been of somewhat lesser quality than that used for small arms.) The moisture content of the powder is 0.67%, which is still within current military specifications.

In terms of the powder's performance under significant confinement, both in an Eprouvette and in Black Powder rifle tests, the Civil War powder produced results consistently within 7 to 10% of that of current production Goex powder of the same granulation. To help put this performance difference into perspective, it should be noted that past evaluations of other current production (non-Goex) Black Powder performed significantly poorer in the same tests than did this sample of Civil War powder. At this time, it is not possible to say whether the small difference between the Goex and Civil War powders under confinement represents a slight degradation of its performance, as opposed to its having been somewhat less effective when originally produced. Such lesser performance could easily have been the result of small differences in the materials used or in the processing methods used at the time of its manufacture.

The physical appearance, physical properties and performance of the Civil War Black Powder are all consistent with there having been very little or no change in this sample over the preceding 140 years. That is to say, for this sample of Black Powder it is fairly obvious that it has remained stable and shows no sign of having deteriorated. This is fully consistent with what would be expected for a pyrotechnic composition stored under reasonably dry conditions.

One reason for reporting these results for this very old Black Powder sample is that too often bomb technicians seem to be of the opinion that all explosives (including properly stored pyrotechnic compositions) deteriorate and become increasingly unstable with age. While most pyrotechnic compositions, when stored under excessively damp conditions, do potentially deteriorate, very few types of pyrotechnic composition become more unstable than they were originally. Almost always, deteriorated pyrotechnic compositions become more stable, possibly even to the point of being essentially inert. That is not to say, when one does not know the nature of a pyrotechnic composition showing signs of having deteriorated, that one should not use added precaution in render-safe and disposal opera-

tions. Rather, one should remember that when speaking of pyrotechnic compositions in general, old does not necessarily mean deteriorated, and that deteriorated pyrotechnic compositions rarely become more sensitive (unstable) as a result of deterioration.

An earlier version appeared in: *Fireworks Business*, No. 254, 2005.

Another Example of Explosively Malfunctioning Comets[1]

K. L. and B. J. Kosanke

This article reports on another batch of comets, imported from China, that tend to malfunction by exploding violently within their mortars as they are being fired. In the last few years, the authors have reported on imported Chinese comets from two other manufacturers, with somewhat similar construction characteristics, that also tended to explode violently upon their firing.[2–6] In each case, it was found that the malfunctioning white (or silver) comets had a high percentage of very fine magnalium (magnesium–aluminum alloy), used potassium perchlorate as the oxidizer, and had internal voids that could function as fire paths.

The comets in question for this article are of two different types: 3-inch solid cylindrical comets, and 3-inch tiger tail comets made by layering comet composition over an internal aerial shell.[1] While some cartons of both types of comets tended to experience the same explosive malfunctions, only the cylindrical comets were carefully studied and will be discussed in this article.

Test Firings and Comet Density Measurements

Initial field testing of the comets was conducted for the purpose of trying to identify which of four remaining cartons of the suspect comets demonstrated a tendency to explode upon firing. In this testing 10 comets from each case were test fired from paper mortars (which had been inspected to confirm that they had smooth interiors and were without obstructions). In these firings, almost all of the 40 comets functioned without a problem. Only one comet exploded violently within its mortar, and three other comets broke apart or had unusually short burn times. All four of the malfunctioning comets were from the same case. Because of the limited number of test firings from this suspect case, another 10 comets from that case were test fired. This time, again only one comet exploded violently within its mortar, and two more malfunctioned less violently. At this point the field testing was halted and the remaining comets from that case (and a few samples from two other cases) were repackaged and transported to the laboratory for further analysis.

It was suspected that comet density might be one of the predictors that determine which comets were most likely to fail explosively. At the lab, before further test firings were conducted, all of the remaining 62 comets (52 from the suspect case and 5 each from two other cases) were disassembled. The density of each comet was determined using the measurement of its mass and physical dimensions. It was found that the comets' density ranged from 1.41 to 1.73 g/cm^3. Given the formulation for the comets (discussed below), the maximum theoretical density of the comets would be approximately 2.4 g/cm^3. Thus the porosity of the comets was found to be quite high, ranging from approximately 30 to 40%.[7]

Once the density of each remaining comet was established, it was ranked from least to most dense. In preparing for further test firings, 42 of the comets were reassembled, drawing most heavily from those test comets with the very highest and the very lowest densities. Of these 42 comets, eight were from two of the cases previously found to have comets that apparently performed well,[8] and 34 were from the case previously found to occasionally malfunction. Of these 42 test comets, four explosively malfunctioned in the mortar as they were being fired. All four of these were from the same case of comets previously found to malfunction occasionally. In terms of density, two comets were among the very lowest density (i.e., the most porous), one had a mid-range density and one comet was from the group having higher density. While these results are somewhat consistent with the suggestion that density is a factor in determining which comets will malfunction, it is

quite far from demonstrating that result to an acceptable degree of certainty.

It terms of establishing the cause of these comets' explosive malfunction, it should be noted that in each case the comet did not explode until it had traveled to nearly the top of the mortar. (For a photograph of a collection of the exploded mortars, see reference 9). Based on previous measurements of the dynamics of shell firings, this means that approximately 30 milliseconds elapsed between the ignition of the comets and their exploding.[10]

Chemical Analysis

Semi-quantitative chemical analyses were performed on comets from both the well-behaving and malfunctioning cartons. The results are summarized in Table 1. The binder in the comet composition was found not to dissolve in water, but it did dissolve in acetone. The amount of binder was determined using simple gravimetric methods. The binder solution was fairly reddish brown in color, suggesting the possibility that it was red gum based; however, the exact nature of this non-aqueous binder was not determined. After the binder was removed from the composition, the oxidizer was dissolved in water, and the amount again determined gravimetrically. The nature of the oxidizer was established using a combination of chemical spot testing and X-ray spectroscopy.[11] The amount of the remaining ingredients (almost exclusively metals) was determined by weighing. As part of a microscopic examination of the remaining ingredients, there appeared to be a trace quantity of charcoal (tiny black particles) mixed with the obviously metal particles. X-ray analysis revealed that the metals were almost exclusively aluminum and magnesium.[12] Further X-ray analysis performed in conjunction with electron-microscopic imaging, found that the metals were a combination of aluminum and magnalium (approximately a 50:50 alloy of aluminum and magnesium).

Table 1. Approximate Chemical Formulations of the Test Comets.

Ingredient	Percentages[a]	
	Well-Behaved	Mal-functioning
Potassium perchlorate	40	40
Aluminum	30	30
Magnalium (50:50)	15	20
Binder (non-aqueous)[b]	15	10
Charcoal	Trace	Trace

a) Percentages are approximate and are reported to the nearest 5%.

b) Based on the amount, it seems likely that the binder also functioned as an additional fuel.

The metal fractions from the compositions of the two groups of comets were subjected to a sieve analysis to determine their mesh fractions (i.e., the range and distribution of particle size). This was followed by an X-ray spectroscopic analysis to determine the ratio of aluminum to magnalium alloy in each mesh fraction. The results of these analyses are shown in Table 2.

The chemical analysis found two important differences between the apparently well-behaving comets and those tending to malfunction explosively. The first difference is in regard to metal content. While both types of comets had

Table 2. Sieve Analyses of the Metal Fractions of the Comet Compositions.

Mesh Range (US Std.)	Mass Percent[a] in the Well-Behaved Comets		Mass Percent[a] in the Malfunctioning Comets	
	Aluminum	Magnalium	Aluminum	Magnalium
+60	30	0	45	0
60–100	35	0	40	0
100–200	30	5	15	0
200–400	5	30	0	15
–400	0	65	0	85

a) Percentages are approximate and are reported to the nearest 5%.

high percentages of very fine magnalium, the comets tending to explosively malfunction had a higher percentage of magnalium (approximately 1/3 more) and a higher percentage of that magnalium was finer than 400 mesh (see again Tables 1 and 2). The result is that the composition of the malfunctioning comets had nearly twice as much of the –400 mesh magnalium, as compared to the apparently well-behaved comets. The second difference between the two batches of comets is in regard to binder content. While both types had relatively high percentages of binder, the apparently well-behaved comets had approximately 50 percent more binder than those comets tending to explosively malfunction. (The potential relevance of these differences will be discussed below.)

Microscopic Analysis

Small solid pieces to comet composition were taken from comets from the two groups (those apparently well behaved and those tending to explosively malfunction). These samples were mounted and sputter coated with gold in preparation for inspection using a scanning electron microscope. Figure 1 presents a pair of images of the typical internal structure of the two types of comet samples. The pieces of composition from the apparently well-behaved comets (see the upper micrograph in Figure 1) were found of have the appearance of being somewhat loosely bound and occasionally had fairly large void spaces. In comparison, the pieces of composition from the occasionally malfunctioning comets (see the lower micrograph in Figure 1) have an even more loosely bound appearance and significantly more and larger void spaces.

Other Testing

Standard fall-hammer impact sensitiveness testing of the comet composition was performed after it had been finely ground using a mortar and pestle. It was found that the comet composition was relatively insensitive to impact when compared with some other commonly used comet compositions. Thus the malfunctions would not seem to be associated with the impact sensitiveness of the comets.

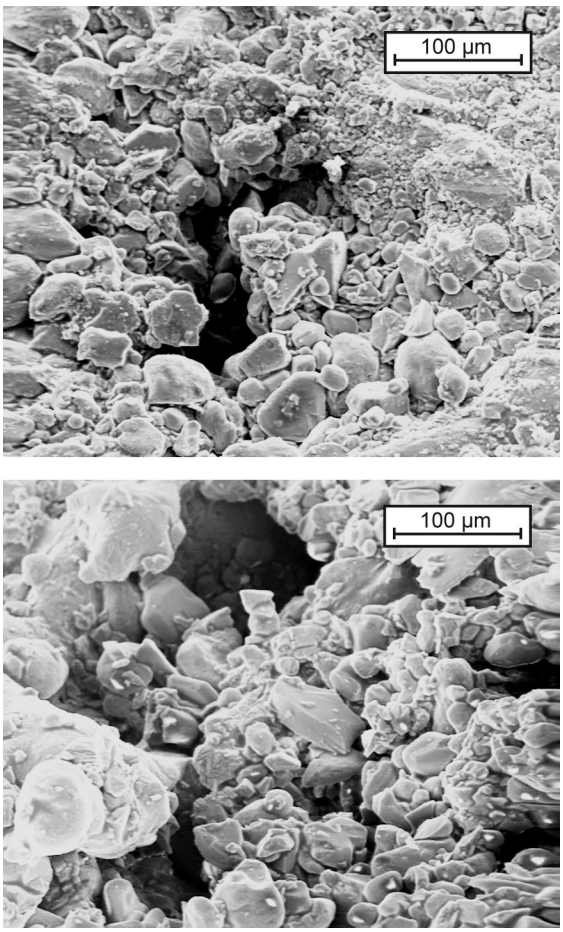

Figure 1. A pair of electron micrographs (200X magnification) comparing the typical internal structure of comet samples from the apparently well-behaved comets (above) and those tending to explosively malfunction (below).

Because the chemical composition of the comets was similar to that of flash powders (which tend to be cap-sensitive) a standard cap-sensitivity test was performed, using a number 8 detonator. While in this single test, the comet did ignite, it merely burned and did not explode.

Discussion

The comets being studied in this instance had construction characteristics in common with the two previously investigated examples of white or silver comets that tended to occasionally malfunction explosively inside their mortar as they were being fired. In each case the comets: 1) contained a high percentage of very fine magnal-

ium, 2) used potassium perchlorate as their oxidizer, and 3) had a significant number of substantially large internal voids. The relevance of the use of a combination of very fine magnalium (–400 mesh) and potassium perchlorate is that it would potentially constitute being a flash powder, if not tightly cemented into a solid mass. The relevance of the internal void spaces is that they can act as fire paths to carry the burning reaction quickly into and throughout the mass of the comet. In combination, these factors can cause the comet to function explosively after a very short delay during which time the burning reaction is accelerating through the mass of the comet. The process by which this can happen is explained more completely in reference 13, which discusses so-called aerial shell detonations or violent in mortar explosions, VIMEs.

Acknowledgments

The authors are grateful to C. Johnson for providing the comets for testing; to C. Johnson, T. Miller, R. Fullam, C. Wallgren and T. Winegar for assistance in performing portions of the testing; and to L. Weinman for commenting on an earlier draft of this article.

End Notes and References

1) As part of the agreement for supplying a substantial number of the suspect comets for testing, the manufacturer's name is being withheld. The authors found this to be acceptable because: a) the comets were imported into the US more than 2 years ago, b) it would seem that these particular comets (and possibly one other batch imported at the same time) were the only ones to experience the malfunctions, and c) it is unlikely that any supplies of these suspect comets currently exist to potentially produce an accident.

2) "'Impossible' and Horrific Roman Candle Accident", K. L. Kosanke, G. Downs and J. Harradine, *Fireworks Business*, No. 225, 2002; *Selected Pyrotechnic Publications of K. L. and B. J. Kosanke, Part 6 (2001 and 2002),* 2005.

3) "Roman Candle Accident: Comet Characteristics", K. L. & B. J. Kosanke, G. Downs and J. Harradine, *Fireworks Business*, 228, 2003; *Selected Pyrotechnic Publications of K. L. and B. J. Kosanke, Part 7 (2003 and 2004),* 2006.

4) "WARNING: Serious Product Malfunction", K. L. Kosanke, *Fireworks Business*, No. 232, 2003; *Selected Pyrotechnic Publications of K. L. and B. J. Kosanke, Part 7 (2003 and 2004),* 2006.

5) "Report on the Initial Testing of Suspect Tiger Tail Comets", K. L. Kosanke, *Fireworks Business*, No. 233, 2003; *Selected Pyrotechnic Publications of K. L. and B. J. Kosanke, Part 7 (2003 and 2004),* 2006.

6) "Further Report on the Testing of Suspect Tiger Tail Comets", K. L. and B. J. Kosanke, *Fireworks Business*, No. 237, 2003; *Selected Pyrotechnic Publications of K. L. and B. J. Kosanke, Part 7 (2003 and 2004),* 2006.

7) What causes comets, or any compacted pyrotechnic composition, to have a density less than its maximum theoretical density is the presence of internal void space. The percentage of the volume occupied by these void spaces is described as a material's porosity. When the amount of void space is large, there is a tendency for the voids to become interconnected. When a significant number of the voids are interconnected, it will be possible for gas to penetrate significantly into the material, and the material is described as being permeable. In terms of a solid mass of pyrotechnic composition, its permeability is important because it will accelerate the burn rate of the composition. If the accelerated burn rate is sufficiently great, it may be possible for the burning to transition into an explosion. (For a further discussion, see reference 13.)

8) The comets are described as "apparently" performing well, because while none were found to explosively malfunction, based on their overall construction characteristics and the relatively small number tested, it cannot be assured that none of these would seriously malfunction.

9) "The Effect on Mortars of Explosions within Them", K. L. and B. J. Kosanke, *Fireworks Business*, No. 251, 2004; *Selected Pyrotechnic Publications of K. L. and B. J. Kosanke, Part 7 (2003 and 2004),* 2006.

10) "Typical Aerial Shell Firing Time Sequence", K. L. and B. J. Kosanke, *Fireworks Business*, No 252, 2005; *Selected Pyrotechnic Publications of K. L. and B. J. Kosanke, Part 8 (2005 to 2007),* 2009.

11) X-ray spectroscopy established that the oxidizer included potassium and chlorine in a ratio of approximately one to one. Spot testing revealed that the oxidizer was not potassium chlorate and that it was potassium perchlorate.

12) X-ray spectroscopy of a bulk sample of the metals found there to be small amounts of copper, zinc and iron present in addition to the aluminum and magnesium. Further X-ray analysis performed in conjunction with imaging individual particles using an electron microscope found that the minor ingredients were associated with only the aluminum metal particles, as some type of alloy.

13) "Hypotheses Regarding Star-Shell Detonations," K. L. and B. J. Kosanke, *Journal of Pyrotechnics*, No. 14, 2001; *Selected Pyrotechnic Publications of K. L. and B. J. Kosanke, Part 6 (2001 and 2002)*, 2005.

An earlier version appeared in: *MAFS Newsletter*, Vol. 34, No. 2, 2005; *Journal of Pyrotechnics*, No. 24, 2006.

Primer Gunshot Residue Detection from the Firing of a Black Powder Revolver

L. T. Briscoe, K. L. Kosanke and R. C. Dujay
Mesa State College, Center for Microscopy, PO Box 2647, Grand Junction, CO 81501

ABSTRACT

A study was conducted to determine the potential for being able to identify primer gunshot residue (PGSR) within the substantial quantities of the particulate residues produced during the firing of a revolver using Black Powder propellant and a percussion cap primer. Samples of gunshot residue (GSR) were collected from the shooter's hands, from surfaces to the side of the shooter, from surfaces near the muzzle of the weapon and from various locations on the weapon itself (both inside and outside). It was found to be relatively easy to identify PGSR from the hand of the shooter, from surfaces to the side of the weapon and from most locations on the weapon. However, using the methods of this study, no PGSR was identified within the large amount of Black Powder residue projected out the muzzle of the weapon and on the inside of its barrel.

Keywords: gunshot residue, GSR, Black Powder, percussion cap primer, scanning electron microscopy, SEM, energy dispersive spectroscopy, EDS

Introduction

When a weapon is fired, gunshot residue (GSR) can originate from the primer, the propellant, the metals contained in the bullet, the bullet jacket, the cartridge case and the gun barrel. For the purpose of determining whether a suspect is likely to have fired a weapon (or has otherwise been exposed to a weapon firing), most generally only those residues originating from the primer are sought in the analysis. For most ammunition these primer gunshot residues (PGSR) contain lead, barium and antimony and are detected using a combination of scanning electron microscopy (SEM) and X-ray energy dispersive spectroscopy (EDS).[1] Unlike weapons using modern propellants, when a Black Powder weapon is fired, a substantial quantity of solid propellant residue is produced in addition to the relatively small amount of PGSR. This gave rise to concern that PGSR might be difficult or impossible to identify in samples taken from many surfaces typically sampled by investigators. The purpose of this brief study was to determine whether the firing of a Black Powder revolver is likely to produce a readily detectable amount of PGSR.

Background

To better quantify the basis for concern regarding the relatively small amount of PGSR produced, consider the following. A common type of primer available for Black Powder weapons is Remington's No. 10 percussion cap, the construction of which is illustrated in Figure 1.

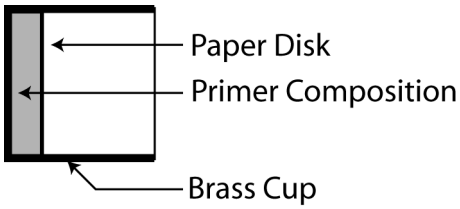

Figure 1. An illustration of the construction of a percussion cap primer. (Not to scale.)

The percussion caps measured approximately 4.5 mm in length and diameter, and they were found to contain approximately 22 milligrams (mg) of primer composition. While the exact chemical formulation of the percussion cap

composition is unknown to the authors, the presence of barium, antimony/sulfur, lead, aluminum, copper/zinc, and iron were identified using EDS, see Figure 2 in which the elements associated with particles of primer composition are identified. (A small metallic appearing filament composed of copper and zinc is thought to have been produced from the brass cup of the percussion primer when the primer composition was being cautiously scraped from it.)

Based on the elements found in the primer composition and information from the material safety data sheet for the percussion caps, it seems most likely that the formulation is similar to one identified in the literature[2] as being among those commonly used. The formulation is presented in Table 1.

Table 1. A Common Percussion Cap (Primer) Composition.[2]

Ingredient	%
Lead styphnate	46
Tetracene	4
Barium nitrate	25
Antimony sulphide	20
Aluminum	5

Using this formulation as input, thermodynamic free-energy modeling predicts that approximately 60% of the reaction products from such a primer will be solids. Thus such a primer can be expected to generate approximately 14 mg of PGSR. On the other hand, a typical load for a Black Powder weapon is 2.6 grams (40 grains) of Black Powder. Upon firing, this is expected to produce approximately 65% solid residues,[3] for a total of approximately 1.7 grams. Thus the relative amount of PGSR produced upon firing under these conditions amounts a little less than 1% of the amount of Black Powder residue.

If such a small amount of PGSR is reasonably well mixed within the substantially greater quantity of Black Powder residue, it is unlikely that the normal protocol for PSGR detection will be successful in finding it. However, if the PGSR is not well mixed chemically with the Black Powder residues, it may still be possibile to locate PGSR from the firing of a Black Powder weapon. There are two mechanisms through which this limited mixing might occur.

The simplest and most obvious mechanism is if some portion of the PGSR escapes the weapon prior to mixing with the high temperature reaction products from the burning Black Powder. Because of the high pressures produced inside a weapon when it is fired, and the necessary clearances (small gaps) between various component parts of the weapon, gunshot residue has the opportunity to exit the weapon at several points. If the weapon is of the type that uses a percussion cap, the area of the nipple (over which the percussion cap is slipped) offers the best chance for undiluted PGSR to escape. (Figure 3 is a conceptualized illustration of one chamber of a Black Powder revolver, in which the basic configuration of the parts of the revolver is shown.)

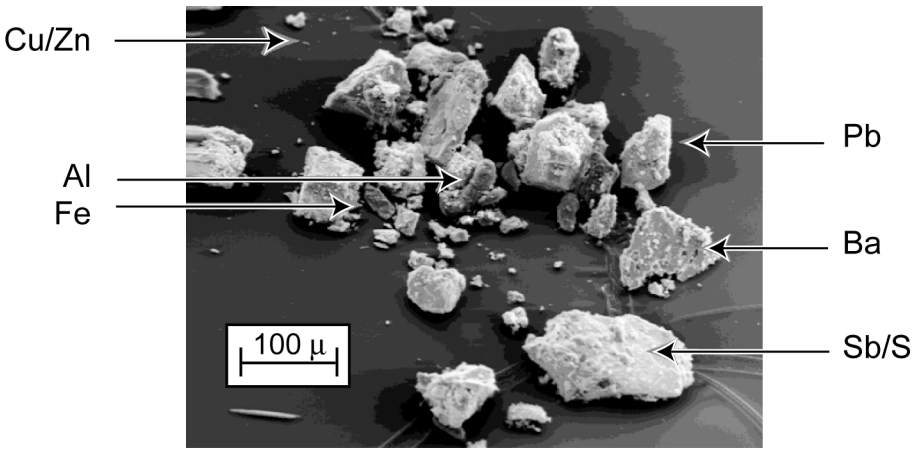

Figure 2. Electron micrograph of the elements found in a Remington No. 10 percussion cap.

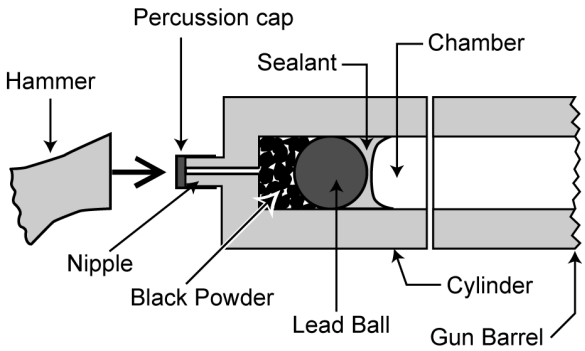

Figure 3. A conceptual illustration of the configuration of a Black Powder revolver. (Not to scale.)

The second means by which detectable PGSR might be produced from a Black Powder weapon arises if there is some mechanism by which the once diluted PGSR might subsequently become concentrated. A process such as this has been observed to occur when there are substantial differences in the melting and boiling points of the mixture of reaction products.[4] In that event, as some chemical reaction products are condensing and solidifying, others can be temporarily left behind as vaporized products to condense and solidify later in the process. In so doing, there can be a segregation of some of the various reaction products.

Table 2 lists the principal reaction products of the primer composition given in Table 1, as well as those from Black Powder.[3] Also given in Table 2 are the melting and boiling points for most of those reaction products.[5] While there are individual differences in the melting and boiling points, it would seem that those differences are neither sufficient nor systematic enough (between the Black Powder residues and PSGR) to produce the type of segregation of reaction products that would allow the relatively easy detection of PGSR. (Note that thermodynamic modeling predicts the reaction temperature to be approximately 1800 °C when burning at a pressure of 100 atmospheres.)

Materials and Methods

Weapon and Ammunition

The weapon used in this study was a 44 caliber "New Army Colt Reproduction in Stainless Steel" revolver made by Fillipietta. The propellant used was 40 grains (2.6 grams) of 3Fg Goex Black Powder. A 185-grain (12-gram) lead ball was then loaded on top of the powder, and a mixture of paraffin and Vaseline was packed over each loaded cylinder to seal it and prevent cross firing of the weapon. (Figure 3 is a conceptualized illustration of one chamber of a Black Powder revolver, in which the basic configuration of the parts of the revolver is shown.) Prior to loading, the weapon was very thoroughly cleaned. Remington No. 10 primers were the only primers used in this study.

Table 2. The Primary Solid Reaction Products Expected when Firing a Black Powder Weapon.

Source	Solid Reaction Products	Weight %	Temperature (°C)[2]	
			Melting	Boiling
Percussion Cap	Barium sulfide	26	1200	—
	Lead sulfide	26	1114	—
	Antimony metal	23	630	1750
	Aluminum oxide	15	2015	2980
	Lead metal	10	327	1740
Black Powder(a)	Potassium carbonate	43	891	- d -
	Potassium thiosulfate	25	>200	- d -
	Potassium sulfate	20	1069	1689

(a) Values are from von Maltitz[3]; (d) = decomposes; "—" = not specified.

Setup of Collecting Surfaces

Three collecting surfaces were prepared prior to the test firings. Each collecting surface had four standard Amray 0.5-inch diameter SEM stubs, with conductive adhesive carbon dots attached. Previous analysis of the blank stubs confirmed that they were free of contamination. The stubs were placed in a four corner arrangement on the cleaned collecting surface. Two such collecting surfaces were positioned to the sides (one right and one left) of the shooter at a distance of approximately 12 inches from the weapon and at a point directly in line with the weapon's cylinder. A third such collecting surface was positioned approximately 12 inches in front of the end of the barrel of the weapon; however, this collecting surface had a hole in the middle to allow the passage of the bullets. Figure 4 is a sketch illustrating the setup for the test.

Firing of the Weapon

The test firings occurred outdoors in an area free from residues from any previous weapon firings. The weather was sunny and clear with only a very slight breeze. Prior to firing the first shot, the adhesive covering was removed from the stub of each collecting surface. The weapon was held in the right hand of the shooter, while the left hand supported the grip of the revolver. Once the weapon was properly positioned in the middle of the three collecting surfaces, a shot was fired through the pre-cut hole in the front collecting surface. One SEM stub on each side collecting surface was removed after the first shot. Because of the large amount of Black Powder residue observed to have been deposited on the front collecting surface, two stubs were removed from the front collecting surface. To avoid contamination, this was done by a researcher other than the shooter. (The shooter's sole responsible was the handling and firing of the weapon.). The stubs that were removed were immediately placed in a storage case and the lid was shut tightly before the second shot.

The shooter proceeded to fire the weapon a second time. Another stub was removed from each of the side collecting surfaces. Again because of the very large amount of residue that had been deposited on the front collecting surface, both of the remaining stubs were removed after the second shot. For the two collecting surfaces located to the side of the shooter, the third stubs were removed after the third shot, and the final stubs were removed after the sixth firing of the weapon.

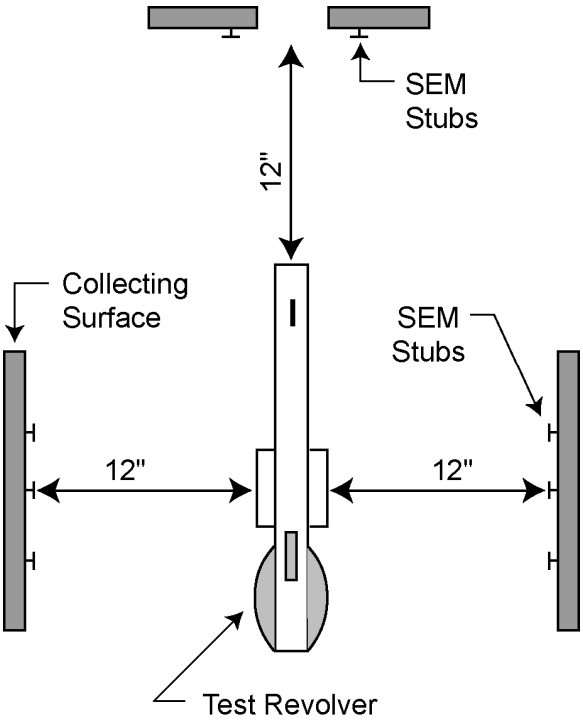

Figure 4. A sketch illustrating the setup for the test.

GSR Sampling of the Weapon and Shooter's Hands

Immediately after completion of the six test firings, the backside and inside surface of the shooting hand as well as the opposing hand were sampled. First the web area on the backside of each hand was dabbed with a conductive adhesive carbon dot a total of thirty times. Then, using a new stub and carbon dot, the entire surface of the inside of each hand was sampled in a similar manner. This sampling was performed by a researcher, not the shooter, to ensure that there was no contamination of the samples. Each sample was immediately placed in a storage case after sampling.

Exterior and interior surfaces of the weapon were also sampled using conductive adhesive carbon dots. Depending on the nature of the surface being sampled, various methods were used. For irregular surfaces the carbon dot was attached to a small piece of Velostat film (conductive plastic film). After sampling, the carbon dot and Velostat were attached to a standard 0.5-inch SEM stub using a second conductive adhesive carbon dot. For sampling some confined surfaces on the interior of the weapon, double-sided conductive adhesive strips were temporarily attached to the end of thin rod and pressed against the surfaces. After sampling, the adhesive dot was carefully peeled off the rod and placed on a stub.

PGSR Analysis

The search for PGSR was accomplished using a manually operated AMRAY 1000 (recently remanufactured by E. Fjeld Co.) and equipped with digital imaging software. The instrument was operated with an accelerating potential of 20 kV. Prior to analysis, the GSR samples were carbon coated to improve the quality of the images produced. The X-ray spectrometer used was energy dispersive, using a Kevex Si(Li) detector (with a thin beryllium window) in conjunction with an American Nuclear System multichannel analyzer (model MCA 4000) using Quantum-X software (version 03.80.20). The EDS system was calibrated prior to analysis using a copper and aluminum sample.

To facilitate the identification of particles of interest on the SEM image screen, backscatter imaging and a careful adjustment of contrast and brightness were required. In the backscatter imaging mode, objects composed of chemical elements with relatively high atomic number appear brighter than those with lower average atomic number. After a brief period of experimentation, imaging settings were found that aided in the identification of PGSR particles among the very large number of non-PGSR particles. For the purposes of the work, a particle of interest was defined as those for which the particle itself appeared noticeably brighter than the bulk of other material. Once a particle of interest was located, an X-ray spectrum was acquired, with the resulting peaks used to identify the chemical elements that were present. Figure 5 is an example of an X-ray spectrum of two PGSR particles. Because of the beryllium window on the detector, X-rays less than approximately 1 keV do not reach the detector. In contrast to the elements found in PGSR, Black Powder residues produce only X-ray peaks from potassium and sulfur. (A prior examination of unreacted and reacted primer composition had confirmed that it contained substantial quantities of three key indicators of PGSR, i.e., lead, barium and antimony). Consistent with commonly used defini-

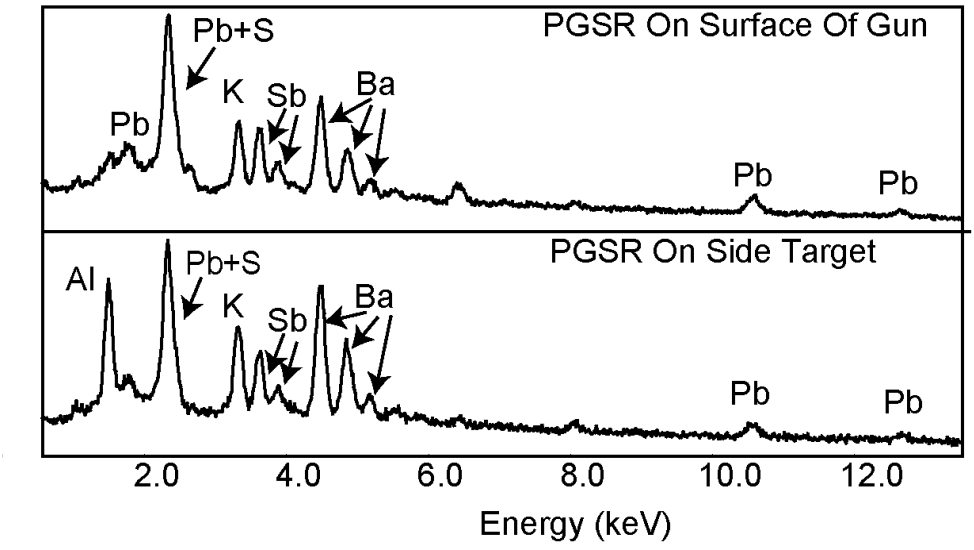

Figure 5. X-ray spectra of typical unique PGSR particles.

tions[1], in this work unique PGSR particles were those producing X-ray peaks for lead, barium and antimony, whereas characteristic PGSR particles were those producing peaks for only two of the three unique PGSR elements.

The propose of this brief study was only to determine whether it was likely that one could detect PGSR particles from the firing of this type of Black Powder weapon. It was not intended to statistically quantify the PGSR distribution or its abundance relative to Black Powder residue particles. In addition, the instrument was manually operated, making the effort labor intensive. Accordingly, in this study the analysis only proceeded until a few particles of interest were located and characterized, this ranged from 5 to 26 particles. See Figure 6 for an electron micrograph of two typical PGSR particles.

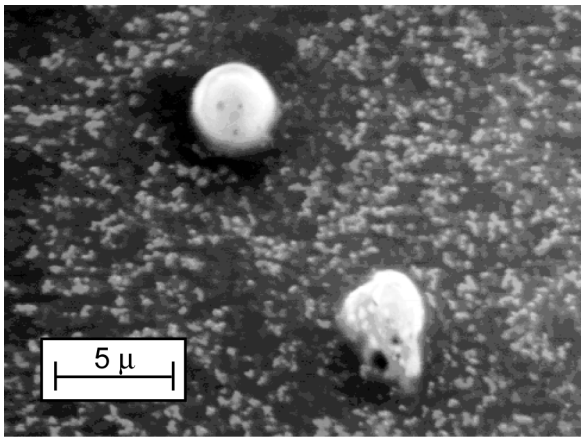

Figure 6. Electron micrograph (secondary electron imaging mode) showing typical PGSR particles.

Results

The results of this study are summarized in Table 3 and in the text below. Although not specifically included in Table 3, the GSR on each of the samples consisted primarily of those residues produced by the burning of the Black Powder propellant.

Shooting Hand

From the sample taken from the shooting hand (the hand that pulled the trigger) 22 particles of interest were examined. Of these, two particles were found to be unique and three particles were found to be characteristic. The non-shooting hand was not examined for PGSR; it was assumed that the results would be consistent with common experience with regard to finding PGSR on non-shooting hands.

Left-Side Collecting Surface

From the stub taken from the collecting surface placed to the left side of the weapon after one shot was fired, 23 particles of interest were examined. Of these, two particles were found to be unique and three particles were characteristic. Because a reasonable number of PGSR was found on the collecting surface to the left side of the shooter after only one shot, only that one sample was examined. It was assumed that simi-

Table 3. A Summary of the Results of the Search for PGSR from the Firing of a Black Powder Revolver.

Sample Source	Number of Particles of Interest				
	Analyzed[(a)]	Unique[(b)]	Pb/Ba	Pb/Sb	Ba/Sb
Shooting Hand	22	2	1	1	1
Left Collecting Surface	23	2	3	0	0
Front Collecting Surface	26	0	0	0	0
Revolver Outside – Surface	15	4	0	0	0
Revolver Outside – Nipple	5	3	0	0	0
Revolver Inside – Nipple Screw	6	2	1	0	0
Revolver Inside – Barrel	12	0	0	0	0

a) This is the number of "particles of interest" that were analyzed by EDS. These particles were selected because their image in the backscatter mode was noticeably brighter than the bulk of the rest of the particles.

b) Unique particles had all three elements (Pb, Ba and Sb) visibly present in the EDS spectra.

lar results would have been found after two, three or even six shots of the weapon. Given the geometry of the weapon it can be assumed that similar results would be found on the collecting surface located to the right of the shooter.

Front Collecting Surface

After an extended search of the large amount of particulate matter expelled from the muzzle of the revolver, after just one shot was fired, 26 particles of interest were found and analyzed. Of these, no unique or characteristic particles were found. Twenty two of the particles were found to contain lead (presumably bullet lead), of which most had a generally spheroidal appearance. No other elements other than those from the Black Powder (potassium and sulfur) were found. This is not to say that absolutely no PGSR was emitted from the muzzle of the weapon, just that its abundance was extremely low compared to the Black Powder residues. Because of time constraints and lack of an automated scanning system, the search for PGSR was abandoned after a few hours, and the entire surface of the collecting stub was not searched. However, it seems clear that, at the very least, it is much more difficult to find PGSR that has been expelled from the muzzle of the revolver than it is to find PGSR that have escaped elsewhere from this type of weapon.

Outside Surface of the Revolver

A total of 15 particles of interest particles were examined from the outer sample collected from the surface of the gun. Of the 15, four of the particles were unique, and none of the particles were characteristic. From the outside of a nipple (over which the percussion cap had been installed), only five particles of interest were examined. Of these, three were found to be unique, and none were characteristic.

Inside Surfaces of the Revolver

From the end of the nipple screw (the end at the entrance to the rear of the weapon's chamber), of the six particles of interest examined, two were found to be unique and one characteristic. From the inside of the barrel, 12 particles of interest were located. Consistent with what was found for material expelled from the muzzle of the weapon, none of the particles were unique or characteristic. Six of the particles contained lead (presumably bullet lead) and somewhat unexpectedly, one of the particles contained a small amount of barium, presumably from the primer composition.

Conclusions

As expected, PGSR can be located with relative ease amid the copious Black Powder residue from certain areas surrounding at least some types of Black Powder weapons after their having been fired. These areas are those from which PGSR can escape prior to its intimate high temperature mixing with the Black Powder combustion products. Specifically, for a revolver using percussion caps, such as used in this study, that includes the shooting hand (and presumably the face) of the shooter, objects to the side of the weapon (presumably including clothing), the outside surfaces of the weapon especially the interior and exterior surfaces near the nipple (over which the percussion cap is positioned). However, it appears that once the PGSR has thoroughly mixed with the high temperature Black Powder combustion products, it becomes so diluted that it is either quite difficult or impossible to locate. Specifically, this includes the material expelled from the muzzle of the weapon and the inside of the barrel (and presumably the inside of the chamber and cylinder ahead of the nipple).

Although not specifically studied in this investigation, these results suggest that significant quantities of PGSR may not be found from the firing of some types of Black Powder weapons. This includes any Black Powder weapon that does not provide a ready path that allows the escape of PGSR without it first having mixed with copious quantities of Black Powder residue. One such example would likely be a weapon using sealed metal cartridges with an integral primer. For such a weapon it would be expected that there will be almost no chance for PGSR to escape without its intimate high temperature mixing with, and dilution by, the much greater quantities of Black Powder combustion products

Obviously much additional research should be performed in this area. It would be preferred to have run an automated scan over the entire stub of material collected from near the muzzle of the weapon. This would more definitely es-

tablish the statistical probability of finding occasional PGSR intermixed with the Black Powder residues. Although it would be expected to yield substantially similar results, it would also be appropriate to test different types of primers and various Black Powder substitutes for their production of PGSR. Finally, it would be appropriate to investigate the production of PGSR from Black Powder weapons using sealed metal cartridges.

References

1) *ASTM E 1588-95: Standard Guide for Gunshot Residue Analysis by Scanning Electron Microscopy / Energy Dispersive Spectroscopy*, ASTM, 1995.

2) J. S. Wallace, "Chemical Aspects of Firearms Ammunition", *AFTE*, Vol. 22, No. 4, p 374, 1990.

3) I. von Maltitz, "Our Present Knowledge of the Chemistry of Black Powder", *Journal of Pyrotechnics*, No. 14, pp 25–39, 2001.

4) K. L. Kosanke, R. C. Dujay, B. J. Kosanke, "Characterization of Pyrotechnic Reaction Residue Particles by SEM/EDS", *Journal of Forensic Sciences*, Vol. 48, No. 3, pp 157–168, 2003; *Selected Pyrotechnic Publications of K. L. and B. J. Kosanke, Part 7 (2003 and 2004),* 2006.

5) *CRC Handbook of Chemistry and Physics*, 75th ed., CRC Press, 1995.

An earlier version appeared in: *Journal of Pyrotechnics*, No. 21, 2005.

Air Blast TNT Equivalency for Rolls of Paper Toy Caps

K. R. Mniszewski, FX Engineering, Inc., Hinsdale, IL, USA
and
K. L. Kosanke, PyroLabs, Inc. Whitewater, CO, USA

ABSTRACT

A study of the explosive output of rolls of paper toy caps, in variously sized assemblages, was conducted. The testing has shown that toy cap rolls are clearly capable of producing a powerful explosive effect if initiated with a sufficiently energetic event. TNT equivalencies based on toy cap composition mass ranged from approximately 10 to 80% for different sized configurations, with the largest equivalences being produced by the largest assemblages of toy caps tested. The results of this study are disturbing, considering that the toy caps (even in bulk packaging) have a UN classification of Explosive1.4S, which by definition should not produce significant blast or fireball effects when initiated. Thus perhaps it is appropriate to consider whether the UN test protocol is adequate for this product.

Keywords: air blast, TNT equivalence, toy caps, Armstrong's mixture, UN test

Introduction

A few years ago, an accident occurred in a toy factory in California. Several workers were killed and others were injured when a number of bulk cases of rolls of paper toy caps exploded with great violence, sufficient to produce traumatic amputations of worker's limbs. The workers involved were repacking the bulk cases of toy caps at a workstation using a blister pack machine. A number of enforcement and regulatory agencies were involved in the accident investigation and reconstruction. However, while it seemed quite clear that the toy caps were the cause of the accident, this was hard to reconcile with the fact that the bulk cases of toy caps were classed as Explosive 1.4 S.

No quantitative information had been produced by the primary investigating agencies regarding the expected explosive output of bulk quantities of toy caps, and a literature search was unsuccessful in locating such data. As part of the continuing accident reconstruction effort, an estimate of the effective amount of energetic material involved in the explosion was sought. The technique used was to determine the TNT equivalence of various quantities of the toy paper cap rolls. As with any condensed phase explosion, a number of effects are produced, including the production of an air blast wave, fireball, ground shock and projectiles. To estimate the yield of such an explosion, the most useful measure is the air blast wave. This paper reports on that study.

Paper Toy Cap Materials

Toy cap composition is typically composed of Armstrong's mixture, generally consisting of approximately 67% potassium chlorate, 27% red phosphorus, 3% sulfur and 3% calcium carbonate by weight.[1] To form the toy caps, the composition is prepared wet and extruded onto a strip of paper as a series of tiny dots, which are then laminated over with another thinner layer of paper and wound into rolls. The dry mixture is extremely sensitive to accidental ignition[1–2] and, even in small quantities (1 gram), is reported to have significant explosive strength (approximately 23% TNT air blast equivalent when initiated using a electric match).[3]

Careful weight audits of sample cap materials in this case were conducted to determine the average mass of toy cap composition per cap. This was determined through a comparison of: 1) the mass of a collection of blank paper dots, taken from the rolls of caps from the areas between the individual caps using a paper punch; and 2) the mass of a collection of individual toy caps har-

vested using the same paper punch that was used to produce the blank paper dots. The result was an average energetic material content of approximately 1.85 milligrams per cap.

The bulk quantities of this particular brand of cap were packaged 100 caps per roll, 12 rolls per thin-walled plastic tube, 12 tubes per paper package, and 100 packages per corrugated cardboard case. Thus a case contained 1.44 million individual toy caps, estimated to contain a total mass of 2.66 kg (5.86 lb) of energetic material.

TNT Equivalence Concept

A blast wave from an explosion can damage structures and injure personnel in the area. From an analysis of this damage an estimate of the charge size involved in an explosion can be calculated. While complicating factors must be considered, such as reflections off structures in the area, the geometry of the charge, etc., the technique is viable and quite useful.[4] However, when practical, the direct measurement of explosive output is preferred. Since in this case there was a sufficient (but not abundant) supply of the paper toy caps, the direct measurement approach was taken.

The information to follow is based on reference 5; however, much the same information can be found in other standard reference texts.[6,7] The ability of explosives to cause damage is often stated in terms of its TNT equivalence (*E),* which can be defined as the ratio of the mass of TNT (trinitrotoluene) to the mass of a test explosive that produces the same explosive output under the same conditions, specifically

$$E_{Test} = \frac{M_{TNT}}{M_{Test}} \qquad (1)$$

where M is charge mass, E is usually expressed in terms of percent, and a common measure of explosive output is peak air blast overpressure.

Using this technique typically begins with measuring the peak overpressure, p^o, produced at a measured distance from a test explosive charge of known mass. Then the amount of TNT that would be needed to produce the same peak overpressure is determined using accepted "standard" data for a charge of TNT under similar test geometry.

The comparison between the measured output of a test explosive charge and that from TNT is accomplished using a so-called mass-scaled distance, Z, defined as

$$Z = f_d \cdot \frac{R}{M^{1/3}} \qquad (2)$$

where R is the distance between the center of the explosive charge and the point of measurement of its output, and f_d (called the atmospheric transmission factor for distance) corrects for the effect of differing air densities. This atmospheric transmission factor is

$$f_d = \left(\frac{P_a \cdot T_o}{P_o \cdot T_a} \right)^{1/3} \qquad (3)$$

where P and T are the absolute atmospheric pressure and temperature. The subscript a denotes ambient conditions at the time of the measurement, and o denotes the standard conditions of the TNT blast data, specifically 1.013 bars and 288 K (15 ºC).

Procedurally, after one determines the peak air blast overpressure for the test explosive charge, it is converted to a relative peak overpressure, p^o/P_a. Then using the data and method of reference 5, the scaled distance, Z, is determined for which a standard charge of TNT (i.e., a spherical 1 kg charge of TNT exploded at 1.013 bars pressure and a temperature of 15 ºC) is known to produce the same relative overpressure as did the test explosive charge. Then, using the value of Z just determined, and the values of R, T and P that existed for the overpressure measurement of the test explosive charge, equation 2 can be rearranged to solve for the mass of TNT, M_{TNT}, which would produce the same peak overpressure under the same conditions as did the test charge. At that point, knowing both the masses in equation 1, the TNT equivalence can be calculated for the test explosive.

In cases where a booster (or initiating charge) is used, the output from that charge may contribute a significant portion of the overall explosive output. When that is the case, it is necessary to account for the booster's contribution. This can be done by measuring the explosive output of the booster exploding alone and calculating its TNT equivalence. Knowing the explosive mass of the booster, M_B, equation 1 can be used

to calculate the booster's equivalent mass of TNT, $M_{(TNT)B}$.

$$M_{(TNT)B} = Z_B \cdot M_B \quad (4)$$

Then in calculating the TNT equivalence for the test charge (less the contribution of the booster), the booster's equivalent TNT mass, $M_{(TNT)B}$, must be subtracted, and equation 1 becomes

$$E_{Test} = \frac{M_{TNT} - M_{(TNT)B}}{M_{Test}} \quad (5)$$

Paper Toy Cap Testing Program

First, a relatively soft initiator was devised for testing the cap materials. The intent was to provide a relatively strong shock without producing much in the way of high density fragments that could act as flyer plates. The first configuration tried was simply to insert an electric match (Daveyfire A/N 28 B) inside one of the tubes of toy cap rolls. This initiator would have been preferred because the explosive charge would be a single electric match with virtually zero explosive output; however, in three tests this initiator was unsuccessful in initiating a reaction of the toy caps.

The next igniter tried was a small acrylic tube filled to capacity with a large number of individual toy caps (obtained from a roll of caps using a paper punch) and carefully stacked on top of one another. After installing an electric match (Daveyfire A/N 28 B) in the tube, which rested against the bottom of the stack of toy caps, the tube was sealed on both ends with a small amount of hot-melt glue. The tube's dimensions (75 mm long, 6 mm ID and 9 mm OD) were chosen because it would fit snugly into the central hole in the rolls of paper toy caps. This initiator had the desirable characteristic of being solely composed toy caps; however, this initiator also failed to function.

A third initiator configuration was tried, in which the stack of toy caps mentioned above was replaced with a 1 gram charge of firework flash powder (70% potassium perchlorate and 30% pyro aluminum). The flash powder configuration performed quite nicely and was chosen as the initiator for subsequent testing. The construction of the initiator is shown in Figure 1.

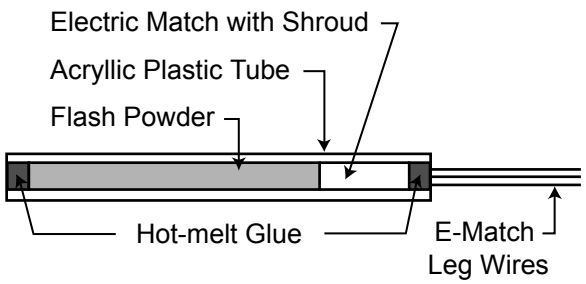

Figure 1. Sketch of the initiator chosen for use in the testing.

This initiator and a number of toy cap configurations were tested in a steel blast chamber (2.5 m in diameter and 5 m long). In each case the test explosive charge was suspended in the chamber approximately on its center axis. Two free-field piezoelectric pressure gauges (PCB model 137A12) were used to measure the side-on pressure from the test devices. The distances to the gauges were chosen to be commensurate with the size of the charges being tested; however, in each case the far gauge was at twice the distance of the near gauge, see Table 1. Digital oscilloscope records were made of the pressure-time history of each explosion.

A series of tests were conducted using increasingly larger assemblages of tubes of toy cap rolls. These configurations were constructed to approximate a right circular cylinder (actually having a hexagonal cross-section) with a height to diameter ratio reasonably close to one. The initiator was always inserted into the middle of one of the tubes of 12 rolls of paper toy caps, and that tube of toy caps was placed at the approximate geometric center of the test charge. Tests were conducted using 7, 28.5, 74, 183, and 676 tubes of toy cap rolls. Figure 2 is a photo of two of the configurations tested, those with 28.5 and 74 tubes. Because there were a limited number of toy caps available, only the test configuration with 7 tubes of toy caps was conducted more than once. Most of the explosion testing was conducted inside the blast chamber described above. The blast chamber tests were conducted at an air temperature of approximately 5 ºC and at a pressure of 0.87 bar (at an elevation of 4600 feet, in western Colorado). Testing of the configuration using 676 tubes of toy cap rolls had to be moved outdoors because, based on the previous testing, it was thought it might exceed the safe

Table 1. Raw Data from the Paper Toy Cap Testing Program.

Number of Tubes of Toy Caps [a]	Composition Mass [b] (kg)	Total Charge Mass [c] (kg)	Near Blast Gauge		Far Blast Gauge	
			Distance (ft) [d]	Pressure (psi) [e]	Distance (ft) [d]	Pressure (psi) [e]
0	0.001 [f]	n/a	2	1.71	4	0.71
				1.52		0.79
				1.82		0.87
0 [g]	0.001 [f]	n/a	2	1.57	4	0.72
7	0.016	0.10	2	4.84	4	1.81
				4.15		1.59
				4.22		1.86
7 [h]	0.016	0.10	2	3.07	4	1.38
28.5	0.063	0.41	3	3.19	6	1.38
74	0.164	1.06	3	6.53	6	2.76
183	0.406	2.16	3	10.2	6	4.11
676	1.50	9.67	6	17.3	12	8.84
1200 [i]	2.66	17.2	10	15.9	20	5.26

a) Each tube of caps had 12 rolls of 100 toy caps for a total of 1200 individual toy caps.

b) This is only the mass of toy cap composition, exclusive of their inert components and initiator. The amount of composition per cap averaged approximately 1.85 milligrams.

c) Total mass of toy caps, including paper and packaging, but exclusive of the initiator. The total mass of a tube of toy caps averaged approximately 14.3 grams.

d) To convert feet to meters, divide by 3.28.

e) This is peak air blast pressure to three significant figures. To convert psi to kPa, multiply by 6.89.

f) No toy caps were used; this was an initiator only, and it used 1.0 gram of a flash powder.

g) No toy caps were used; this was an initiator only, but it was wrapped with paper approximating the confinement provided by the rolls of toy caps

h) This was the same as the other 7 tube tests, but used an initiator with only 0.5 gram of flash powder.

i) This was one case of toy caps in an unaltered condition, with the exception of placing an initiator in a tube of toy caps in the approximate center of the case. The case consisted of 100 packages of 12 tubes of toy caps.

capacity of the blast chamber. In addition, one final test was performed that used a full case of the bulk toy caps, which consisted of 1200 tubes of toy caps, for a total of 1.44 million individual caps (100 packages of 12 tubes of 12 rolls of 100 toy caps). This test also needed to be conducted outdoors because of the large size of the test charge. The outdoor testing was conducted with the test charges and free field blast gauges at approximately 3 feet above the ground, and at an air temperature of approximately 27 ºC and a pressure of 0.86 bar.

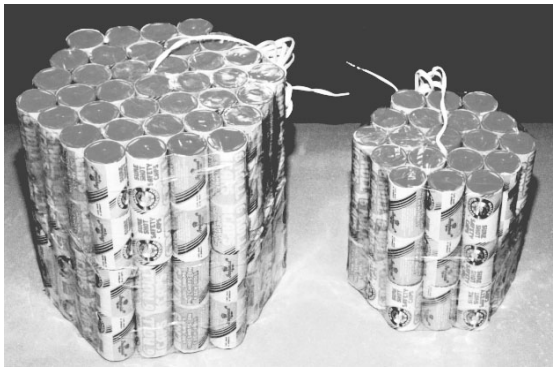

Figure 2. A photograph showing two of the toy cap test configurations, those containing 74 (left) and 28.5 (right) tubes.

Results

The three tests conducted using the chosen initiator in the absence of any toy caps produced an average overpressure TNT equivalency of 47%, see Tables 1 and 2. Given the construction of the initiator, the result is reasonable. With a mass of 1.0 gram of flash powder, the booster weight contribution ($M_{(TNT)B}$ in equation 5) used in subsequent testing was 0.47 grams TNT equivalent. One test was performed to determine whether the stronger confinements produced by insertion of the initiator into a roll of paper toy caps would result in a significant difference in its performance (see Table 1). While the peak air blast overpressures were less than the average from the three previous tests of the initiator, the overpressures were within the range of the three previous measurements. Thus it was concluded that the effect of wrapping the initiator with paper (or rolls of toy caps) was negligible.

The results of testing the assemblages of toy caps are presented in Tables 1 and 2, including the calculated TNT equivalencies—based on the mass of toy cap composition alone and on the total mass of the rolls of caps—for the variously sized configurations. After three tests of the smallest test charge (7 tubes of toy cap rolls), an additional test again using 7 tubes of caps was conducted; however, in this case the flash powder charge in the initiator was reduced to only 0.5 gram. The result was a significant drop in the explosive output of the toy caps. This suggests that the 1.0 gram initiator, at best, may only be marginally sufficient for the purpose. However, there was not enough space inside the rolls of toy caps to have used an initiator with a larger charge of flash powder, and the use of a non-pyrotechnic (high explosive) initiator was thought to be excessive for the purposes of these output tests.

Table 2. TNT Equivalence Results for Paper Toy Caps.

Number of Tubes of Toy Caps [j]	Equivalent TNT Mass (kg) [k]	TNT Equivalence (%) [l] Composition Only [m]	TNT Equivalence (%) [l] Total Toy Cap Mass [n]
0 [o]	0.00047	47	n/a
7	0.0024	15	2.4
7 [p]	0.0012	9	1.4
28.5	0.0057	9	1.4
74	0.020	12	1.9
183	0.056	14	2.6
676	0.81	54	8.4
1200 [q]	1.9	81	12.5

j) Each tube of caps had 12 rolls of 100 toy caps for a total of 1200 individual toy caps.

k) Based on peak air blast overpressure and correcting for the contribution of the initiator. This is the average of the results from the near and far blast gauges. When multiple tests were performed, this is the overall average of the results. The results are reported to two significant figures.

l) Calculated using the average of the near and far equivalent TNT masses.

m) Calculated based only on the mass of toy cap composition, but correcting for the initiator. The results are reported to the nearest 1%.

n) Calculated based on the total mass of toy caps, including paper and packaging, but correcting for the initiator. The results are reported to the nearest 0.1%.

o) No toy caps were used; this was an initiator only.

p) This was the same as the other 7 tube tests, but used an initiator with only 0.5 g of flash powder.

q) This was one case of toy caps in an unaltered condition, with the exception of placing an initiator in a tube of toy caps in the approximate center of the case. The case consisted of 100 packages of 12 tubes of toy caps.

The output from the smaller assemblages of paper toy caps (those comprised of 7 to 183 tubes and using the 1.0 gram initiator) ranged from 9 to 15% TNT equivalence based on composition mass, and there was no obvious trend in the data. This is in significant contrast with the results from the two larger assemblages (those comprised of 676 and 1200 tubes), which produced TNT equivalences of 54 and 82%, respectively, based on composition mass.

The physical debris produced in the tests of the smaller assemblages of paper toy caps consisted of a moderate amount of cap paper and unexpended caps, indicating the non-homogeneous nature of the rolls of toy caps and the incomplete propagation throughout the test charges. However, the amount of visible paper and unexpended caps present after the largest two test configurations (676 and 1200 tubes) was substantially less than in the smaller test configurations. This is consistent with a more complete propagation of the explosive reaction through the assemblages and accounts for the significantly higher TNT equivalencies obtained for these larger assemblages of toy caps.

The propagation mechanism involving the rolls of paper toy caps is not fully understood but is assumed to be one of sympathetic explosion, where the initiation of one cap may on average initiate one or more caps as a result. Given the construction of the cap rolls, the transfer mechanism may be one of impact through the thin paper separating the individual caps. Tube-to-tube transfer may be similar, through the plastic tube separations which are much thicker. To some extent, the efficiency of propagation was evidenced by the amount and nature of the debris left after each test. As described above, larger charges were shown to be more efficient in their ability to propagate.

Differences in the shape of the overpressure decay curve (the portion of the air blast positive phase after reaching peak overpressure) change the efficiency with which the blast wave propagates in air. Thus the air blast TNT equivalences found at various distances from a non-TNT test charge depend on details of the shape of the blast wave produced by that explosive, as compared with a blast wave from TNT.[8] This is certainly true for this study, due to the non-ideal explosive involved and to a lesser extent the non-spherical geometries. A comparison of the air blast results in this toy cap study reveals that the far gauge consistently resulted in significantly higher TNT equivalences. (It was verified that this was not a calibration or other problem with the instrumentation.) Accordingly, in Table 2, the TNT equivalences reported are the average of the near and far gauge results. While this is a reasonable approach, it must be realized that had the gauges been placed at other distances than those in this study, the TNT equivalences would be somewhat different as well.

Both high and low speed video cameras were setup to record the two test explosions produced outdoors. However, in the first test (that using 676 tubes of caps) the unexpectedly large air blast shock cause a circuit breaker to trip-off, which caused the high speed video record to be lost. Other than that, the recorded results of both tests were quite similar although somewhat different in scale. Figure 3 is a series of 1/60 second video fields, with a shutter speed of 1/60 second, recorded using the low speed video camera. (The low speed video images are reproduced here because they were captured with a more appropriate *f*-stop setting and the images are more distinct.) The numbers on these images are the number of video fields elapsing after the first image, which was the last image recorded prior to the explosion. The field of view in the images, at the location of the explosion, is approximately 18 feet high by 26 feet wide (5.5 by 8 m). In image number zero, the full carton of paper toy caps and the near blast gauge have been highlighted with circles.

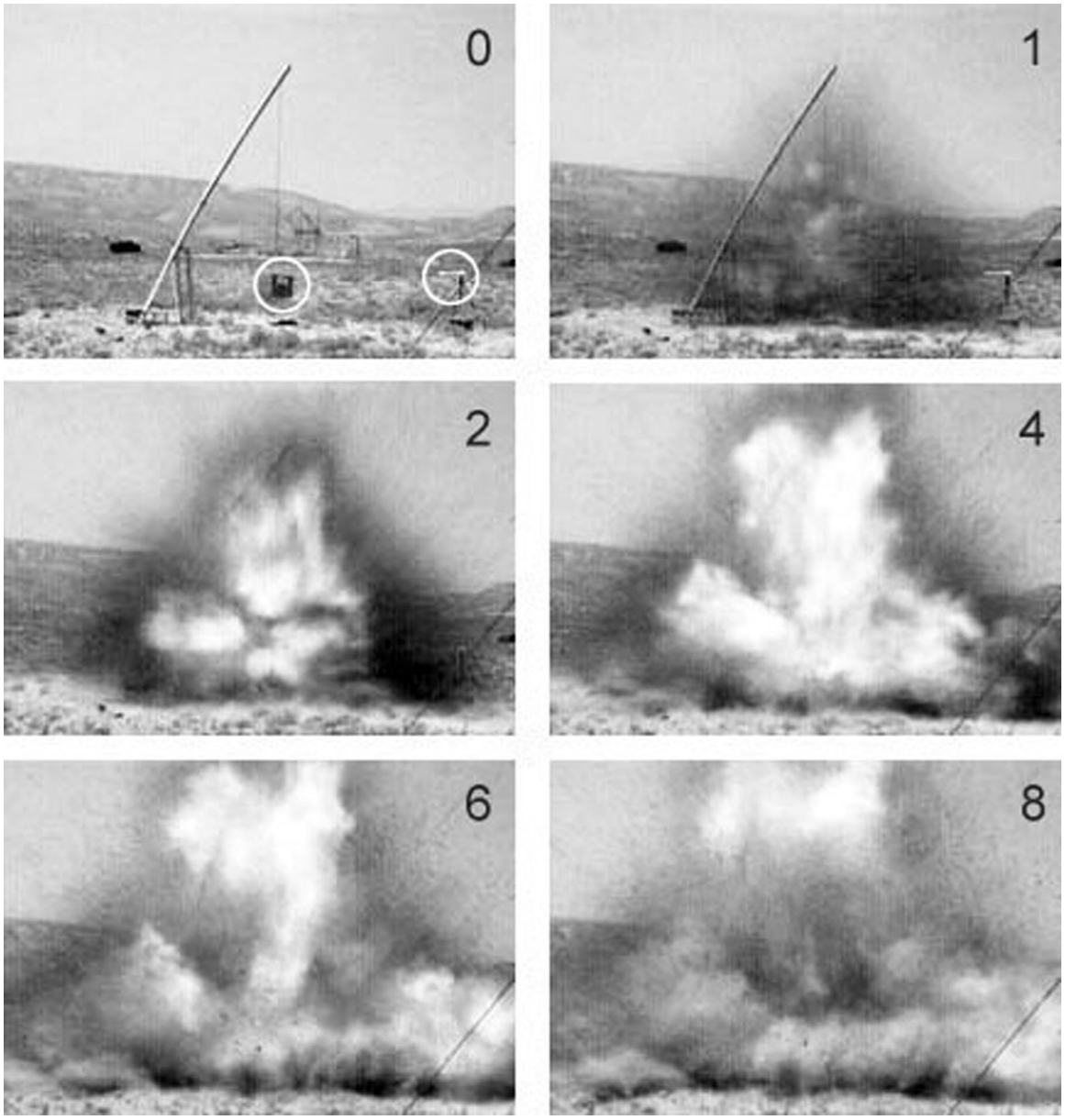

Figure 3. Video images just before and during the test involving a full case of paper toy caps. The field of view at the approximate distance of the explosion is 18 by 26 feet (5.5 by 8 m), and the numbers on the images are the number of 1/60 second video fields elapsing after the first image.

It is of interest to note that in the first image of the explosion (#1) that, while some of the debris from the explosion (appearing dark in the image) has been propelled to a diameter of approximately 16 feet (4.9 m), essentially no flash of light is discernable. In the next image (#2) the debris has expanded to approximately 21 feet (6.4 m), and a fireball has started to develop. In the next image (#4) the fireball has developed fully and thereafter decays. It is thought that the fireball is not part of the explosive reaction, but rather the burning in air of the finely shredded paper debris from the toy caps. This is consistent with the observation of a near total lack of paper debris after the explosion, including remnants of the heavy cardboard carton. The lack of a significant flash during the initial stages of the explosion and the subsequent development of a fireball was confirmed in the high frame rate video record.

Conclusion

Had greater quantities of toy caps been available for study, more tests could have been performed. This would have produced greater certainty in the results and other aspects of the case could have been investigated, such as identifying possible causes for the initiation of the caps in the accident. Nonetheless, the testing has shown that bulk quantities of paper toy cap rolls are clearly capable of producing a powerful explosive effect if initiated with a sufficiently energetic event. TNT equivalencies, based on toy cap composition mass, ranged from approximately 10 to 80% in different sized configurations, with the largest equivalences being produced by the largest assemblages of toy caps tested. This was unexpected, as the authors had thought that the opposite would likely have been the case, with very large assemblages tending to fail to efficiently propagate the explosion.

The results of this study are disturbing, considering that paper toy caps (even in bulk packaging) have a UN classification of Explosive 1.4S, which by definition should not produce significant blast or fireball effects when initiated. In the UN test protocol it is only required to initiate one item near the center of one case used in the testing. As part of this study of TNT equivalence, some very limited testing was performed in an attempt to learn how the accident might possibly have come to occur. During that testing, it seemed clear that a single toy cap functioning, or even a significant fraction of a single roll of caps functioning, was unlikely to have been sufficient to propagate well enough to produce the massive explosion that caused the fatalities or those explosions observed in the TNT equivalencies tests. Thus, it is understandable that the current UN test would conclude that the proper classification for the toy caps was Explosive 1.4S. Nonetheless, massive explosions certainly are possible (and have accidentally occurred at least once) for bulk cases of paper toy caps. This would generally not have been thought to be possible for items with an Explosive 1.4S classification. Accordingly, perhaps some consideration should be given to changes in the UN test protocol or the classification of paper toy caps.

Acknowledgments

The authors gratefully acknowledge P. Cooper and D. Chapman for providing comments on an earlier daft of this paper.

References

1) T. L. Davis, *The Chemistry of Powder and Explosives*, Angriff Press, 1970 [reprint of 1941 book published by J Wiley], p 105.

2) R. R. Rollins, *Potassium Chlorate / Red Phosphorus Mixtures*, Contract number DAAA-21-67-C-0682 for Picatinny Arsenal, available from Franklin Research Laboratories, (date unknown).

3) K. L. and B. J. Kosanke, "Explosive Limit of Armstrong's Mixture", *American Fireworks News*, No. 177, 1996; *Selected Pyrotechnic Publications of K. L. and B. J. Kosanke, Part 4 (1995 to 1997),* 1999.

4) R. Merrifield and J. Mackenzie, "Methodology for Estimating the Explosion Yield of Incidents Involving Conventional or Improvised Explosives", *Proceedings of the 8th International Symposium on the Effects of Interactions of Munitions with Structures*, Washington, D.C., 1997.

5) G. F. Kinney and K. J. Graham, *Explosion Shocks in Air*, Springer-Verlag, 1985.

6) W. E. Baker, *Explosions in Air*, Univ. of Texas Press, 1973.

7) P. W. Cooper, *Explosives Engineering*, VCH Publishers, 1996.

8) P. W. Cooper, "Comments on TNT Equivalence", *Proceedings of the 20th International Pyrotechnic Society Seminar*, 1994.

An earlier version appeared in: *Fireworks Business*, No. 258, 2005.

Mortar Plug and Recoil Problems

K. L. and B. J. Kosanke

(Note that this article contains a number of explanatory notes at its end. These are identified in the text as superscript letters in square brackets. While these notes may be of interest to some readers, they are ancillary in nature and readers may wish to ignore them until and unless they want further information.)

As is so often the case, this is an instance where one might take a useful lesson from someone else's unfortunate experience. This article recounts a relatively minor incident experienced by a display company, but one that could have been of significantly greater consequence.[a] The purpose of the article is to use this incident as the basis for discussing potential problems regarding mortar plug attachment and mortar recoil forces, which others in the industry may benefit from considering in greater detail.

As part of a firework display, a volley of 4-inch double-break spherical aerial shells[b] were to be fired from three racks positioned side by side. The shells were loaded into the company's normal mortars in their standard racks. These mortars and racks had been successfully used many times previously to fire single-break spherical shells of the same diameter. However, on this occasion, heavier and more powerfully-lifted double-break shells were being fired from the relatively weak and flexible deck of an old wooden barge. On this occasion, upon firing the shells, the mortars recoiled with enough collective force for the racks to break through the wooden deck of the barge (see Figures 1 and 2). In addition, most of the mortars blew (lost) their plugs (see Figure 3).

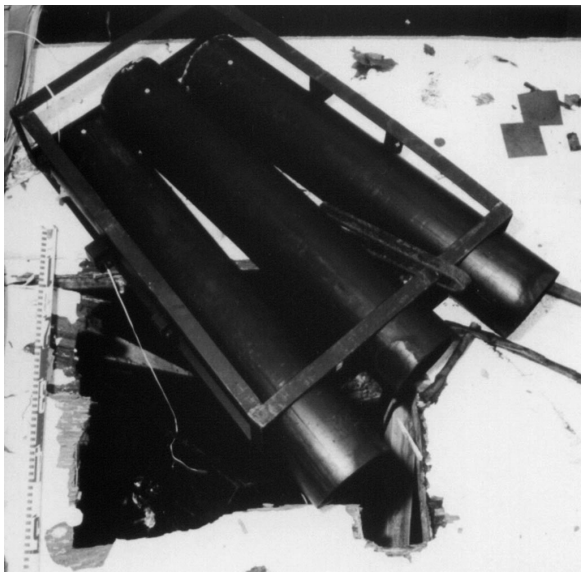

Figure 1. A photograph of deck of the wooden barge, with one of the three mortar racks partially covering the hole in the deck.

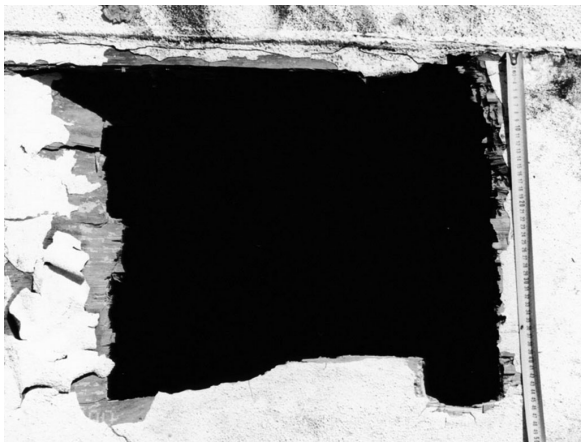

Figure 2. A photograph of the approximately 18-inch square hole in the deck of the wooden barge where the three mortar racks had broken completely through.

Where the mortar plug attachment in this incident was sufficient for the firing of typical shells in the past, it was not sufficient for the shells on this occasion when fired from the barge deck. It can reasonably be concluded that two factors combined to produce the mortar plug failure, one fairly obvious and one not so obvious. The fairly obvious factor is that the internal mortar pressures for these double-break spheri-

Figure 3. A photograph of the bottom of one of the mortar racks in which two of the three mortars had completely lost their plugs.

cal shells are expected to have been roughly double that for typical single-break spherical shells,[c] thus requiring a mortar plug attachment strength that was also approximately double.

The not so obvious factor contributing to the mortar plug attachment problem is the role played by the relatively weak and flexible barge deck. When firing a mortar that has been placed in firm contact with a very strong and unyielding supporting surface (like pavement or firmly compacted ground), it can be considered that the attachment between the plug and mortar is not so much to keep the plug from blowing downward out of the mortar, but rather to keep the mortar tube from lifting upward off from the plug. That is to say, there is an upward force on the bottom of the plug produced by the very strong and unyielding support surface below the mortar plug that approximately balances the downward force on the top of the plug produced by the high pressure lift gas inside the mortar. Figure 4 is an attempt to illustrate this, where it can be seen that the forces acting against the top and bottom of the mortar plug are approximately balanced.[d] Because of this approximate balance, there will be essentially no tendency for movement of the plug.[e]

There is, however, another much smaller upward force that acts to lift the mortar up from the plug. This upward force acting on the mortar is primarily a result of frictional forces produced by the upward flow of lift gas escaping from around the aerial shell. Thus, in the case of firing the mortar from a very strong and unyielding supporting surface, for the most part the attachment of the mortar plug need only be sufficiently strong to safely counter this relatively small upward force on the mortar.[f]

Now consider the situation where the same mortar and shell are fired from a comparatively weak and flexible support surface. In this situation, when the shell fires, the downward force from the lift gas on the top of the mortar plug is not balanced by an upward force from the support surface. Thus the mortar plug begins to move downward. As a result of the attachment

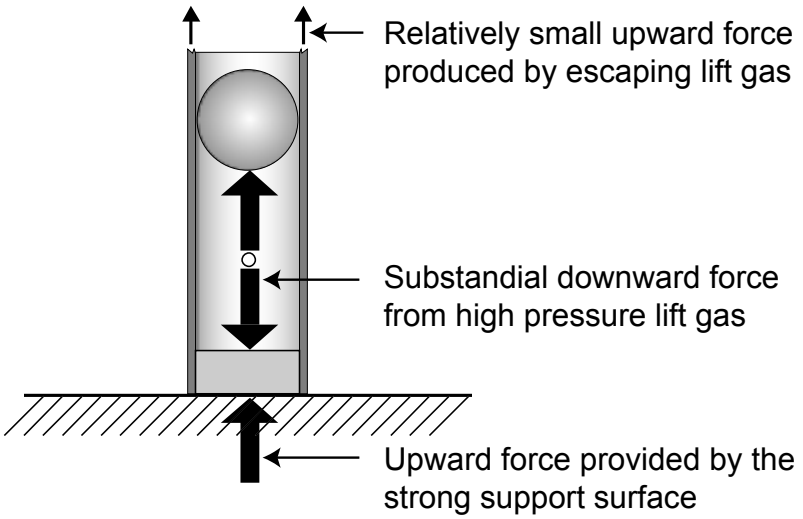

Figure 4. An illustration of the nearly balanced forces acting on the mortar plug that is resting on a very strong and unyielding supporting surface.

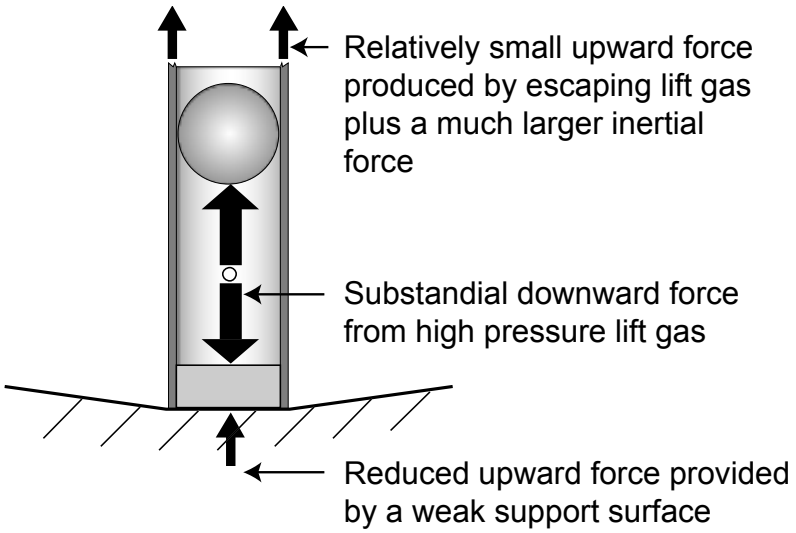

Figure 5. An illustration of the unbalanced forces acting on the mortar plug that is resting on a comparatively weak and flexible supporting surface.

between the plug and mortar tube, the downward movement of the plug acts to pull the mortar tube down. Because the mortar tube has mass, a force is developed as a result of the tube's inertial resistance to its sudden downward movement. In this case the attachment of the mortar plug needs to not only counter the relatively small upward force from escaping lift gas trying to lift the mortar up from the plug (as was discussed above), the attachment also needs to be strong enough to counter a much larger inertial force developed due to the sudden downward movement of the mortar tube. Figure 5 is an attempt to illustrate this.

The length, strength and number of nails securing the mortar plugs used in the incident being discussed, would appear to have been marginally sufficient at best (see again Figure 3). Nonetheless, the mortars had been used many times in the past to successfully fire single-break spherical shells and on occasion double-break spherical shells. If that was the case, why then did the mortar plug attachment fail on the occasion of being fired from the wooden barge deck? It can be surmised that on those past occasions, when the mortar plugs remained attached, the mortars had been placed on much more solid and unyielding support surface than the barge deck (such as illustrated in Figure 4). However, when the shells and mortars were fired on the relatively weak and flexible barge deck, the deck was unable to provide a sufficient upward force on the bottom of the mortar plug to approximately balance the downward force from the lift gas (such as illustrated Figure 5). This resulted in a substantially greater stress on the mortar plug attachment; more stress than it was capable of withstanding. Accordingly, what had proven sufficiently strong attachment in the past was not sufficient for the relatively weak and flexible barge deck.

As regards the failure of the barge deck, it can reasonably be concluded that there were two factors that combined to produce the deck failure, one fairly obvious and one not so obvious. The fairly obvious factor is that the internal mortar pressures for double-break spherical shells are expected to have been roughly double that for typical single-break spherical shells,[c] thus producing recoil forces also approximately double[g] and requiring a support surface with a correspondingly greater strength.

The not so obvious factor is associated with the design of the three mortar racks. For a ruggedly designed mortar rack, one with substantial support running the length of the rack below the mortars, the recoil force produced by the firing of individual mortars will be delivered somewhat uniformly across the entire area below the rack. In addition, when multiple racks are held tightly together as a single unit, to some extent the load will be further distributed across a

wider area below the group of racks. In such a situation, the load strength (in pounds per square foot) of the support surface can be relatively modest. However, in the incident described above, the racks were made of fairly thin and narrow angle iron, with no interconnection between the two pieces of angle iron forming the bottom of the rack except at the two ends of the rack (see again Figure 3). In addition, the racks were loosely held together in such a way that allowed virtually free vertical movement of the individual racks. One can imagine that these racks will perform reasonably well when positioned vertically on a strong and unyielding support surface. However, such is not the case when the mortars in these racks are fired from a relatively weak and flexible surface.

When racks such as in this incident are fired from a relatively weak and flexible support surface, the recoiling mortars will cause the thin angle iron to twist and spread apart, even to the point of potentially allowing the mortars to slip between the two pieces of angle iron. When that happens, the recoil force from each individual firing mortar is applied to only that relatively small area of the barge deck immediately below the firing mortar. With the full mortar recoil force being applied to such a small area of the barge deck, for the deck to successfully withstand that concentrated force requires that the deck have substantially greater load strength. Then too, once the barge deck begins to fail at one point, the remaining load strength of the barge deck is lessened and the collective individual firings of the other mortars can more easily continue the process of deck failure, ultimately producing a total failure of the deck such as documented in Figure 2.

It is hoped that the discussion of the incident has provided some useful information that might be helpful to others in avoiding similar problems when firing a display from a relatively weak and flexible mortar support surface.[h]

Acknowledgements

The authors are grateful to Larry Weinman for commenting on earlier versions of this article and to John Mercer for having performed some of the internal ballistic calculations.

Notes

a) As is often the case when investigating accidents, some of the facts may be in dispute. For the purpose of this article, the details presented are as thought to be correct by the authors.

b) Double-break spherical aerial shells are also sometimes called peanut shells or double-bubble shells.

c) Estimates of the internal mortar pressures were generated using data produced by T. Shimizu's internal ballistics model[1] and with the assistance of J. Mercer using his ballistics model.[2]

d) Not shown in Figure 4 are the outward forces from the lift gas pressure acting in opposing directions on the mortar walls, which are thus balanced around the circumference of the mortar. It is primarily on the aerial shell where the force from the high pressure lift gas is not balanced, and this is what causes the shell to accelerate rapidly up the length of the mortar.

e) In the case of a strong and unyielding support surface, Newton's Second Law of Motion ($F = m\ a$) implies that for there to be no motion of the mortar plug upon firing (i.e., for the plug not be accelerated) there must be no net force on it (i.e., the force from the lift gas must be counter-balanced with an equal and opposite force provided by the support under the mortar).

f) This was confirmed by rough measurements suggesting that the upward force from the escaping gas around the shell acting to lift the mortar tube from the plug is only about 5 to 10% of the downward force acting on the mortar plug because of the pressure of the lift gas. In another test, a shell was fired from a mortar placed on a very strong and unyielding surface (a thick concrete slab). The mortar plug was not attached to the mortar in any way and was loose enough to slip out of the mortar tube when raised off the surface. When the shell fired, it was propelled to roughly half its normal height, the mortar plug did not noticeably move, and the mortar tube lifted off of the mortar plug and rose roughly two feet into the air.

g) Estimates of the recoil forces were derived from peak and average internal mortar pressures using the method described previously.[3]

h) Somewhat similar lack of support problems can occur even when firing from a strong and unyielding support surface, when that firing is from angled mortars. This is because the entire bottom of the mortar (or mortar rack) is not firmly resting against the supporting surface. The portion of the mortar plug that is not in contact with the support surface will not have the benefit of an upward force to balance the downward force from the lift gas pressure acting on the plug. In the incident being described in this article, note that two of the three mortars in each rack were angled slightly (fanned outward). This can be expected to have further increased the tendency for the mortars to slip through the bottom of the racks. In addition, the angling will further increase the tendency for the recoiling mortars to break through the barge deck, because the recoil force is concentrated along only that portion of the edge of the plug that first makes contact with the deck.

References

1) "Shimizu Aerial Shell Ballistics Predictions (Parts 1 and 2)", K. L. and B. J. Kosanke, *PGI Bulletin*, Nos. 72 and 73, 1990; and *Selected Pyrotechnic Publications of K. L. and B. J. Kosanke, Part 2 (1990 through 1992)*, Journal of Pyrotechnics, 1995.

2) "Thermodynamics of Black Powder and Aerodynamics of Propelled Aerial Shells", J. E. Mercer, *Journal of Pyrotechnics*, No. 16, 2002.

3) "Typical Mortar Recoil Forces for Spherical Aerial Shell Firings", K. L. Kosanke and L. Weinman, *Fireworks Business*, No. 242, 2004; *Selected Pyrotechnic Publications of K. L. and B. J. Kosanke, Part 7 (2003 and 2004),* 2006.

An earlier version appeared in: *Fireworks Business*, No. 259, 2005.

Avoiding Making Comets That Explosively Malfunction

K. L. and B. J. Kosanke

In recent years, there have been at least three separate instances where white (or silver) comets, which were manufactured in China, have demonstrated a tendency to malfunction by powerfully exploding when they are fired.[1–5] In each instance, the comets were solid masses of composition, as opposed to being crossettes or some other type of intentionally exploding comets. In studying these comets, even though there were three different types of comet devices under three different brand names, it was discovered that they shared some characteristics in common that understandably account for their explosive malfunctions. After providing a limited amount of background information, it is the purpose of this article to identify the problem characteristics and to recommend an easy and cost effective means for manufacturers to avoid similar malfunctions in the future.

The first product[1,2] was a type of 2-inch 8-shot Roman candle that exploded upon firing with such force as to shatter a thick steel mortar used for support, which resulted in one fatality plus traumatic limb amputations for two other people. The second product[3,4] was a type of 5-inch comet shell, improperly described as being a Tiger Tail, that shredded HDPE mortars and fragmented the racks holding them, fortunately without injury. The third product[5] was a 3-inch comet of normal construction that shredded paper mortars and completely disassembled the racks used to hold them, again fortunately without injury. (In each of the three cases, further accidents and injuries were avoided by withdrawing the inventory of these products from use.)

For more detailed information about the specifics of the comet malfunctions as well as information about the analysis of the comets, see the references cited in the previous paragraph.

The Problem

Each of the comets used potassium perchlorate as their oxidizer, see Table 1. The remainder of the composition was a combination of aluminum and magnalium (a 50:50 alloy of magnesium and aluminum) and a binder. A substantial portion of the metal fuels consisted of very small particles, see Table 2. As a practical matter, for these three formulations, those metal particles smaller than about 100 mesh will be consumed in the flame of the burning comet and are not useful in producing a spark trail. Further, those metal particles smaller than about 200 mesh will potentially participate in explosive burning of the compositions. Accordingly, these compositions could be considered to be little more than a type of flash powder containing larger spark producing metal particles and that had been bound together to form solid masses of composition. The nature of their chemical composition is the first of the two comet characteristics that combined to produce the powerfully explosive malfunctions of these comets.

Table 1. Approximate Chemical Formulations of the Problematic Comets.

Ingredient[a]	Case 1	Case 2	Case 3
Potassium perchlorate	50	40	40
Aluminum[b]	20	30	30
Magnalium (50:50)[b]	20	25	20
Binder[c]	10	5	10

a) Ingredients are reported as percentages and are rounded to the nearest 5%. See the various article references for more information on the methods used to determine the ingredients and their percentages.

b) See Table 2 for metal fuel particle size.

c) In each case the chemical nature of the binder seemed to be different, but its exact nature was not determined.

Table 2. Approximate Mesh Fractions of the Metal Fuels in the Problematic Comets.[a]

Mesh Range	Case 1[b]	Case 2		Case 3	
	Al + Mg/Al	Al	Mg/Al	Al	Mg/Al
+60	0	65	10	45	0
60 – 100	5	25	10	40	0
100 – 200	15	10	35	15	0
200 – 400	30	0	25	0	15
–400	50	0	20	0	85

a) Mesh fractions are reported as percentages, rounded to the nearest 5%.

b) In this study, there had been no attempt to separately determine the mesh fraction of the aluminum and magnalium. The reported values were estimated using information reported in reference 6, which also contains information suggesting that it is magnalium that was the finer of the two metal powders.

Microscopic inspections of the various comets revealed that they all had structures that were either poorly consolidated (i.e., they were highly porous in cases 2 and 3) or otherwise provided internal channels that would allow the ready penetration of gases (in case 1). Thus, in each case it seemed apparent that upon burning, there would be the likelihood for substantial penetration of burning gas into the core of the comets. This is significant because it would result in much more rapid burning of the comets, rapid burning that could potentially accelerate to explosion.[7] (This potential was confirmed in Case 1, where the burning of some of the problematic comets, when completely unconfined, produced powerful explosions.) The potential for accelerated burning is the second of the two comet characteristics that combined to produce the powerfully explosive malfunctions of these comets.

Understandably the tendency for these comets to explosively malfunction was the result of the combination of: (1) the flash-powder-like nature of the comet compositions (combining an energetic oxidizer with an excessive amount of very fine metal powder), and (2) the internal structure of the comets (one that potentially allows the ready penetration of burning gas to more-or-less simultaneously ignite the entire mass of composition).

The Solution

Besides being a safety imperative, a possible solution to the problem is simple. Further, the solution has both has an economic advantage and it likely provides an esthetic improvement as well.

It is simple: Remove the very small particle size magnalium from the composition and replace it with a less reactive fuel like red gum. It seems somewhat likely that the very fine magnalium is present only because it is not being screened from the magnalium being purchased.

It has an economic advantage: It seems to be relatively common for Chinese manufacturers to use magnalium in making flash powder for their salutes. The very small particle-size magnalium is needed for making these salutes, and generally this fine mesh material is the most expensive. If it is screened from the magnalium used in making the comets, an overall cost savings should result. Further, the substituted fuel (e.g., red gum) that replaces the very fine magnalium is also less expensive.

It likely has an esthetic improvement: When the comets function as currently formulated, the heads of those comets will be excessively bright, tending to detract from the main feature of comets, their attractive tails. By replacing a portion of the metal fuel in the comet with something like red gum, the head will be less brilliant and the tail should appear enhanced.

One possible alternative solution would be to use a high percentage of binder and make sure the comets are very solidly compacted with small and relatively few internal voids. However, as a practical matter when manufacturing, there is always the chance that an occasional comet will be minimally compacted for any number of reasons, and one under-compacted comet may mean one dreadful accident. Thus this is not a guaranteed solution, and it does not have the economic and esthetic benefits.

Another possible solution might be to replace the potassium perchlorate with a less powerful oxidizer like potassium nitrate. This would have an economic advantage, but might make it difficult for the burning comet to ignite the primary spark producing fuel, which is the large particle size aluminum.

The Implementation

Major US importers and the more influential fireworks organizations need to recommend (and if necessary insist) that their Chinese suppliers immediately make this change (or some other effective change).

Acknowledgment

It must be acknowledged that while the cause of the explosive malfunctions seems to be well established, the effectiveness of the solutions suggested above have not been confirmed by laboratory testing.

It is gratefully acknowledged that L. Weinman commented on an earlier draft of this article.

References

1) "An 'Impossible' and Horrific Roman Candle Accident", *Fireworks Business*, No. 225, 2002; *Selected Pyrotechnic Publications of K. L. and B. J. Kosanke, Part 6 (2001 and 2002),* 2005.

2) "Roman Candle Accident: Comet Characteristics", *Fireworks Business*, 228, 2003; *Selected Pyrotechnic Publications of K. L. and B. J. Kosanke, Part 7 (2003 and 2004),* 2006.

3) "WARNING: Serious Product Malfunction", *Fireworks Business*, No. 232, 2003; *Selected Pyrotechnic Publications of K. L. and B. J. Kosanke, Part 7 (2003 and 2004),* 2006.

4) "Further Report on the Testing of Suspect Tiger Tail Comets", *Fireworks Business*, No. 237, 2003; *Selected Pyrotechnic Publications of K. L. and B. J. Kosanke, Part 7 (2003 and 2004),* 2006.

5) "Another Example of Explosively Malfunctioning Comets", *Fireworks Business*, No. 254, 2005; *Selected Pyrotechnic Publications of K. L. and B. J. Kosanke, Part 8 (2005 thorugh 2007),* 2009.

6) "Investigation Report, Bray Park Fireworks Tragedy 20 May 2000", Natural Resources and Mines, Queensland, Australia, 2002.

7) "Hypotheses Regarding Star-Shell Detonations", *Journal of Pyrotechnics*, No. 14, 2001; *Selected Pyrotechnic Publications of K. L. and B. J. Kosanke, Part 6 (2001 and 2002),* 2005.

An earlier version appeared in: *Fireworks Business*, No. 260, 2005.

Lessons from a Fatal Accident

K. L. and B. J. Kosanke

There was a fatal accident not too long ago while a worker was preparing aerial shells for use in a firework display.[1] What makes a discussion of this accident particularly relevant is that it involved: a) a smaller amount of pyrotechnic material than is often worked with at display companies, b) materials that were significantly less explosive than are often worked with at display companies, and c) a number of work practices that are somewhat common at many display companies. It is hoped that a discussion of this accident may help to identify some work practices and work facilities that should be considered for improvement from the standpoint of worker safety.

Background

In this instance, the work was being performed in a small metal shed, approximately 10 x 15 feet in dimension and 8 feet high. Present in the shed were probably 28 (and no more than 40) 3-inch aerial shells; in addition there were relatively small quantities of other pyrotechnic materials present (mostly electric matches and some quick match). The worker was assembling groups of seven of the 3-inch aerial shells into clusters to be fired simultaneously. This was accomplished by trimming the shell leaders' exposed black match to a length of about an inch, aligning a set of seven shell leaders together, inserting an electric match into the center of the cluster of black match tips, and securely taping the shell leaders to hold the set of shells together as a unit.

During the course of the accident the worker never exited the shed. Although the worker's body was virtually incinerated, there was little if any evidence of blast injury, and the most immediate cause of death was smoke inhalation. Thus, it seems fairly clear that his death was not the result of an explosion that might have rendered him unconscious. Rather it was the result of being unable to successfully exit the shed before succumbing to the flame and smoke from the burning pyrotechnics.

It is unknown whether the accident was initiated while cutting the shell leaders, an accidental ignition of an electric match, or some other cause. What is known is that there were a number of factors that potentially contributed to the cause of the accident or contributed to its severity. The remainder of this article is devoted to discussing those factors.

Potential Causal Factors

Although some razor knives (box slitters) were available in the work shed, it was common practice at that facility to use a scissors to cut quick match, and in this case the black match from the ends of the shell leaders. While this method of cutting fuse is expedient and is not uncommon, it does have the potential to cause an ignition of the fuse. Although not particularly expedient, one of the often recommended methods for safely cutting fuse is to use a razor knife and to cut the fuse against a block of wood. There is, however, a slight variation on this method that is at least as expedient as using a scissors but is much safer. That method is to use a so-called anvil cutter (e.g., a garden pruning tool) that employs a razor knife cutting against a plastic stop. One such cutting tool (using replaceable blades and costing less than $5) is shown in Figure 1.

While the use of a proper fuse cutting tool will substantially reduce the probability of causing an ignition, that probability is not absolutely zero. Accordingly, when cutting fuse, it should always be on one's mind that an ignition could occur. Thus one should perform fuse cutting in an environment: a) that is relatively free of other pyrotechnic materials that would present a hazard if ignited (in this case, the total collection of aerial shells being worked with), b) that provides

Figure 1. An example of an anvil cutter for use in cutting various types of fuse.

a degree of separation between the fuse being cut and the pyrotechnic materials to which the fuse is attached (in this case, the aerial shell attached to the fuse), and c) that provides one with the ready ability to quickly flee to a safe distance should that become necessary.

Although the shed was made of metal (aluminum), the shed was not electrically grounded and the floor was covered with vinyl flooring. This type of flooring can readily contribute to the build up of electrostatic charges and does not provide for the safe discharge of those electrostatic charges.[2] Also there was no provision for safely discharging personnel working within the shed. The electric matches were of a type commonly used and which are (as are many types of electric matches[3]) quite sensitive to discharges occurring from the bridgewire through the composition[4] (see Figure 2). It was the practice at that facility to expose the electric match by removing its safety shroud before attaching it to the shell leaders. This further increased the potential for an accidental ignition of an electric match from an electrostatic discharge.

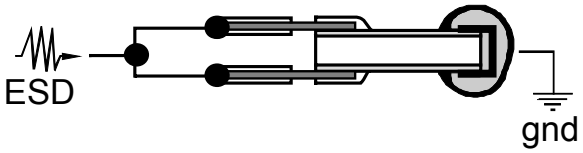

Figure 2. An illustration of an electrostatic discharge (ESD) occurring from the bridgewire through the composition of an electric match.

An estimate of the likely temperature and relative humidity inside the shed at the time of the accident is approximately 60 ºF and 55%, respectively. Although the humidity was not especially low, it was easily low enough to have allowed the buildup of a sufficient electrostatic charge to produce a through-the-composition ignition of an electric match. It should also be noted that even if the leg wires of the electric matches are kept shunted, this provides no protection for discharges occurring from the bridgewire through the composition.

Many of the tools present in the work shed were made of steel and some of the furniture had substantial metal parts. This could have been causal because of the possibility of incendive sparks, such as from the dropping of a tool. Also, since the safety shrouds were removed from the electric matches, the match tips were exposed and readily subject to an ignition from impact or friction.[5]

Factors Contributing to Severity

Several of the factors contributing to the severity of the accident relate to the ability (or inability) of someone to quickly exit the work shed in the event of an accident. These factors are:

1) There was only a single exit door. It is greatly preferred that a worker have the option of choosing from at least two exits such that the worker is more likely to be able to locate one that is safely remote from the accident with its flame, exploding shells, etc.

2) The exit door was immediately adjacent to the work tables where presumably the accident started and then progressed. The natural reaction of a worker experiencing an ignition of the materials being worked on is to recoil or retreat from the developing accident. Thus this is greatly preferred that the exit(s) be in the general direction the worker will already be moving (i.e., backward away from the work tables in this instance).

3) The door was approximately 28 inches wide, which is relatively narrow, especially since it was the only exit from a shed in which pyrotechnic materials were being worked with. Based on other accidents, the panic resulting

from being enveloped within a fireball makes it very difficult to locate even a full-sized exit.

4) The door opened inward. Thus, even if the worker successfully found the door and still had relatively fully functioning hands, it was necessary to locate the door knob to open the door. Further, since the shed was somewhat tightly constructed, if the internal pressure inside the shed, and acting on the door, had momentarily increased by even 0.1 psi, a typical person would have difficulty opening the door against the pressure acting on it. Such a momentary gas pressure could have easily been produced by the gaseous products of the burning pyrotechnics, plus the collateral pressure rise produced by the expansion of the air inside the shed due to the overall temperature rise inside the shed.

Another factor contributing to the severity of the accident was the amount of pyrotechnics being worked on. Each of the 3-inch shells in the groups of seven shells had a lift charge of 40 grams, for a total of 280 grams for each group of shells. The fireball produced by the ignition of just the lift charges on just one group of shells is more than sufficient to fully engulf the head and torso of a worker. (See Figure 3 for the ranges of fireballs produced by various amounts of Black Powder.) Based on documented experience, those persons caught within a pyrotechnic fireball in normal clothing (street clothes) have no more than a 50 percent chance of survival.[6] Further, even if the person does not die from the burns received, that person will be very seriously impaired and will have a most unpleasant existence for the rest of their life.

Given the dimensions of the fireball produced by just the lift charges from a small collection of aerial shells, in addition to taking measures to reduce the likelihood of there being an ignition, it is appropriate to provide a means of protecting workers from such a fireball in the event that there is an ignition. One frequently used method is to load the shells being worked on into mortars, such that if there is an accidental ignition, the shells will fire into the air. This provides a relatively high degree of protection from the explosions of the shells (assuming the mortars are outdoors at the time). However, if one is working in close proximity to the mortars

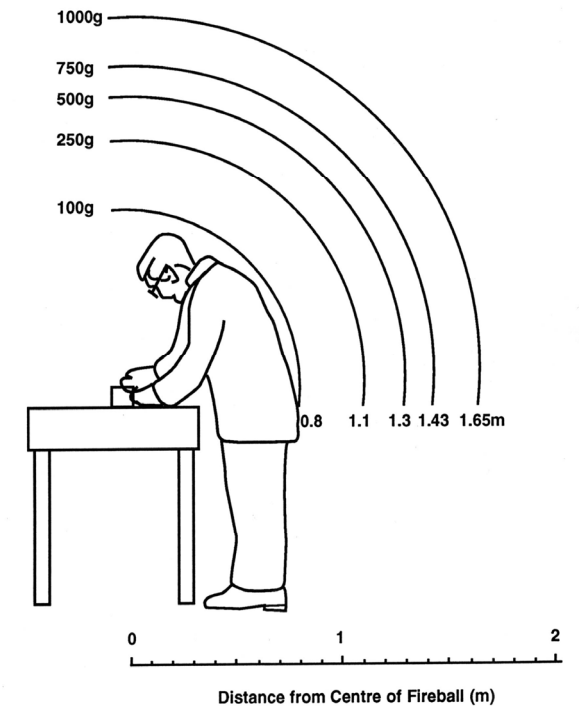

Figure 3. Fireball ranges from various amounts of burning Black Powder.[6] (For conversion to English units, 1 m = 3.3 feet and 100 g = 3.5 ounce.)

at the time the shells fire, such as when working with the shell leaders, the protection from the burning lift gas may be marginal and there is the potential for workers to have their hand(s) over the mortars at the time of their firing.

Another employee protection method would be to provide a barrier between the worker and the fireworks. This does not need to be an absolutely tight barrier. Even a partial barrier such as a small shield (see Figure 4) in front of the worker would tend to deflect most of a modest fireball from their torso, face and eyes.[7] For such a safety shield, the worker operates by looking through the window (made of Lexan™) and extending their arms around the barrier to perform various needed tasks. Similarly, the barrier does not need to provide complete blast protection, assuming the layout of the work area is such that it will allow a worker to retreat a reasonable distance during the interval taken by the time fuse to burn through and explode the aerial shell(s).

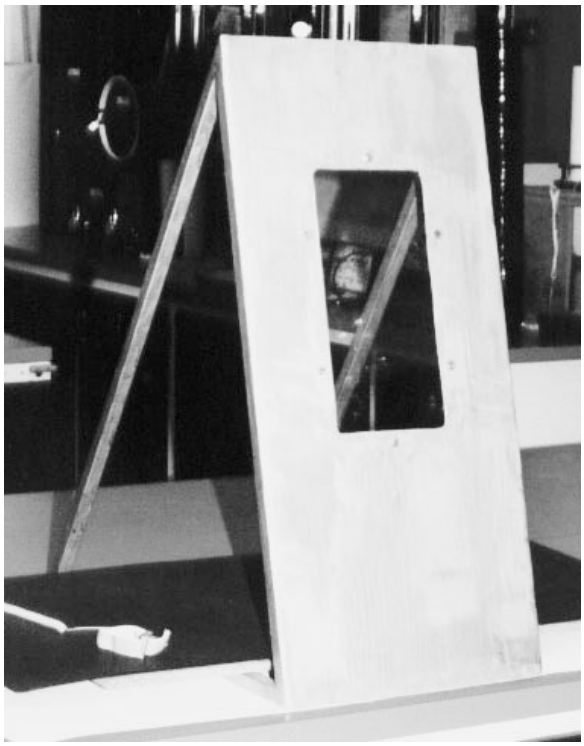

Figure 4. A photo of a small, inexpensive and convenient to use personal safety shield.

Conclusion

Since display companies are not involved with what is normally considered to be firework manufacturing, it seems to be fairly common for them to assume that the risks[8] to their on-site employees are comparatively minimal. The risks may be considerably less than for manufacturing operations, but the risks are still significant. The authors are aware of five on-site accidents that resulted in 11 fatalities at firework display companies in recent years.

Certainly display companies are not especially profitable businesses, and certainly there is some cost in taking measures that minimize risk to their on-site employees. However, the cost of accidents can be extreme, and some of the measures to minimize employee risk involve very little cost. Examples of such measures are: providing proper fuse cutting tools, cutting fuse in locations 10 or 20 feet remote from aerial shells when possible, working outdoors when practical, storing unused pyrotechnic materials in closed cabinets, and limiting the total amount of pyrotechnic materials in the immediate work area.

In general, there are probably three things that are needed to substantially reduce the risk to on-site employees at firework display businesses; their management and personnel both need to: 1) recognize that there are significant risks involved with their on-site operations, 2) spend a little time thinking about cost effective ways to minimize those risks, and 3) develop a positive and vigilant attitude regarding safety in general.

Acknowledgment

The authors are grateful to L. Weinman for commenting on an earlier draft of this article.

Notes and References

1) As is often the case when investigating accidents, some of the facts may be in dispute. For the purpose of this article, the details presented are as thought to be correct by the authors. Particulars about the company and date of the accident are being withheld because that information is not relevant within the context of this discussion.

2) A metal shed with insulating vinyl flooring and the metal furniture that was on top of that flooring would constitute an electrical capacitor of sort. While such a capacitor would be capable of storing electrostatic charges, it is not clear whether this was also a causally related factor in the accident.

3) "Studies of Electric Match Sensitiveness", K. L. and B. J. Kosanke, *Journal of Pyrotechnics*, No. 15, 2002; *Selected Pyrotechnic Publications of K. L. and B. J. Kosanke, Part 6 (2001 and 2002),* 2005.

4) It is fairly common for the sensitiveness of electric matches to accidental ignition from electrostatic discharges occurring through-the-composition to be on the order of 100 times greater than that for discharges occurring through-the-bridgewire.[3] Note that discharges so very small as to be less than can be sensed (felt) by a person, are still

possible to cause the accidental through-the-composition ignition of an electric match. While a fully intact coating on electric matches can provide a high level of protection from through-the-composition discharges, that coating often has slight defects that can render it almost completely ineffective.

5) As a practical matter, when the safety shroud is in place on an electric match, it is highly unlikely to accidentally cause its ignition from impact or friction.

6) "Thermal Hazards from the Accidental Ignition of Pyrotechnic Compositions", R. K. Wharton and R. Merrifield, *Journal of Pyrotechnics*, No. 6, 1997.

7) Even a small safety shield such as that shown in Figure 4 may be of more value than some might recognize. Apparently there is an autonomic reflex response to extreme stress (such as being engulfed by a fireball) that causes one to involuntarily inhale, even in circumstances where that is clearly inadvisable. Although in the case of a fireball, inhaling the burning gases may not produce instant death, it will produce lung damage that will soon result in death. Even the use of a limited safety shield, such as described above, provides a useful measure of protection to keep this from occurring.

8) Risk considers both the probability of the accident occurring, as well as the likely consequences of that accident if it does occur.

An earlier version appeared in: *Fireworks Business*, No. 262, 2005.

Initial Tests of Barge Safety Shelter Resistance to Penetration by Aerial Shells

K. L. and B. J. Kosanke

In the 2000 edition of the National Fire Protection Association's *Code for Fireworks Display*, a chapter was added with requirements for performing displays on barges and floating platforms. One of those requirements for manned displays when fired electrically (or as an alternative fired manually) is to provide a safety shelter for the on-board crew. (In the 2006 edition of the code, a safety shelter is also required for roof-top and limited-access displays, unless the electrical firing crew is located at least 75 feet from the nearest mortar.)

One requirement for the construction of the safety shelter is that it be made using at least the equivalent of 3/4-inch plywood.[1a] While it might reasonably be concluded that some number of standard dimensional 2×4's would also be used in the construction that is not specified in the NFPA code. One requirement for the placement of the safety shelter is that it be placed at least 2 feet per inch of mortar diameter away from mortars up to 6-inch in diameter and at least 4 feet per inch of mortar diameter away from mortars larger than 6-inch diameter.[1b]

In drafting the 2000 version of the code it was widely accepted by the NFPA's Technical Committee on Pyrotechnics that a safety shelter was a good idea and that the construction and placement requirements were reasonable. However, at that time no one had any test data to offer in support of the concept of a safety shelter, its manner of construction, or its positioning with respect to the mortars in the display. Thus, it seemed worthwhile to the authors to conduct some testing of safety shelters. (Unfortunately, it has taken several years for the authors to find the time to begin to work on this project.)

Of particular interest in the current testing is the ability of a safety shelter to resist the penetration of aerial shells fired directly at it from mortars, as this is probably the most intensive abuse it will be subjected to. This brief article is a report on initial testing of safety shelter construction material's resistance to direct penetration from fired aerial shells.

The basic setup for the testing is shown in Figure 1. Seen near the center in this photo is a mortar with two vertical support columns and a test target positioned above. The test target is a 2 foot square piece of new ¾-inch AC exterior plywood well secured to a wooden frame made with standard 2×4 dimensional lumber around the edge of the plywood square. The target location is centered over the mortar at a distance of 8 feet above its mouth. The target was placed with the plywood side facing down toward the mortar and the 2×4 frame on top. The test target is not secured in place; rather it is merely resting on top of a support collar at the top of the support columns. To the left of the mortar in Figure 1 is a set of portable steps used to facilitate putting the target in place. To the right of the mortar in Figure 1 is a shelter used to house the cameras and their operator (and on occasion, instruments for measuring aerial shell muzzle and impact

Figure 1. A photograph of the setup for recording videos of the aerial shell impact tests.

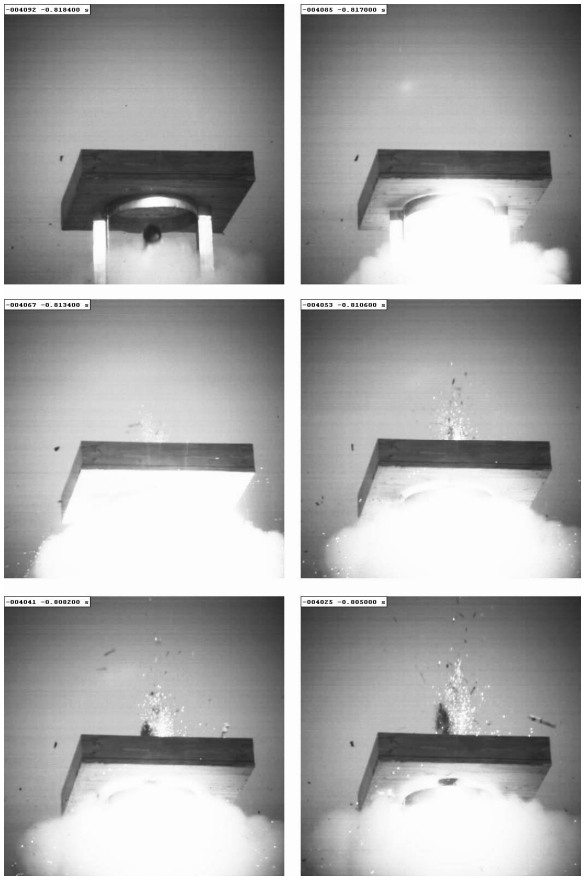

Figure 2. A series of images captured during a 3-inch aerial shell's impact with a reinforced section of 3/4-inch plywood.

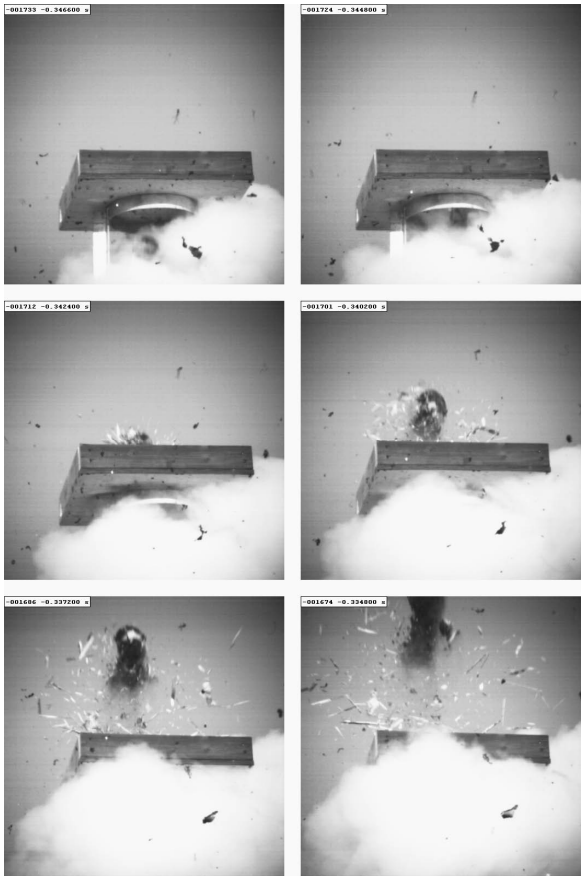

Figure 3. A series of images captured during a 4-inch aerial shell's impact with a reinforced section of 3/4-inch plywood.

velocities, mortar pressure profiles and aerial shell exit times).

Figures 2 and 3 present a collection of images documenting the results from two of the three initial tests of the ability of the shelter's 3/4-inch exterior grade plywood to withstand the direct impact of 3- and 4-inch aerial shells, respectively. In each case, the total span of time covered by the images in the Figures was approximately 12 milliseconds (0.012 second). The primary video camera was operated at 5000 frames per second. The 6 images presented in the Figures were selected from approximately 60 frames (spanning the time interval) in an attempt to well characterize the sequence of events occurring around the time of shell's impact.

In Figure 2, which shows the impact of a 3-inch aerial shell (Horse Brand), the plywood was breached, but only a portion of the contents of the shell passed through the plywood. In the first image (upper left), the aerial shell can be seen a few inches below the target, emerging ahead of the smoke and fire from the mortar. In the second image (upper right), the aerial shell is seen striking the target and there is a flash of light. The light was apparently produced by the impact of an attached comet on the exterior of the shell. (This is thought to be the case because not until approximately 0.12 second or another 600 images after the impact, are the contents of the shell seen to ignite in a much larger and much more sustained output of light.) In the 3rd through the 6th images, the plywood is being breached and some of the fire and contents of the shell are seen emerging from the back (2×4 reinforced side) of the target. Although not readily apparent in this brief series of images, the test target has begun to rise relatively slowly from the support collar. This is somewhat appar-

ent in the 6th image (lower right) where a bright gap can be seen between the support collar and the target, and what appears to be a portion of the not fully penetrating aerial shell can be seen imbedded in the plywood at that point.

In Figure 3, showing the impact of a 4-inch aerial shell (Yung Feng), the plywood was completely breached with the mostly intact shell passing through the plywood. In the first image (upper left), the aerial shell can be seen a few inches below the target, emerging ahead of the smoke and fire from the mortar. In the second image (upper right), the aerial shell is striking the target, but is not clearly visible. In the 3rd image, fragments of the plywood can be seen projecting above the test target. In the 4th image, the plywood has been completely breached and the mostly intact shell can be seen emerging above the target. In the 5th and 6th images, the aerial shell is seen to continue upward, but with some of its contents leaking out and trailing behind. Although not seen in the images, the contents of the shell ignited following the impact and gave the appearance much like that expected for a flowerpot malfunction. Again in this brief series of images, it is not readily apparent that the test target has moved; however it will eventually rise about 2 feet before falling back.

At this point, it is probably appropriate to consider whether the tests as staged provide reasonably reliable results. This will be done in the following series of paragraphs.

In these tests, the 8-foot separation between the mortar the test target was chosen partially as a matter of convenience and partly because of the NFPA's required separation of 2 feet per inch of mortar diameter between small caliber mortars and the safety shelter. Eight feet is then the minimum separation distance for a 4-inch mortar. However, if a mortar that was initially at the minimum separation distance from the shelter, then tipped over in the direction of the shelter, its muzzle could end up approximately one mortar length closer to the shelter. Because an aerial shell firing from the mortar is initially traveling in a column of air that is rapidly moving in the same direction as the shell, it is should not be expected that the aerial shell will slow detectably over a distance of a few feet after leaving the mortar. Any small differences between the distances used in these tests and what might occur during a worst case accident can certainly be ignored; if anything, the plywood is only more likely to be breached if the target were slightly closer to the muzzle of the mortar.

The vertical orientation of the target over the mortar was chosen as a matter of both convenience and safety. The amount of gravitational slowing of the shells will be insignificant over the 8-foot distance. There is no reason to suspect that this choice of orientation significantly affected the results; if anything, the plywood is only more likely to be breached if the shells were fired horizontally into the plywood targets.

The decision to not rigidly secure the target in place was made after an initial test. In that case, a 4-inch shell impacted the plywood target that was weighted down with approximately 20 pounds of water contained in four plastic two-liter soda bottles placed in the four corners of the test target. While the target eventually rose approximately half a foot into the air following the shell impact, by the time the target did so the 4-inch shell had long since passed through the target and was well out of the field of view of the cameras. It was obvious that gravity and the inertia of the target were sufficient to hold the target in place during the aerial shell's impact. This was confirmed in subsequent tests such as seen in Figures 2 and 3, wherein the unsecured targets remained virtually in place during the course of the impact of the aerial shells. Another reason for using unsecured targets is that some degree of wall flexibility is expected for a typically constructed safety shelter. Thus, the use of targets that were not rigidly secured is thought to have better simulated a likely safety shelter. Finally, an aerial shell impacting a rigidly secured target will deliver more of its energy to the act of penetrating the target. That is to say, if an aerial shell is capable of penetrating an unsecured target, the same shell will certainly have penetrated a rigidly secured target.

Because it is only the approximately worst case scenarios that are being considered, and the 4-inch shell proved capable of completely breaching the plywood target, there is little need to test either more 4-inch shells or larger caliber shells. Since the 3-inch shell only partially breached the test target, it might have been worth looking at the results from a few more 3-inch shell firings to see if any are successful in

completely passing through the plywood. (Perhaps if time and interest allows, this will be done, but there are no immediate plans for this.)

While the NFPA code does not specify the use of 2×4 dimensional support lumber behind the ¾-inch plywood, almost certainly this will be the most commonly used method for supporting the wall and roof sheets of plywood. It is also quite likely that the spacing between the 2×4 supports will be either 16 or 24 inches. Thus the choice of 24 inch square test targets with 2×4 around the edge should have a resistance to penetration that is approximately equivalent to a typical safety shelter.

In the tests reported on in this article the mortar was always firmly supported and was not able to freely recoil upon firing. In addition the angle of impact was perpendicular to the surface of the test target. If the firing mortars on a barge come to be tipped in the general direction of the safety shelter, it is likely that some amount of mortar recoil motion will occur, and the shell's trajectory is not likely to be exactly perpendicular to the front wall of the safety shelter. When the mortar is free to recoil to some extent upon firing, there will be a modest reduction of the muzzle velocity of the aerial shell[2] and a decrease in the likelihood of the shell penetrating the wall of the shelter. Similarly, when an aerial shell strikes the safety shelter at an angle other than perpendicular, there will be a decrease in the likelihood of the shell penetrating the wall of the shelter. Estimating the effects of recoiling mortars and non-perpendicular shell trajectories is a complex engineering problem. However, it was the purpose of these initial tests to only test the penetrability of safety shelters under the most extreme conditions. Thus the effects of recoiling mortars and non-perpendicular trajectories can be ignored in this initial study.

The authors agreed with the proposal requiring a safety shelter as defined by the NFPA's Technical Committee on Pyrotechnics, and this has not changed as a result of the test results being reported here. It is important, however, for firing crews to understand that, while the use of a safety shelter provides a useful level of protection from some of the things that can go wrong during a display, that protection is far less than complete, even for a relatively small caliber aerial shell.

Acknowledgment

The authors are grateful to L. Weinman for commenting on earlier drafts of this article and for performing calculations of the approximate effect of freely recoiling mortars on aerial shell muzzle velocity.

Reference and Note

1) *Code for Fireworks Display,* NFPA-1123, 2006, (a) Paragraphs 4.2.3 and 4.4.1(4), (b) Paragraph 4.3.2.

2) L. Weinman performed calculations to estimate the likely reduction in aerial shell muzzle velocity when its firing mortar is completely free to recoil. Depending on the relative mass of the aerial shell and mortar, the reduction in a 4-inch shell's muzzle velocity ranges from approximately 3 to 15 percent.

An earlier version appeared in: *Fireworks Business*, No. 263, 2005.

Evaluation of "Quick-Fire" Clips

K. L. and B. J. Kosanke

Quick-Fire clips are a product of Martinez Specialties[1] and come in two varieties. One is the "VF" clip, which is primarily intended to couple to and ignite visco-like[2] fuse products using an electric match. The other is the "LC" clip, which is primarily intended to ignite the lift charge of aerial shells using an electric match.[3] (However, both clip types have other useful applications as well.) Supplies of both types of Quick-Fire clips were provided by Martinez Specialties for an evaluation of their effectiveness.[4] This article is a brief report of those product evaluations.

Quick-Fire VF Clips

With the wide spread use of large cake items in firework displays, many with visco fuse as the point of ignition, there is need for a reliable means of igniting those item using electric matches. Based on the testing reported here, the Quick-Fire VF clip (connector) should effectively fill that need. The clip and its attachment to a small cake item are illustrated in Figure 1. The upper most photograph shows two views of the clip as supplied (i.e., without an electric match installed in it). The first step in the process of attachment to the firework is to install a non-shrouded electric match into the left half of the clip.[4] This process requires only a few seconds, is well described in the literature supplied with the clips, but is not illustrated in Figure 1. The upper-middle photograph shows the visco fuse of the firework after the ignition end was uncovered and freed from its attachment to the firework. The lower-middle photograph is after the Quick-Fire VF clip has been secured to the visco fuse. Again, this process requires only a second or two, is well described in the literature supplied with the clips, but is not illustrated in Figure 1. The lower most photograph is with the Quick-Fire VF clip and visco fuse secured to the firework using tape.

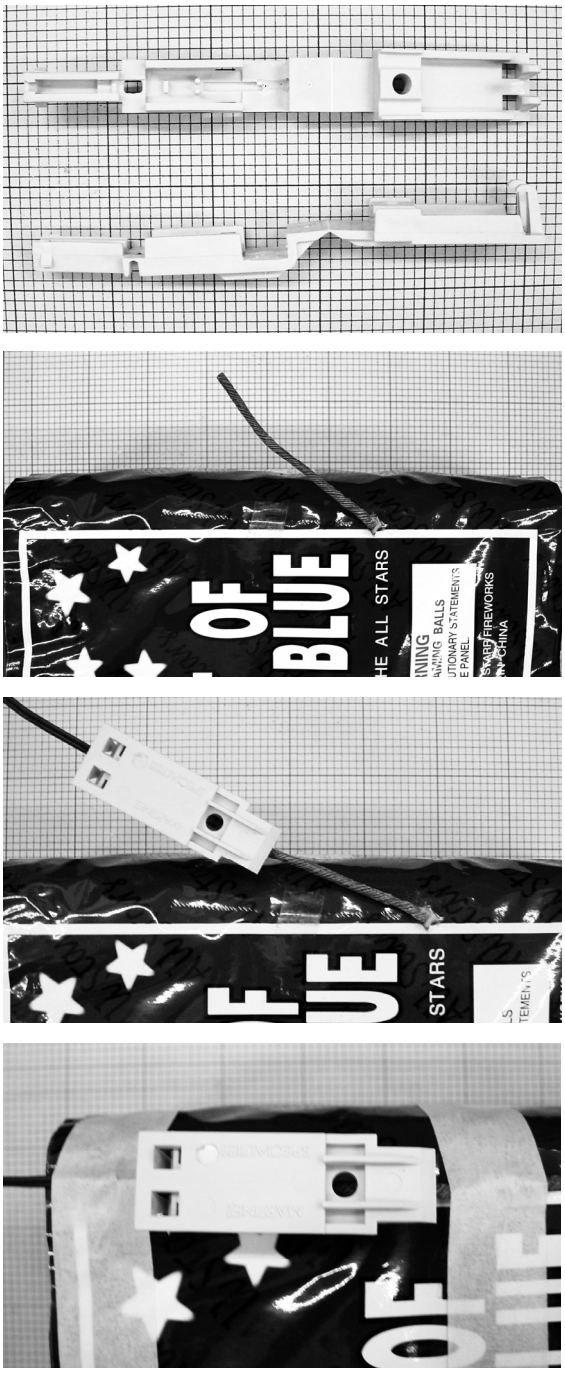

Figure 1. Photos of the Quick-Fire VF clip and its attachment to a small firework cake item.[4]
(Each square in the background is 0.1 inch.)

In the course of the evaluation a total of 30 test ignitions of visco-like fuse were conducted. This included 10 each of ignitions of: a) high quality visco fuse, b) low quality visco fuse, and c) the fast burning visco-like fuse commonly used on reloadable consumer firework aerial shells. All 30 ignitions were successful. Further, it was found that the process of loading the electric match into the clip and installing the clip onto the visco fuse was quick and relatively easy to accomplish.[4]

During the course of evaluating the effectiveness of the Quick-Fire VF clips a limited number of trials of their utility in initiating Lightning Thermo Tube were conducted. (Lightning Thermo Tube is an interesting new product, somewhat similar to shock tube, that is being introduced to the firework trade.[5]) It was found that the Quick-Fire VF clip provided an effective means to couple an electric match to Thermo Tube and accomplish its initiation.

Quick-Fire LC Clips

The greatest precision in the firing time of an aerial shell is accomplished when the electric match is installed directly into its lift charge.[6] Probably the best way to accomplish this is to have the electric match installed by the shell's manufacturer. However, it is common for users to install their own electric match, often by simply poking a hole into the shell's lift bag, inserting the electric match (often, but inappropriately, with the safety shroud removed), and taping over the hole. This is somewhat problematic because of the potential for leaking lift powder and the use of electric matches without their safety shrouds.[7] Based on the testing reported here, the Quick-Fire LC clip (connector) should effectively solve the problem of a user installed electric match into the lift charge. The Quick-Fire LC clip is shown in Figure 2. The upper photograph is of two views of a clip as supplied. The lower photograph shows the clip after a non-shrouded electric match has been installed.[4] This process requires only a few seconds, is well described in the literature supplied with the clips, but is not shown in Figure 2.

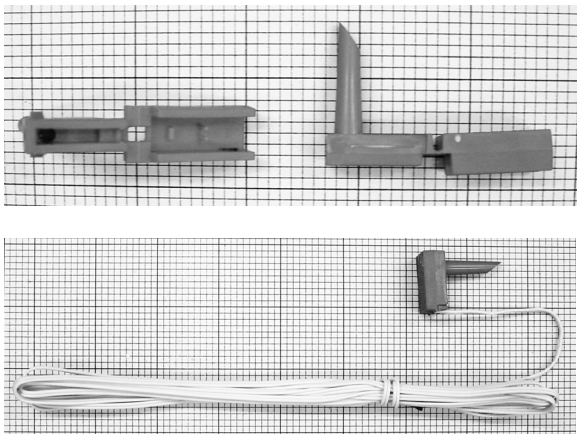

Figure 2. Photos of the Quick-Fire LC clip before and after installation of an electric match.[4] (Each square in the background is 0.1 inch.)

Figure 3 illustrates the process of installing the Quick-Fire LC clip into the lift charge of an aerial shell. The top photograph shows the aerial shell and Quick-Fire LC clip (with an electric match) ready for installation. The middle photograph shows the LC clip pressed partially into the lift charge of the shell. This insertion is facilitated by the relatively sharp point on the LC clip. The bottom photograph shows the Quick-Fire LC clip fully inserted and secured in position using tape. The taper of the LC clip aids in limiting the leakage of lift charge powder. The typical user will probably want to leave the shell leader attached on smaller caliber shells for use in lowering the shell into its mortar.

Only a very limited number of test firings of the Quick-Fire LC clip installed into the lift charge of an aerial shell were carried out. In part this was for the sake of economy, but it was mostly because of the abundant fire and sparks that project from the clip when it fires. Figure 4 is one video field (1/60 second) recorded during the firing of an LC clip using a Martinez Specialties e-max electric match. The LC clip is seen illuminated to the left in Figure 4, and the fire and sparks projecting from the clip extends fully 10 inches to the right. With such a robust projection of fire and sparks, ignition of an aerial shell's lift charge is essentially assured.

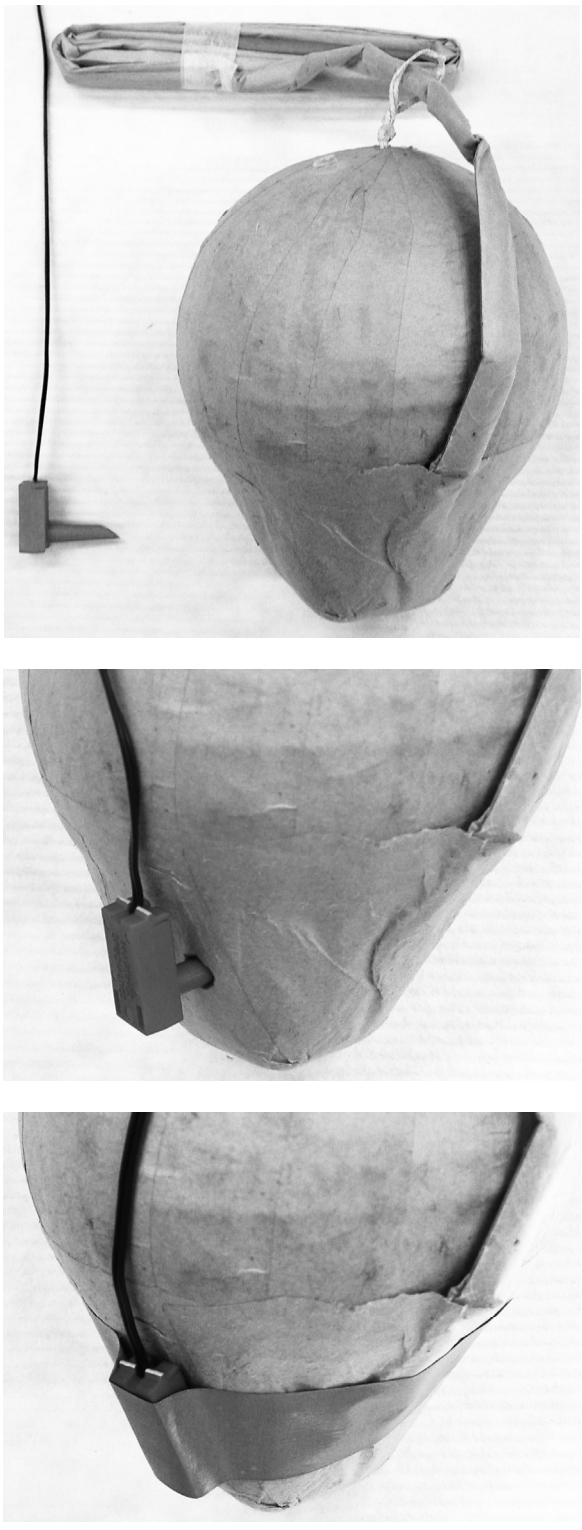

Figure 3. Photographs illustrating the process of installing a Quick-Fire LC clip into the lift charge of an aerial shell.

Figure 4. A photograph documenting the 10-inch jet of fire and sparks projecting from a Quick-Fire LC clip.

Although Quick-Fire LC clips are primarily intended for use in quickly and safely installing an electric match into a standard aerial shell, it is possible to use the clip to install an electric match into shell's leader fuse. This can be accomplished in at least two ways, one of which is demonstrated in Figure 5. In this case, a portion of the shell leader has been cut off, the LC clip inserted into the quick match between the black match and the match pipe, and clip is held in place by bending over the end of the leader fuse and securing the clip with the electric match leg wire. Another method of installing the Quick-Fire LC clip (not illustrated herein) is to slit the leader fuse, insert the LC clip into the slit alongside the black match, and then secure the clip in place.

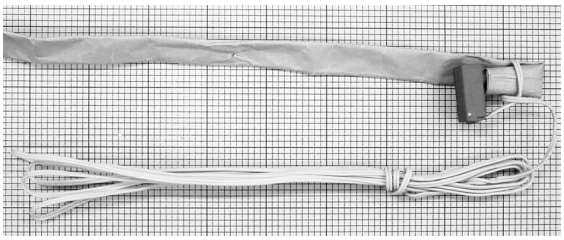

Figure 5. A photograph demonstrating an alternate use of an Quick-Fire LC clip to attach an electric match to an aerial shell's leader fuse.

Conclusion

The use of Quick-Fire VF and LC clips is an expedient and effective means of attaching electric matches to visco-fused items and standard

aerial shells. In addition, although not specifically investigated in this brief study, use of the clips should provide abundant safety with respect to the installation and removal of electric matches. This is because the electric matches are well encased and are not in direct contact with other pyrotechnic materials. This virtually eliminates or at least greatly reduces the possibility of their accidental ignition due to impact, friction, and the type of electrostatic discharges of greatest concern.[8–9]

References and Notes

1) Martinez Specialties, Inc., 205 Bossard Rd. Groton, NY 13073, 607-898-3053.

2) Visco fuse is also called hobby fuse, cannon fuse and sometimes fireworks safety fuse.

3) "New E-Match Attaching Clip", *Fireworks Business*, No. 262, 2005.

4) The clips supplied for evaluation, and shown in the top photographs of Figures 1 and 2, did not have electric matches preinstalled. However, while Martinez Specialties will supply clips without an electric match already installed, it is intended that the clips will generally be supplied with an electric match preinstalled to save time for the user.

5) Lightning Thermo Tube is a product intended for use in fireworks that was subsequently evaluated by the authors. "An Evaluation of Lightning Thermo-Tube™ as a Pyrotechnic Ignition System", K. L. and B. J. Kosanke, *Journal of Pyrotechnics*, No. 24, 2006; *Selected Pyrotechnic Publications of K. L. and B. J. Kosanke, Part 8 (2005 through 2007),* 2009.

6) "Firing Precision for Choreographed Displays", K. L. and B. J. Kosanke, *Fireworks Business*, No. 194, 2000; *Selected Pyrotechnic Publications of K. L. and B. J. Kosanke, Part 5 (1998 through 2000),* 2002.

7) Transporting an aerial shell with a non-shrouded electric match installed in the lift charge would also be a violation of a requirement of the standard APA87-1, incorporated by reference into US DOT regulations.

8) Typical electric matches are far more sensitive to electrostatic discharges that occur through the pyrotechnic composition, rather than those that occur through the bridgewire. Since electric matches installed in LC clips are isolated from close contact with external objects, electrostatic discharges occurring through the composition are very highly unlikely.

9) "Studies of Electric Match Sensitiveness", *Journal of Pyrotechnics*, No. 15, 2002; ; *Selected Pyrotechnic Publications of K. L. and B. J. Kosanke, Part 6 (2001 and 2002),* 2005.

An earlier version appeared in: *Journal of Pyrotechnics*, No. 22, 2005.

Thermodynamic and Spectroscopic Analysis of a Simple Lilac Flame Composition

B. T. Sturman[a] and K. L. Kosanke[b]

[a] 6 Corowa Court, Mount Waverley, Victoria 3149, Australia

[b] PyroLabs, Inc., Whitewater, CO, USA

ABSTRACT

A simple lilac flame composition consisting of 80% potassium nitrate and 20% shellac was investigated by emission spectroscopy and thermodynamic modeling. The flame from the burning composition had a reddish-pink core with a brighter pale lilac outer envelope. The core of the flame is presumably close to the equilibrium conditions predicted by thermodynamic modeling. The calculated equilibrium flame temperature is 1526 K; seven gases (CO, H_2O, N_2, CO_2, H_2, KOH, K) and one liquid (K_2CO_3) account for 99.7% of the molecules in the core of the flame. Of these, liquid potassium carbonate (mole fraction 9.6%) is expected to emit a continuous spectrum while atomic potassium (mole fraction 2.5%) imparts a red colour from the resonance doublet (766.491 and 769.897 nm), which is considerably broadened by self-absorption. The outer flame envelope is presumably a diffusion flame in which flammable gases from the core burn in entrained air. The maximum adiabatic temperature of such a flame was calculated as 1723 K; seven gases (N_2, CO_2, H_2O, KOH, K, Ar, $K_2O_2H_2$) account for 99.8% of the molecules in the outer flame envelope. The emission spectrum of atomic potassium superimposed on a continuous spectrum arising from the combining of atomic potassium with OH radicals to form gaseous KOH is responsible for the lilac colour of laboratory flames containing potassium and is the likely cause of the lilac colour of the outer regions of this pyrotechnic flame. The article includes a brief tutorial outline of some relevant aspects of the atomic spectroscopy of potassium.

Keywords: lilac flame colour, potassium nitrate, shellac, thermodynamic modeling, visible spectrum

Introduction

Potassium nitrate, potassium perchlorate and potassium chlorate are very widely used in pyrotechnics as oxidizers. One of the advantages of potassium salts is that in most compositions they contribute little colour to the flame. It is well known, however, that potassium compounds emit visible light in laboratory flames[1] and it is to be expected that they would have some effect on the colour of pyrotechnic flames. Webster[2] studied the effect of potassium salts in magnesium-fueled flares and noted that visible emission from potassium may be part of the reason that high purity colours are not obtained from signal flares that incorporate a potassium salt as an oxidizer. Jennings-White[3] noted that mixtures of potassium perchlorate or potassium chlorate with shellac burn with white or off-white flames respectively, but a mixture of potassium nitrate and shellac burns with a lilac flame and has been used as a composition for a coloured lance. In 1980 Winokur[4] presented a comprehensive review of pyrotechnic mixtures for producing purple fire and listed a very simple composition for a violet lance: 80% potassium nitrate and 20% shellac. The source was an Italian work[5] published in 1845 (which the authors have not seen). Since the first publication of the present article, the authors have found that the same formula appears in the first edition of F.-M. Chertier's 'Nouvelles Recherches des Feux d'Artifice' (chez l'auteur, Paris, 1843, p. 420), two years earlier than the Italian work cited by Winokur.

Chertier described the composition as 'Saltpeter Pink for Lances and Stars".

Recently Jennings-White[6] observed for the potassium nitrate and shellac composition that

> …close examination of the flame shows the red is in the interior of the flame, with lilac on the outside. I had some observers look at this from a greater distance with a strontium pink for comparison. The consensus was that the flames were clearly similar pink, but the potassium (nitrate) one had a bluish fringe.

The authors decided to attempt to provide an explanation for these observations.

Background

1. Possible Sources of the Flame Colour

Flames emit light by several processes including:

1) Emission of continuous spectra by incandescent solids or liquids
2) Emission of line spectra by atoms
3) Emission of band spectra by molecules
4) Emission of continuous spectra by chemiluminescent recombination reactions.

Band emission from molecules is an extremely important source of pyrotechnic colour,[7] but does not appear to be relevant in the case of the lilac flame being discussed.

It is well known that potassium salts impart a lilac colour to laboratory flames. The colour is attributable to the combination of the following:[1a,8,9a]

1) Atomic emission from potassium. Possible lines include the pair of resonance lines at the far red extreme of the visible spectrum (at 766.491 and 769.897 nm) and another pair at the violet end of the spectrum (at 404.414 and 404.721 nm).
2) Continuum emission, extending from about 570 to 340 nm[9a] and peaking in the violet around 400 nm,[1a] arising from the chemiluminescent combination of atomic potassium with hydroxyl (OH) radicals to form gaseous potassium hydroxide.[10]

2. Tutorial Outline of Relevant Aspects of the Atomic Spectroscopy of Potassium[1,11,12]

According to the quantum theory, electrons in an atom occupy regions of space around the atomic nucleus called *orbitals*. Different arrangements of electrons in orbitals correspond to different energy states of the atom. In atoms having more than one electron (such as the potassium atom) most of those electrons occupy very stable orbitals and do not participate in the electron rearrangements associated with chemical reactions or with interactions of atoms with light. Such changes involve rearrangements of only the outermost electrons, which are the most loosely bound. The potassium atom has only one electron that is not locked up in a highly stable inner orbital. That outer electron can occupy many different orbitals, but only the lowest energy one is stable. An electron in that orbital can stay there forever. If the atom gains energy, for example by colliding with another atom, the outer electron can move into another orbital that corresponds to a higher energy state, but it cannot remain there indefinitely. Most commonly, the atom will lose energy in the same way it gained it – in a collision with another atom. Even if the atom were completely isolated, however, quantum theory predicts that the electron will eventually return to the stable orbital. The time that any one atom remains in a higher energy state is unpredictable, but the average time (referring to a large number of such atoms) is known and is called the *radiative lifetime* of the energy state. When an atom spontaneously changes from a higher energy state to a lower one, the excess energy is emitted as light. The energy difference (ΔE) between the two states corresponds to the energy of one photon of the emitted light (E_p). The wavelength of the emitted light (λ) is related to the photon energy by the Planck equation,

$$\Delta E = E_p = h\nu = hc/\lambda \qquad (1)$$

where energy is expressed in joules (J), h is Planck's constant (6.626×10^{-34} J s), ν is the frequency (s^{-1}) of the emitted light, c is the velocity of light (2.998×10^{8} m s^{-1}) and λ is the wavelength in metres. Similarly, the opposite process can take place, wherein the atom can absorb a light

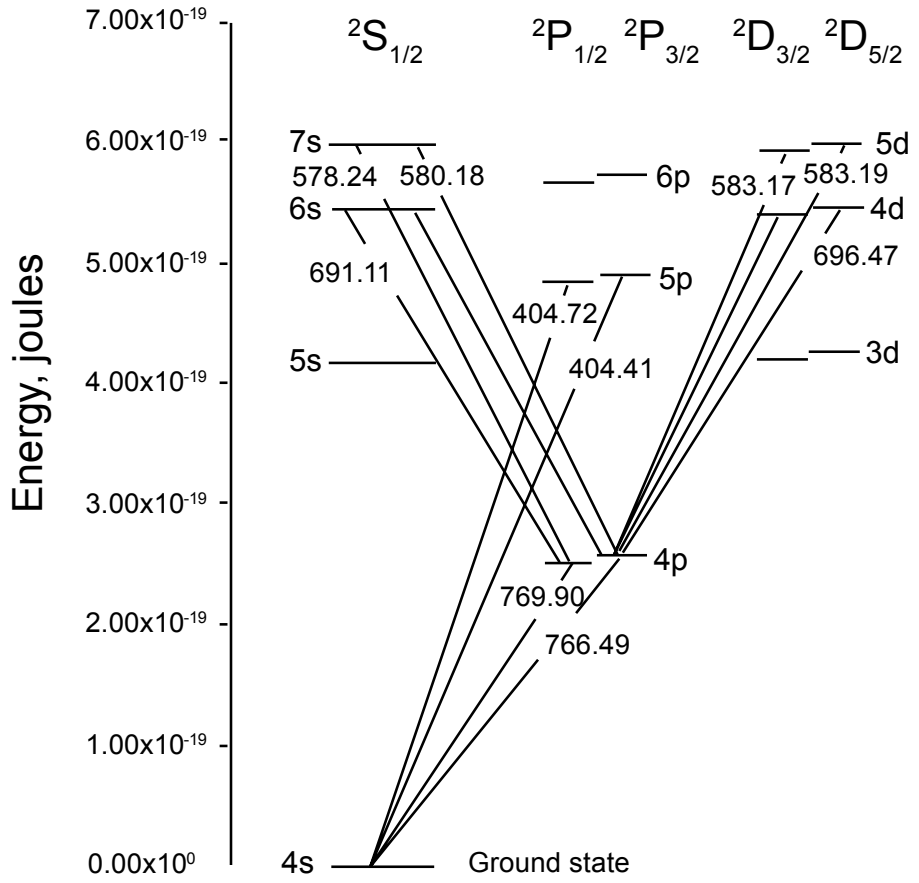

Figure 1. A simplified diagram of electronic states (energy levels) in the potassium atom.

photon having an energy E_p that corresponds to the difference ΔE between two energy states of the outermost electron; in this process the electron temporarily moves from a lower energy state to a higher one.

Figure 1 shows some of the energy states of the potassium atom, together with some of the energy transitions giving rise to the emission lines discussed in this article. Not all lines are labeled, and not all possible lines are shown. Energy states above the lowest one are called *excited states* and atoms in such states are said to be *excited*. The lowest energy state is called the *ground state*. Emission lines that result from transitions from excited states to the ground state are called *resonance lines*. The four resonance lines indicated in Figure 1 are the most intense potassium emission lines in flames.[1a]

Most potassium atoms in a flame will be in the ground state. Consequently, whenever potassium atoms are present in a flame, photons having energies corresponding to potassium resonance lines can be absorbed when they pass through the flame.

In Figure 1, the columns labeled 'S, P, D' indicate families of atomic energy states that differ from each other in the shape of the electronic orbitals. According to quantum selection rules, electrons can participate in transitions where they move between S and P states, and between P and D states, but not between S and D states or between states having the same label (such as between S and S states). By convention, the superscript before the letter is one more than the number of unpaired electrons in an atom in that energy state. A potassium atom has one unpaired electron, so the superscript is 2. It is read as "doublet", for the historical reason that spectral lines associated with atoms having one unpaired electron often occur in pairs that are called "doublets". The subscript after the letter indicates the *total angular momentum* of the energy state, which depends on whether the angular momentum associated with the spin of the unpaired electron adds to, or subtracts from, the angular momentum associated with the motion of the electron around the nucleus of the atom (the elec-

tron's *orbital angular momentum*). The electronic energy states in each family are labeled with lower case letters indicating the shape of the orbital preceded with a number (the *principal quantum number*), which increases with increasing energy. In some cases, there are pairs of electronic energy states (e.g., 4p*1/2*, 4p*3/2*) that have the same principal quantum number and are labeled with the same letter, but have different angular momenta as a result of electron spin. The energy differences between the atomic energy states (e.g., $4_2P_{1/2}$, $4_2P_{3/2}$) are very small in the potassium atom. In Figure 1 these energy differences have been exaggerated for clarity – if shown to scale, the difference would be lost in the thickness of the line. Electronic transitions from these energy states result in the characteristic "doublets" in the potassium spectrum (e.g., 766.491 and 769.897 nm). The energy state diagram, Figure 1, is based on data from the NIST *Handbook of Basic Atomic Spectroscopic Data*.[8]

The measurement of the intensity of resonance lines emitted from laboratory flames has long been used for the determination of potassium concentration in analytical samples by flame emission spectrometry.[9] The success of this analytical method requires that the number of potassium atoms in the path through the flame of the light being measured is so low that a photon emitted by one atom will have a high probability of escaping from the flame rather than being reabsorbed by another atom. Such a flame is described as being *optically thin*.

The gases in a flame can often be considered as being in *local thermodynamic equilibrium*. This means, amongst other things, that the number of potassium atoms in a particular excited state (n) is related to the total number of free potassium atoms (n_t) by the *Boltzmann equation*

$$n = n_t \frac{g}{z} e^{-\Delta E / kT} \qquad (2)$$

where g is the *statistical weight* of the excited state, z is the *partition function* of the potassium atom (2 at the temperatures of interest), e is the base of natural logarithms (2.718…), ΔE is the *excitation energy* (the energy difference in joules between the excited state and the ground state), k is *Boltzmann's constant* (1.38×10^{-23} J atom^{-1} K^{-1}) and T is the absolute temperature (K). If the number of excited atoms is consistent with the Boltzmann equation, the excitation process is described as *thermal* or *collisional* excitation.

In some flames, particularly in relatively cool flames or in the primary reaction zone of normal flames, the number of atoms in a particular high energy state sometimes greatly exceeds that predicted by the Boltzmann equation. In these circumstances the formation of excited atoms is attributed to *chemiluminescence*.[13,14] Several different chemiluminescent processes have been described.[13,14] In all of them a population of excited atoms or molecules arises as a result of energy released in the formation of chemical bonds being transferred directly to electrons in an atom or molecule, causing the most loosely-bound electron in that atom or molecule to move to a higher energy state.

Irrespective of the mechanism that produces the excited species, the intensity of emission (I), expressed as photons per second, is simply

$$I = n / t \qquad (3)$$

where n is the average number of excited atoms and t is the radiative lifetime. (To convert from photons per second to joules per second, one multiplies by the photon energy E_p; see equation 1.)

Table 1. Spectroscopic Parameters of Potassium Resonance Lines and their Relative Intensities.

Wavelength (nm)	Excitation Energy (J)	Statistical Weight of Excited State	Lifetime of Excited State (s)	Normalized Relative Intensity[(a)]
404.41	4.91×10^{-19}	4	1.16×10^{-6}	2.7
404.72	4.91×10^{-19}	2	1.07×10^{-6}	1.5
766.49	2.59×10^{-19}	4	2.67×10^{-8}	100000

[(a)] Intensities were calculated in joules per second per unit atom concentration, assuming thermal excitation at 2275 K, and then normalized to 100,000.

The maximum temperature calculated for the air–propane flame by thermodynamic modeling is 2275 K. The expected thermally excited emissions from potassium atoms at this temperature are shown in Table 1. The intensity of the 766.49 nm line has been arbitrarily set to 100,000 and the intensities of the other lines have been normalized to this value.

As shown in Table 1 the two deep red lines are very intense and the two violet lines are much less so. Both pairs of lines lie in regions of the spectrum to which the human eye is not particularly sensitive, but they have been known for a long time and are shown in some of the very early drawings of flame spectra.[15] Kirchhoff and Bunsen[16] referred to the pair of deep red lines as "Ka α" and the pair of violet lines as "Ka β". (The symbol "Ka" indicated potassium.) The prism spectroscope used by these researchers was evidently unable to resolve each pair of lines into their two components. Kirchhoff and Bunsen[16] reported another very weak red line in the potassium flame. This line coincided with Fraunhofer line B. It was visible from a "highly intense flame" and described as "not very characteristic". It can be identified with an unresolved group of five lines (696.47, 694.42, 693.88, 693.63, and 691.11 nm), arising from transitions between excited states.[8] The coincidence of these red potassium lines with Fraunhofer line B is of no significance; Fraunhofer line B arises from absorption of sunlight by oxygen in the air.[17] Two of the lines from this group of potassium lines are identified in Figure 1. These red lines are of comparable intensity to the other potassium lines at the high temperatures prevailing in the electric arc,[8] but would be very weak in flames.

When Shimizu[18a] described the flame spectrum of potassium he did not mention the deep red resonance lines and described the violet lines as "intense". He wrote "The lines are very strong, but they are in the ultraviolet, at the outer edge of the eye's visibility, and have no color influence". Shimizu's assessment of the intensity of the violet lines is certainly valid, given that he was comparing them to some faint yellow and green potassium lines arising from transitions between excited states that would be very sparsely populated at flame temperatures. Compared to the deep red lines, however, the violet lines are extremely weak. The literature suggests, however, that in some flames the violet lines are not always as weak as would be expected from calculations that assume thermal excitation. For example, referring to the use of these lines in flame photometry, Dean[19a] states that "the sensitivity of the violet doublet is one tenth the sensitivity of the red doublet". This is very different from the ratio of 2.8×10^{-5} calculated in Table 1. The issue is clouded by the fact that the detectors used in flame photometry vary greatly in sensitivity across the wavelength range,[9b] but this variation is not sufficient to account for the difference in the ratios of the calculated and reported intensities of the two doublets. The implication is that the violet doublet can be excited by chemiluminescence in some laboratory flames. An example is given by Alkemade,[19] but the enhancement over thermal excitation was not large. Whatever the excitation mechanism, the intensity of the violet doublet is always very much less than that of the red doublet. If the colour of the potassium flame were attributable solely to a combination of the deep red and violet lines, the flame would be red. Clearly there is another contributor to the colour of the potassium flame that changes the colour from red to lilac.

It has long been known that the distinctive lilac colour of the potassium flame is easily masked by the yellow light from sodium and that this can be overcome by viewing the flame through blue cobalt glass. This glass transmits almost no light between about 500 and 700 nm but transmits quite efficiently at each of the extreme ends of the visible spectrum. The potassium flame, when seen through blue cobalt glass, is not lilac but purplish-red; when seen through green glass it is bluish-green.[20] Green glass transmits blue, green and yellow light but absorbs light at each of the ends of the visible spectrum. Accordingly the lilac colour of the potassium flame must result from a combination of the red light expected from the potassium resonance lines and light that is largely absorbed by blue cobalt glass but largely transmitted by green glass. That light is attributable to a continuum in the flame spectrum of potassium. This continuum has been known for a long time. It was described by Kirchhoff and Bunsen,[16] who wrote "In the flame the volatile potassium compounds give a very long continuous spectrum with only two characteristic lines…", and was subsequently studied by other spectroscopists.[21,22a,10] It was once thought to

originate from the recombination of electrons and potassium ions,[22a] but in 1958 James and Sugden[10] demonstrated that it was the result of the combination of hydroxyl radicals and potassium atoms to form gaseous potassium hydroxide. Shimizu[18a] mentioned this continuum, attributing it to the potassium atom and noting that "it does tend to whiten the flame and interfere with other flame colors".

The pale lilac colour of laboratory flames that are coloured by a vaporized potassium salt can thus be attributed to a combination of the deep red resonance lines from atomic potassium with the potassium hydroxide recombination continuum. The violet potassium resonance lines contribute very little to the colour, being much less intense than the red lines and the continuum. The fact that the continuum is a substantial contributor to the colour accounts for the pale, washed-out appearance of the lilac flame.

The observation of a lilac colour in a pyrotechnic flame containing potassium salts is consistent with observations of laboratory flames into which potassium has been introduced, and provides the explanation of the lilac colour of the outer regions of the flame from the potassium nitrate−shellac composition. The pink colour of the core, however, was not so readily explained.

The discussion so far implies that each spectral line consists of photons having exactly the same energy, corresponding to exactly the difference between two atomic energy levels. In reality, the photons in each line have a range of energies and the emission "lines" might be better described as "peaks". While each line (peak) has its maximum at the photon energy (or wavelength) predicted from the energy of the corresponding atomic transition, it tails away on either side. There are several factors that contribute to this *line broadening*.[12a] In flames, the dominant effect operating at low concentrations of emitting/absorbing atoms is the collision of excited atoms with other atoms and molecules.[12a] At higher atom concentrations emission lines can become extremely broad. When there is a relatively high concentration of emitting/absorbing atoms in the source, a photon emitted by one excited atom is very likely to be absorbed by another ground state atom. The chance of a photon being re-absorbed depends on its energy; a photon having an energy corresponding to the maximum of the emission line will have a much greater chance of being absorbed than a photon having energy that is slightly greater, or slightly less, than the maximum. The resulting excited state atom will then either transfer its extra energy to another atom or molecule in a collision or re-emit a photon. If the re-emission occurs after a collision, it is very likely that the energy of the emitted photon will be slightly different from that of the photon that was absorbed. Accordingly that emitted photon is likely not to correspond to the energy corresponding to the maximum of the emission line (peak). At these higher atom concentrations, this process occurs many times before a photon finally escapes from the flame. The result of these many emissions and re-absorptions before photons eventually manage to escape from the flame is greatly to broaden the energy distribution of those emitted photons. Such a flame is described as *optically thick*. The characteristics of spectral lines from atoms in optically thick sources are well documented in the literature.[11a,12a,23]

The emission of light from an optically thick source can be thought of as intermediate between what happens in optically thin sources and in a *black body*. A black body is an object in which matter (atoms) and electromagnetic radiation (including light) are in thermal equilibrium. The rate of emission of radiation by atoms exactly equals the rate of absorption by other atoms. For such perfect equilibrium, all emitted radiation is reabsorbed and no light leaves the object, which is why the object ("body") is called "black". An ideal black body can be approximated by the inside of a hollow object, so well insulated that there is no exchange of energy between the object and the outside world. The only way the spectrum of such an object can be viewed is to make a tiny hole in it, a hole so small that the effect on the equilibrium between atoms and radiation is not significantly disturbed by the slight loss of radiation through the hole. The spectrum of such an object is continuous, and the relationship between light intensity and wavelength at any given temperature can be calculated theoretically from the fact that radiation and matter are in thermal equilibrium.[11b,12b]

Recall that for an optically thin source a photon emitted by an atom in the source has a high probability of leaving the source without ever

interacting with another atom. In contrast, a photon emitted by an atom in an optically thick source is highly likely to be absorbed by another atom as just described, but photons do eventually escape. Photons having energies corresponding to the theoretical maximum of the emission line are more likely to be absorbed than photons having energies away from the maximum. Eventually, if the concentration of emitting and absorbing atoms becomes sufficiently high, the rate of absorption at the peak's maximum approaches the rate of emission. In other words, the photons having energy corresponding to the line's maximum are close to being in equilibrium with the atoms. For photons of that energy, the source then behaves like a black body. The intensity of the emitted light at the line's maximum approaches the intensity of light of that same wavelength that would be predicted for a black body at the same temperature as the source. Accordingly, at a given temperature, as the concentration of atoms of the emitting element increases, the intensity at the centre of the emission line only increases until it reaches the intensity that would be emitted at that wavelength by a black body at the same temperature. Thereafter, it is only the intensity of light having wavelengths on either side of the maximum that continues to increase with increasing concentration of emitting atoms. The result is that as the concentration of emitting atoms increases, the radiation from the emission line is spread over an increasingly wide region of the spectrum on either side of the line's maximum. This line broadening process is described as *self-absorption*.

Douda[24–28] has shown that the light from sodium nitrate–magnesium flares arises predominantly from sodium resonance lines that have been broadened by self-absorption. Such a substantially broadened line may be referred to as a *resonance line continuum*. Douda also demonstrated that in these flares, the light emitted by sodium atoms in the core of the flame is reabsorbed by sodium atoms in the cooler outer regions of the flame, resulting in a distinct dip in the centre of the broadened emission line where there would otherwise be a maximum. This is called *self-reversal* of the emission line. Of greater relevance to the discussion of lilac flame is the observation by Douda *et al*.[25] of broadened self-reversed potassium resonance lines in the spectra of potassium nitrate–magnesium flares.

The fact that self-absorption and self-reversal of sodium lines can transform the familiar amber-yellow sodium flame into the yellowish-white of the sodium nitrate–magnesium flare, coupled with the observation by Douda and his colleagues[25] of similar processes in potassium nitrate–magnesium flares, led the authors to consider whether the same mechanisms, applying to the deep red potassium lines, could account for the pink core of the potassium nitrate–shellac flame.

Experimental

The spectroscopic measurements were made using three slightly different configurations. However, each used an Ocean Optics CHEM-2000 spectrometer. The first configuration was one in which solutions are aspirated into a propane–air flame. This apparatus is sketched in Figure 2 and was previously described more completely.[29] The other two configurations were used to record spectra from burning pellets of pyrotechnic composition and tiny specially made tubes of lance composition. In these latter two configurations, the flame burner in Figure 2 is replaced with a holder for 6-mm (1/4-inch) diameter test pellets or 6-mm (1/4-inch) diameter lance. In one of these configurations, a fish-eye lens was used to fully integrate the light emitted from the entire area of the flame. In the other configuration the lens was removed and a collimator used to limit light collection to a spot no more than approximately 5 mm in diameter. In this way, and by carefully positioning the flame source and by collecting data for only a fraction of a second, light could be collected from a relatively small portion of the flickering flame.

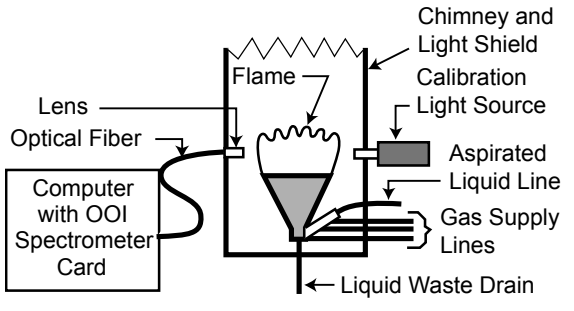

Figure 2. Illustration of the apparatus for taking spectral data from solutions of interest.

The potassium nitrate (KNO_3) used in this study (purchased from Service Chemical, USA) and the shellac (purchased from William Zinser & Co., USA) were each of a grade normally used in the firework industry. The raw flame spectrum of potassium nitrate was obtained using the test configuration shown in Figure 2 with a 0.1 molar solution in distilled water. The spectrum was first corrected by subtracting a background flame spectrum (distilled water only) taken under the same measurement conditions as used for the potassium nitrate test solution. Then the background corrected spectrum was corrected for the wavelength dependent response function of the detector.[29] The final result is the potassium nitrate spectrum shown in Figure 3. For comparison purposes, the flame spectrum of a 0.1M solution of analytical reagent grade potassium nitrate (Mallinckrodt, USA) is presented in Figure 4.

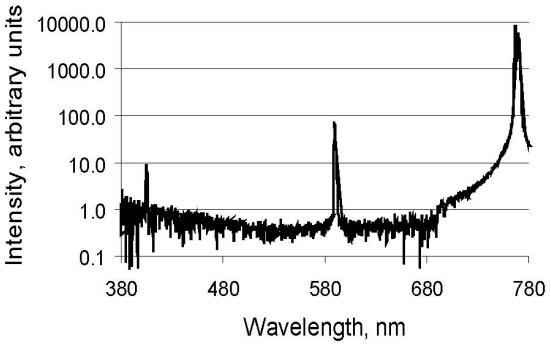

Figure 3. Spectrum of a solution of technical grade potassium nitrate aspirated into an air–propane flame, corrected for instrument background and detector response.

The 80% KNO_3 and 20% shellac lilac test composition was prepared by first thoroughly mixing the two components using a mortar and pestle. Then the composition was divided in two portions; one for use in making bound test pellets and the other for loading into the lance tubes. To make the bound pellets, sufficient denatured ethanol was added to make a pliable mass. This dampened composition was then compacted into a series of 6-mm (0.25-inch) diameter and approximately 20-mm (0.8-inch) long test pellets. The test pellets were first allowed to air dry at approximately 20 ºC (68 ºF) for a day and were

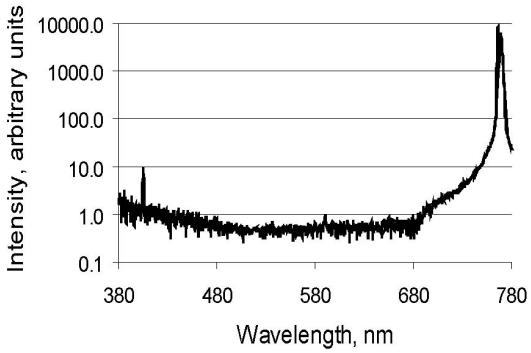

Figure 4. Spectrum of a solution of analytical reagent grade potassium nitrate aspirated into an air–propane flame, corrected for instrument background and detector response.

then raised to approximately 50 ºC (122 ºF) for approximately 1 hour. Figure 5 is a photograph of a burning test pellet, in which the brighter and lighter outer flame envelope is readily apparent.

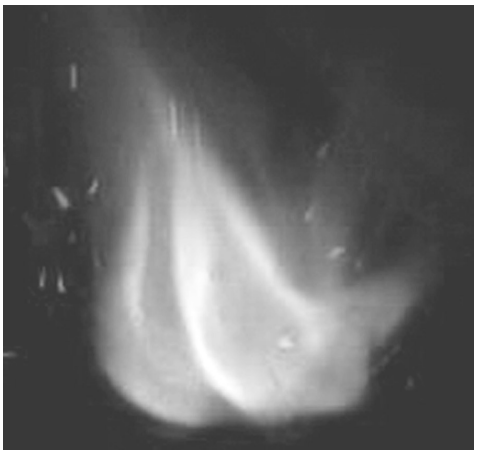

Figure 5. A photograph of a burning pellet of the lilac composition showing the brighter and lighter outer flame envelope

The raw flame spectra of the test pellets were obtained by burning them in a darkened area using the test configuration described above using the fish-eye light collecting lens, which integrated the light from the entire flame. The raw spectra were corrected for instrument background (dark current) and then corrected for the instrument response function.[29] The final result is the spectrum shown in Figure 6.

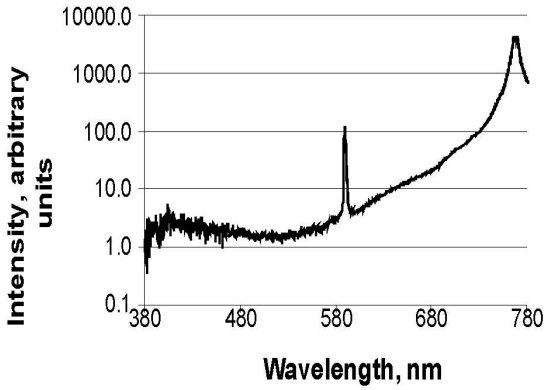

Figure 6. Spectrum of the flame of a burning pellet of 80% potassium nitrate and 20% shellac mixture, corrected for instrument background and detector response.

Using the un-dampened portion of the lilac flame composition, a series of lances was prepared. The lance tubes were specially made using just two wraps of thin tissue paper. This was done so as to limit the interfering effect of the burning lance tube. The lance tubes were 6 mm (1/4 inch) in diameter and approximately 25 mm (1 inch) long. The composition was carefully loaded using the traditional rod and funnel method. The spectra of the lances were recorded using the instrument configuration described above using the collimator. By properly positioning the burning lance in front of the collimator, it was possible to collect spectra somewhat selectively concentrating on the emissions from either the inner or outer portions of the flame envelope. Lances were used for these measurements because they produced a more steady flame, which facilitated the collection of spectra from the two regions of interest within the flame. Nonetheless, the movement of the flame was still sufficient to require that the data collection intervals be kept to only 0.1 second to aid in limiting the light acquired from other portions of the flame. (The burning pellets of composition flickered greatly, which facilitated the taking of a photograph more clearly showing the difference between the inner and outer flame envelope, see Figure 5.)

The spectra collected from the inner and outer parts of the flame, corrected as described above, were smoothed with a 9-point moving average to remove some of the "noise" resulting from the low light intensity in this mode of measurement. Finally the intensity data points in each spectrum were normalized to the maximum value in that spectrum. The use of normalized intensities allows the different line widths in the spectra to be seen more clearly. Furthermore, the colour of the flame depends on the relative intensity of the various spectral features, not their absolute intensity. Results are presented in Figure 7. The data used to generate the spectrum of technical grade KNO_3 in the air–propane flame shown in Figure 3 were re-processed in the same way and the resulting spectrum is included in Figure 7 for comparison.

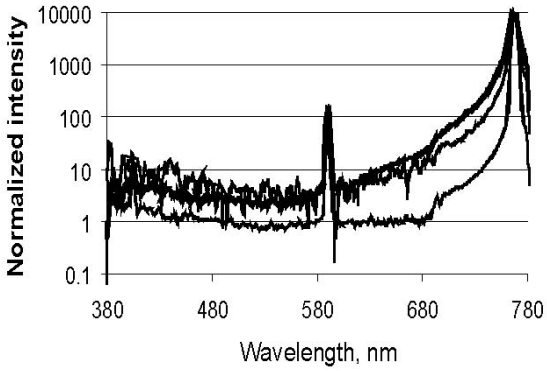

Figure 7. Spectra of the inner and outer parts of the flame of a burning lance made with 80% KNO_3 and 20% shellac. Bold trace: Inner part of the flame. Upper non-bold trace: Outer part of the flame. Lower non-bold trace: technical grade KNO_3 solution aspirated into the air–propane flame.

Additional spectra were derived from each of the test technical grade potassium nitrate and test composition spectra produced as described above. The purpose was an attempt to quantify the effect of the sodium impurities present in the raw chemical ingredients. This was accomplished by simply stripping out the sodium peaks from the two corrected test spectra. Finally, all spectra were converted to their CIE colour values using a program provided by Will Meyerriecks.[30] These results are presented and discussed below.

Results and Discussion

1. Flame Spectra

The visible spectrum of the technical grade KNO_3 solution aspirated into the air–propane flame is presented as Figure 3. Note that the intensity scale is logarithmic. The most prominent feature is the partially resolved pair of deep red potassium resonance lines. The yellow line (actually an unresolved pair of lines at 589.0 nm and 589.6 nm) from sodium impurities is also obvious. The (unresolved) pair of violet potassium resonance lines can be discerned, but, as expected, its intensity is very low. The continuous spectrum is evident by the offset of the spectrum from the 0.1 unit intensity line in Figure 3. Figure 4 presents the corresponding spectrum of analytical reagent grade KNO_3 solution aspirated into the air–propane flame. The obvious difference between this spectrum and that of the technical grade material is the very much lower intensity of the yellow sodium line.

Figure 6 presents the visible spectrum of the flame from the burning of a bound pellet of the 80% KNO_3–20% shellac mixture. The spatial resolution of the apparatus used as configured and the dynamic flickering of the flame did not allow the separation of the spectrum of the reddish-pink core from that of the lilac outer regions of the flame. The pair of deep red potassium resonance lines is again the dominant feature of the spectrum The extent to which these lines have broadened and extend well into the shorter wavelengths of the red region of the spectrum to which the eye is more sensitive, can be seen by comparing Figure 6 with Figures 3 and 4. This broadening is attributed to self-absorption caused by a high concentration of potassium atoms in the flame. The sodium line is evident, as expected. The unresolved pair of weak violet potassium lines cannot be discerned above the background noise. It is clear from Figure 6 that the continuum is greatly increased in intensity compared to that in Figure 3. This is attributable to two sources: (a) potassium–hydroxyl recombination, as expected for a flame containing potassium, hydrogen and oxygen, and (b) possibly from particles of solid or liquid suspended in the flame. There was no attempt to calculate the contribution of the latter, but there would presumably be a considerable effect from the rather high concentration of molten potassium carbonate in the flame. The spectrum of a black body at ~1500 K would peak in the infrared, with sufficient "tailing" into the visible to make the body appear yellowish-orange. Flame particles are likely to be very small, with the result that the "black body" spectrum would be shifted to shorter wavelengths, making the emitted light whiter.[31]

Figure 7 presents spectra attempting to concentrate on the inner and outer parts of the lance flame, collected using the collimated light collection configuration. Because of the limited special resolution and the motion of the flame, it is likely that spectra of the edge of the flame included at least part of that from the inner flame. Further, the inner part of the flame had to be viewed through the outer part. Thus it must be expected that both the spectra are, to a significant extent, mixtures of the emissions from both the inner and outer regions of the flame. Nonetheless, there are distinct differences in the spectra from the inner and outer parts of the flame. (As expected, most of the spectra collected were of intermediate character to the two presented in Figure 7.)

The spectrum of the inner part of the flame is similar to that of the burning pellet (Figure 6). The most notable difference is that the unresolved violet resonance line pair is clearly visible, but is still of low intensity. The spectrum of the outer part of the flame is different in several ways: the pair of red potassium lines is less broad, the continuum in the shorter wavelength region is relatively more intense and the pair of violet lines is not discernible above the background noise. The spectrum of potassium nitrate in the air–propane flame is different from either of the lance flame spectra, with the pair of red lines being less broad, the continuum much less intense and the unresolved violet lines distinctly more intense. The wavelength resolution of the spectrometer used in this work was not sufficient to show whether or not self-reversal of the potassium resonance lines was present.

Table 2. CIE *x* and *y* Coordinates Calculated from the Spectra and their Corresponding Colours.

Spectrum or Spectral Feature	CIE *x*	CIE *y*	Colour
Analytical reagent KNO_3 in air–propane flame	0.323	0.276	Pale reddish-purple
Technical KNO_3 in air–propane flame	0.479	0.371	Pink
Technical KNO_3 in air–propane flame, Na resonance lines removed	0.335	0.287	Pale reddish-purple
Burning pellet of 80% KNO_3, 20% shellac	0.507	0.348	Pink
Burning pellet of 80% KNO_3, 20% shellac, Na resonance lines removed	0.484	0.319	Pink
Inner core of lilac lance flame	0.493	0.354	Orange-pink
Inner core of lilac lance flame, Na resonance lines removed	0.434	0.298	Pink
Outer envelope of lilac lance flame	0.399	0.305	Pink
Outer envelope of lilac lance flame, Na resonance lines removed	0.327	0.253	Pale reddish-purple
Potassium resonance lines from air–propane flame (calculated relative intensities, assuming thermal excitation at 2200 K)	0.722	0.259	Red
Sodium resonance lines	0.569	0.430	Yellowish-orange
Black body at ~1520 K[12b]	0.583	0.394	Orange

2. CIE Chromaticity Diagram

Table 2 shows the CIE *x* and *y* coordinates (using the 1931 2º Chromaticity Diagram) of some relevant spectra and spectral features. Some of these colour coordinates are plotted on a CIE chromaticity diagram in Figure 8. The colours indicated on the diagram for the KNO_3 in the propane gas flame and for the lilac flame composition are consistent with observations, bearing in mind that the CIE descriptions cover quite a broad range of perceived hues. The CIE results and visual observations both find the inner part of the flame to be "redder" than the outer part. The results for the colours expected when the sodium lines were removed from the experimental spectra indicate that there would be a definite improvement in the colour of the lilac flame if there were less sodium present.

3. Thermodynamic Modeling

It seemed obvious that the colour of the flame from the potassium nitrate–shellac composition was attributable to potassium, but no data for the composition and temperature of the flame were available to support this. Thermodynamic modeling was used to obtain an indication of the potassium concentration in the flame and the flame temperature. It was assumed that at the core of the flame the temperature and composition were close to those expected at thermodynamic equilibrium. Moving away from the core, the effects of entrained air would presumably be increasingly significant.

Thermodynamic modeling was done using the NASA-CEA program.[32,33] The combustion was modeled at a pressure of 1 bar. The required inputs were the quantities of the reactants (relative weight), their chemical composition and their enthalpies of formation. The enthalpy of formation and chemical composition of potassium nitrate are included in the database that forms part of the NASA-CEA program. The data for shellac were taken from Meyerriecks.[34] The empirical formula was $C_6H_{9.5}O_{1.6}$ and the enthalpy of formation was −440 kilojoules per gram formula weight. As noted by Meyerriecks[34] this enthalpy value is subject to considerable uncertainty; the results of the modeling must therefore be regarded as semi-quantitative. Furthermore, no ac-

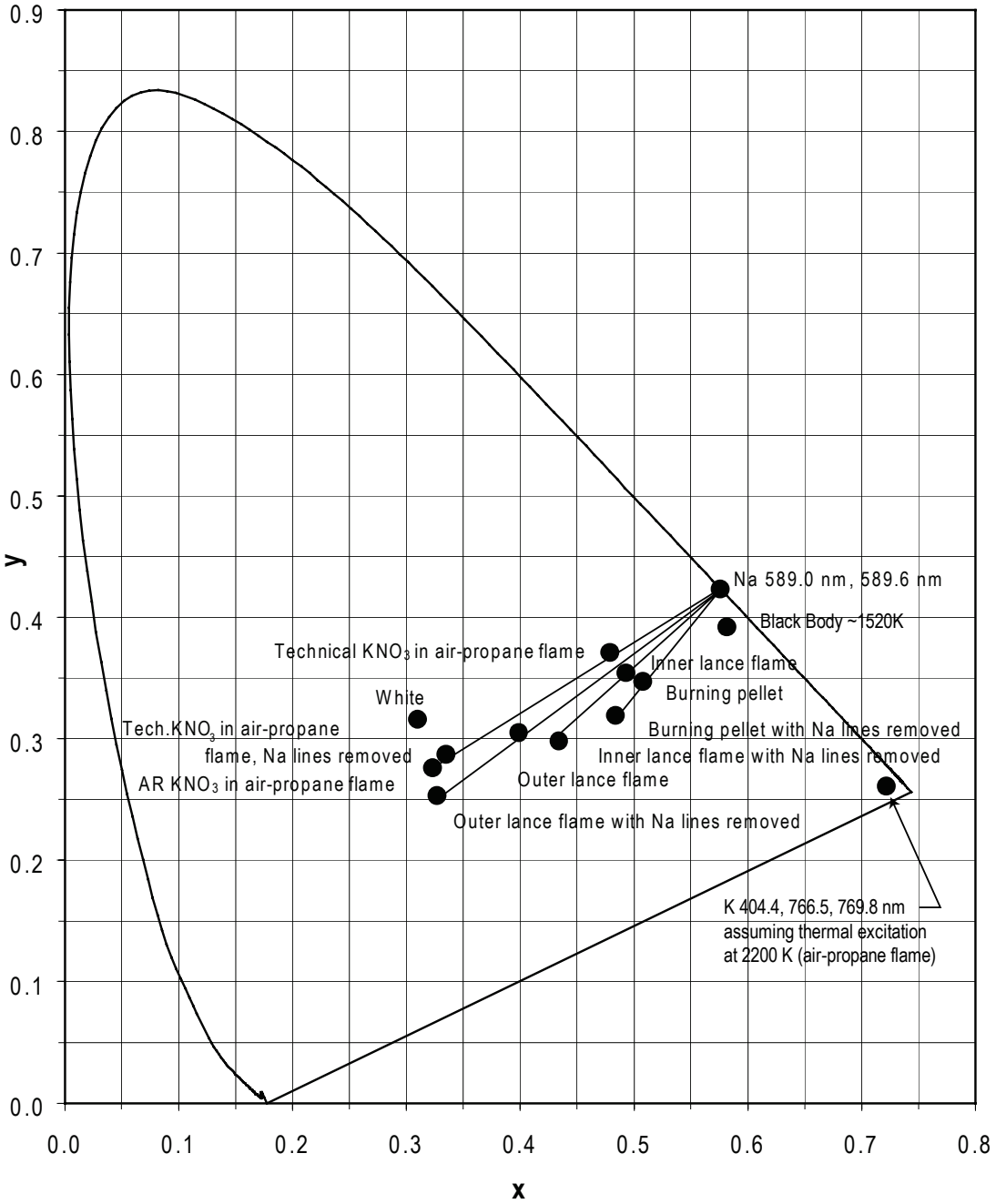

Figure 8. CIE chromaticity diagram showing the positions of the various flame colours, plotted from the coordinates in Table 2.

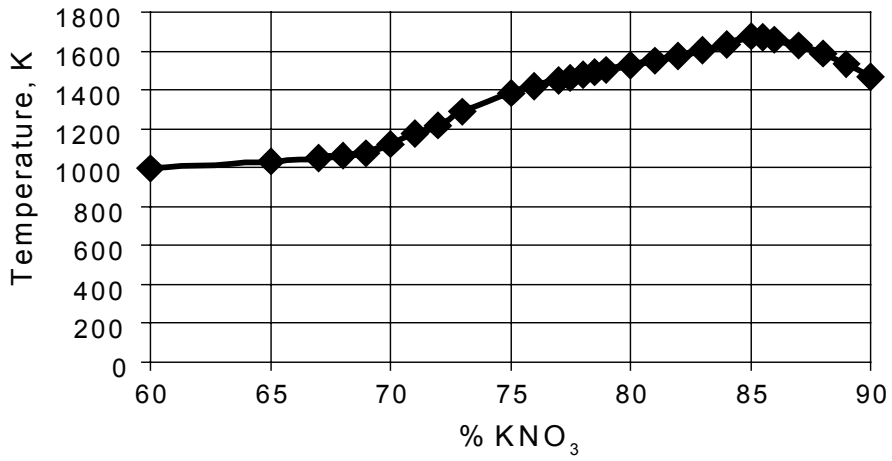

Figure 9. Equilibrium flame temperatures for the combustion of binary mixtures of potassium nitrate and shellac.

count of energy loss from the flame by radiation was considered. Despite these limitations it was thought that thermodynamic modeling would provide a useful basis for an explanation of the spectrum of the flame from the burning composition.

The output of the program included the equilibrium temperature and the mole fractions of the combustion products. The number of significant figures in the values reported in this paper does not indicate the uncertainty in the values, as no attempt was made to estimate the uncertainties. The aim was only to produce a plausible, consistent account of the flame colour. This certainly required an indication of the flame temperature and composition, but a fully detailed quantitative analysis was not necessary and probably not possible. The program took ionization effects into account but these turned out to be insignificant.

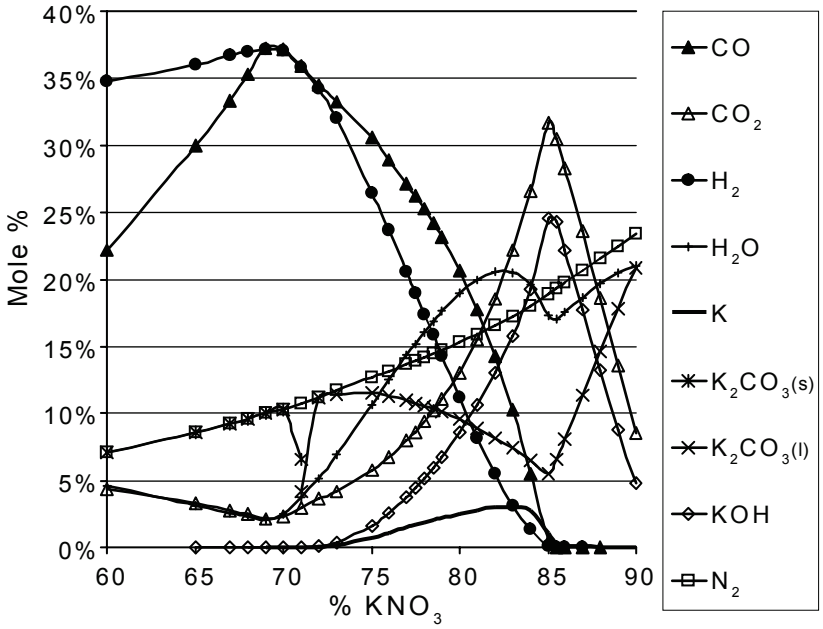

Figure 10. Equilibrium flame compositions for binary mixtures of potassium nitrate and shellac. Trace components (<1%) have been deleted for clarity

No species are included in the output unless they are present at mole fractions greater than 5×10^{-6},[29] and no ions were reported in the output of the program.

A plot of equilibrium adiabatic temperature predicted for the combustion of a series binary mixtures of potassium nitrate and shellac is shown in Figure 9. For the 80% KNO_3 and 20% shellac mixture, the predicted flame temperature is 1526 K and the maximum temperature is predicted to be reached by a mixture of 85% KNO_3 and 15% shellac. The equilibrium composition of the flame gases from these binary mixtures, each at their predicted flame temperature, is shown in Figure 10. The 80% KNO_3 and 20% shellac mixture is close to that producing the greatest concentration of atomic potassium in the flame. As indicated in Figure 10, the maximum atomic potassium concentration occurs at about 83% KNO_3.

Figure 11 shows the major components of the flame gases for the 80% KNO_3 and 20% shellac mixture. Of these, carbon monoxide (CO), hydrogen (H_2) and potassium (K) are expected to burn in the air, forming a diffusion flame around the flame core. Modeling such a flame is difficult because there are two competing factors operating: (a) the reaction of combustible gases with air, which tends to heat the flame, and (b) the cooling of the flame gases by the loss of heat into the surrounding cold air.

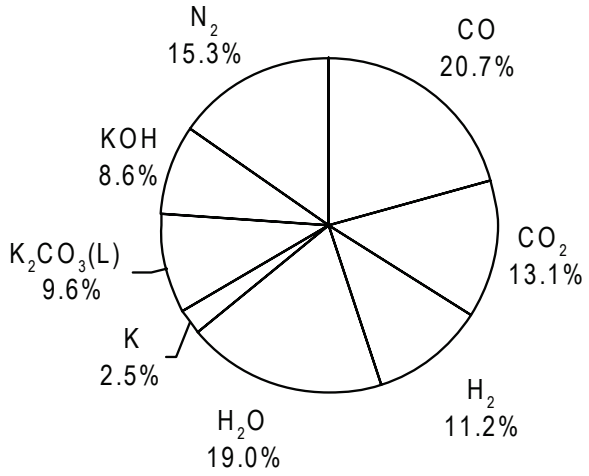

Figure 11. Equilibrium composition of the flame of 80% KNO_3 and 20% shellac mixture (1526 K).

The maximum possible temperature of the diffusion flame was calculated by modeling the combustion of the 80% KNO_3 and 20% shellac mixture in varying amounts of air. The maximum temperature (1723 K) occurred with a mixture of 50.66% KNO_3, 12.66% shellac and 36.68% air by mass and produced the products shown in Figure 12. As shown in Figure 12 there is still a significant concentration of atomic potassium in the diffusion flame, but the number of potassium atoms per unit volume (2.2×1016 atoms cm^{-3}) is only approximately 18% of that calculated to be present in the flame core (1.2×1017 atoms cm^{-3}). Concentrations of the various species in atoms or molecules per cubic centimetre were calculated from the mole fractions and the molar volume at the flame temperature and a pressure of 1 bar, as found from the ideal gas law. The calculated concentrations of potassium atoms in the diffusion flame and in the flame core were of a similar magnitude to the concentration calculated by Douda and Bair[26] for sodium atoms in the flame of a sodium nitrate–magnesium ($NaNO_3$–Mg) flare (4×10^{17} atoms cm^{-3}).

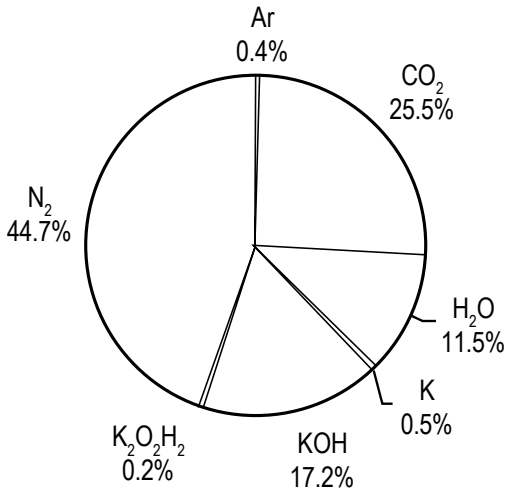

Figure 12. Equilibrium composition of the flame of 80% KNO_3 and 20% shellac mixture with sufficient entrained air to reach the maximum adiabatic flame temperature (1723 K).

Despite the substantial decrease in the concentration of potassium atoms in the diffusion flame, the intensity of the deep red resonance lines is expected to be similar to (approximately 0.75 times) that from the core. This is because

the diffusion flame is hotter, with the result that the fraction of potassium atoms excited to emit these lines is approximately 4.1 times greater in the diffusion flame than in the core. However, the lower concentration of ground state potassium atoms in the diffusion flame compared to the core would result in the deep red lines being less subject to broadening by self-absorption. Thus there would be less emission in the shorter wavelengths of the red region of the spectrum, making the diffusion flame appear less red than the core. The same considerations indicate that the violet potassium resonance lines would be approximately 2.7 times more intense in the diffusion flame than in the core, because the fraction of potassium atoms excited to emit these lines is approximately 14 times greater in the hotter diffusion flame.

It was not possible to test all of these predictions with the results of Figure 7, because the sampled volume of the flame was almost certainly not the same for each spectrum. Absolute intensity comparisons are meaningful only if the sampled volume is constant. The possibility of normalizing the intensities to that of the sodium line was rejected because this normalization would be valid only if the temperatures were the same in each part of the flame. Figure 7 does show, however, that the red lines are relatively less broadened, and the short-wavelength continuum relatively more intense, in the outer part of the flame than in the inner part, the standard of comparison being the maximum intensity of the red potassium line in each spectrum.

The calculated concentration of potassium hydroxide (KOH) in the diffusion flame (7.2×10^{17} molecules cm^{-3}) is greater than that in the flame core (4.1×10^{17} molecules cm^{-3}). Accordingly, assuming that the chemiluminescent potassium hydroxide emission is proportional to the equilibrium potassium hydroxide concentration, one can predict that the ratio of red potassium emission to the bluish-violet KOH continuum would be less in the diffusion flame than in the core. This would make the diffusion flame appear bluer than the core. Another source of blue light in the diffusion flame could be the blue emission associated with the combustion of carbon monoxide.[22b] (This is the principal source of the familiar blue colour of the outer mantle of flames in which fuels containing carbon are burnt in air or oxygen).

Conclusions

The pink colour of the core of the flame from the 80% KNO_3–20% shellac mixture is attributable to broadening of the deep red potassium resonance lines by self-absorption, which extends the emission into the region of the spectrum to which the eye is more sensitive. The potassium emission is superimposed on a continuum produced by a combination of thermal emission from droplets of molten potassium carbonate suspended in the flame and chemiluminescent emission from potassium–hydroxyl recombination. The lilac colour of the outer regions of the flame presumably arises from the same combination of emission lines from potassium atoms and the potassium–hydroxyl recombination continuum, with very much less thermal emission from liquid droplets. The visible intensity of the red potassium emissions is reduced because of less self-absorption broadening of the 766.491 and 769.897 nm resonance lines, and the intensity of the violet chemiluminescent emissions is increased. The result is the lilac colour of the outer (diffusion) flame envelope.

References

1) R. Mavrodineanu and H. Boiteux, *Flame Spectroscopy*, Wiley, New York, 1965; [a] pp 368–371; [b] pp 507–508.

2) H. A. Webster III, "Emission From Molecular Species in Pyrotechnic Flames", *Proceedings of the 5th International Pyrotechnics Seminar*, 1976, pp 551–565.

3) C. Jennings-White, "Nitrate Colors", *Pyrotechnica*, Vol. XV, 1993, pp 23–28.

4) R. M. Winokur, "Purple Fire", *Pyrotechnica*, Vol. VI, 1980, pp 21–31.

5) V. Pacini, *Il dilettante di pirotechnicia, ovvero regole da tenersi per lavorare i fuochi d'artificio e colorati (The Amateur Pyrotechnist, Or Rules To Be Observed When Working with Fireworks and Colours),* Campolmi, Florence, 1845 (cited by Winokur, *loc. cit.*).

6) C. Jennings-White, personal communication, 2004.

7) R. F. Barrow and E. F. Caldin, "Some Spectroscopic Observations on Pyrotechnic Flames", *Proceedings of the Physical Society (London)*, 62B, 1949, pp 32–39.

8) J. E. Sansonetti, W.C. Martin and S.L. Young, *Handbook of Basic Atomic Spectroscopic Data (version 1.1)* [Online]. Available: http://physics.nist.gov/Handbook. National Institute of Standards and Technology, Gaithersburg, Maryland, 2004.

9) J. A. Dean, *Flame Photometry*, McGraw-Hill, New York, 1960; [a] pp 167–173; [b] pp 82–83.

10) C. J. James and T. M. Sugden, "Photometric investigations of alkali metals in hydrogen flame gases, III: The source of the alkali metal continuum", *Proceedings of the Royal Society of London*, Vol. A248, 1958, pp 238–247.

11) A. Thorne, U. Litzen and S. Johansson, *Spectrophysics*, Springer-Verlag, Berlin, 1999; [a] pp 214–217, [b] pp 164–166.

12) J. D. Ingle, Jr., and S. R. Crouch, *Spectrochemical Analysis*, Prentice Hall, Upper Saddle River, New Jersey, 1988; [a] pp 209–219; [b] pp 88–89.

13) T. M. Sugden, "Excited species in flames", *Annual Reviews of Physical Chemistry*, Vol. 13, 1962, pp 369–390.

14) C. Th. J. Alkemade, Tj. Hollander, W. Snelleman and P. J. Th. Zeegers, *Metal Vapours in Flames*, Pergamon Press, Oxford, 1982, pp 634–652.

15) H. E. Roscoe, *On Spectrum Analysis*, Macmillan, London, 1869, frontispiece.

16) G. Kirchhoff and R. Bunsen, "Chemical Analysis by Observation of Spectra", *Annalen der Physik und der Chemie* (Poggendorff), Vol. 110, 1860, pp 161–189. English translation available at http://dbhs.wvusd.k12.ca.us/webdocs/Chem-History/Kirchhoff-Bunsen-1860.html

17) *Fact Sheet 5: Absorption Lines in The Solar Spectrum*, Faculty of Pure and Applied Science, York University, available at http://resources.yesican.yorku.ca/trek/scisat/final/grade9/fact_sheet5.html

18) T. Shimizu, *Fireworks from a Physical Standpoint*, transl. A. Schuman, Vol. II, Pyrotechnica Publications, Austin, TX, 1983; [a] p 75; [b] p 114.

19) C. Th. J. Alkemade, in J. A. Dean and T. C. Rains, Eds., *Flame Emission and Atomic Absorption Spectrometry*, Vol. 1, Marcel Dekker, New York, 1969, p 146.

20) R. C. Weast, ed., *CRC Handbook of Chemistry and Physics*, 63rd ed., CRC Press, Boca Raton, Florida, 1982–1983, p D138.

21) T. N. Panay, "Sur le spectrum continu de potassium dans la flame" ("On the continuous spectrum of potassium in the flame"), *Comptes Rendus de l'Academie des Sciences*, Vol. 204, 1937, pp 251–253.

22) A. G. Gaydon, *The Spectroscopy of Flames*, Chapman & Hall Ltd, London, 1957; [a] p 224; [b] pp 95–101.

23) N. Omenetto, J. D. Winefordner and C. Th. J. Alkemade, "An expression for the atomic fluorescence and thermal-emission intensity under conditions of near saturation and arbitrary self-absorption", *Spectrochimica Acta*, Vol. 30B, 1975, pp 335–341.

24) B. E. Douda, "Formation of the Sodium Resonance Line Continuum", *RDTN No. 95*, Naval Ammunition Depot, Crane, IN, 1970.

25) B. E. Douda, R. M. Blunt and E. J. Bair, "Visible Radiation from Illuminating-Flare Flames: Strong Emission Features", *Journal of the Optical Society of America*, Vol. 60, 1970, pp 1116–1119.

26) B. E. Douda and E. J. Bair, "Visible Radiation from Illuminating-Flare Flames: II. Formation of the Sodium Resonance Continuum", *Journal of the Optical Society of America*, Vol. 60, 1970, pp 1257–1261.

27) B. E. Douda and E. J. Bair, "Radiative Transfer Model of a Pyrotechnic Flame", *Journal of Quantitative Spectroscopy and Radiative Transfer*, Vol. 14, 1974, pp 1091–1105.

28) B. E. Douda and R. J. Exton, "Optically Thick Line Widths in Pyrotechnic Flares",

Journal of Quantitative Spectroscopy and Radiative Transfer, Vol. 15, 1975, pp 615–617.

29) W. Meyerriecks and K. L. Kosanke, "Color Values and Spectra of the Principal Emitters in Colored Flames", *Journal of Pyrotechnics*, No. 18, 2003, pp 1– 22; *Selected Pyrotechnic Publications of K. L. and B. J. Kosanke, Part 7 (2003 and 2004),* 2006.

30) W. Meyerriecks, personal communication, 2003.

31) A. G. Gaydon and H. G Wolfhard, *Flames: Their Structure, Radiation and Temperature*, 2nd ed., Chapman & Hall, London, 1960, p 231.

32) S. Gordon and B. J. McBride, *Computer Program for Calculation of Complex Chemical Equilibrium Composition and Applications I. Analysis*, NASA Reference Publication 1311, National Aeronautics and Space Administration, Lewis Research Center, Cleveland, Ohio, 1994.

33) B. J. McBride and S. Gordon, *Computer Program for Calculation of Complex Chemical Equilibrium Composition and Applications II. Users Manual and Program Description*, NASA Reference Publication 1311, National Aeronautics and Space Administration, Lewis Research Center, Cleveland, Ohio, 1996.

34) W. Meyerriecks, "Organic fuels: Composition and Formation Enthalpy Part II – Resins, Charcoal, Pitch, Gilsonite and Waxes", *Journal of Pyrotechnics*, No. 9, 1999, pp 1–19.

An earlier version appeared in: *Fireworks Business*, No. 268, 2006.

Spark Travel Distance

K. L. and B. J. Kosanke

It is generally recognized that spark particle size is one of the factors controlling how far sparks will be propelled from various firework items. However, there is relatively little quantitative information in the pyrotechnic literature documenting the distance sparks travel as a function of their initial size. This article reports on a brief study of maximum titanium spark particle travel distance as a function of the mesh size of sponge titanium included in two sizes of relatively small flash powder salutes.

The flash powder used in the test salutes was made using the formulation described in Table 1. The amount (weight) of titanium was adjusted for each mesh fraction to limit the total number of spark particles produced by each test device. This was done to facilitate the tracking of a reasonable number of individual spark particles in each test. The test salutes contained 3.5 grams of flash powder in the smaller salutes and 35 grams in the larger salutes. Both sizes of test salutes were made using appropriately sized small polyethylene bottles. This confinement method was chosen to better assure reproducibility compared with salutes made using paper, glue and string. The test salutes were fired using an electric match placed at the approximate center of the flash powder charge. The blast pressure characteristics of the two salute sizes are given in Table 2. The air blasts were measured at a distance of 10 feet, with both the salutes and free field blast gauges placed at a height of 4 feet above the ground.

Table 1. Flash Powder Formulation Used in the Test Salutes.

Ingredient	Percentage
Potassium perchlorate	60
Magnalium (50:50) 325 mesh	30
Sulfur (flour)	10
Titanium (sponge)	+ Various

Table 2. Test Salute Output Characteristics.

Size	Flash Mass (g)	Peak Pres. (psi)	Pos. Phase (ms)	Impulse (psi ms)
Small	3.5	0.42	0.6	0.25
Large	35	1.4	1.1	1.54

Small calibration lights were positioned on either side of the test salutes to calibrate the measurement of the maximum travel distance of the sparks produced. A normal frame-rate video camera was used to record the progress of the sparks every 1/60 second while using a shutter speed of 1/250 second. Figure 1 is a sample of three of the six tests conducted using the small test salutes. The images are reproduced as negatives to more clearly see the spark trails. These composite images were produced by superimposing every other of the individual video fields during the course of the event, thus documenting both the location and velocity of the sparks throughout their range. In this brief study, only one test salute of each size and titanium mesh fraction was fired. The full set of test results (each Ti particle mesh range and both salute sizes) are presented in Table 3 and are shown as a graph in Figure 2.

As expected, for both salute sizes, the titanium particles were propelled increasingly far as their particle size was increased. The maximum spark travel distance for the smallest titanium particles (40–50 mesh) is not highly dependent on salute size. In this case, the larger salute only propelled the spark particles about 25% further than the small salute. This suggests that small spark particles are relatively easily accelerated, and that their travel distance depends largely on their aerodynamic characteristics and their burn time. To some extent this is confirmed in Figure 2, where the spark particles can be seen to burn-out before slowing appreciably and before they

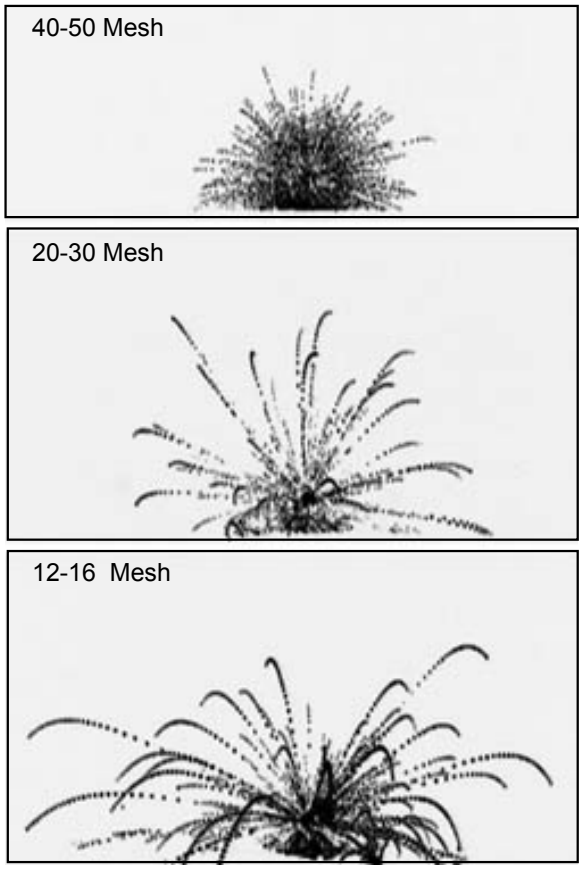

Figure 1. Spark travel distance results for three of the mesh fractions used in the small test salutes. (These are negative images with a field of view that is approximately 85 feet wide.)

begin to curve downward under the force of gravity. To the contrary, the maximum spark travel distance for the largest titanium particles (8–12 mesh) is more strongly dependent on salute size, with the larger salute propelling the spark particles about 60% further than the small salute. In this case, the greater pressure impulse (blast pressure times time) provided by the larger salutes was useful in accelerating the spark particles to higher velocity and they have a sufficiently long burn time to persist until they have slowed substantially.

Table 3. Titanium Spark Spread Test Results.

Test No.	Ti Mesh Fraction	Ti Mass Used[(a)]	Maximum Spark Travel[(b)] (feet)	
			Small Salute	Large Salute
1	8–12	10	50	80
2	12–16	8	40	70
3	16–20	6	35	65
4	20–30	5	25	50
5	30–40	4	25	40
6	40–50	3	20	25

a) This is the additional mass of sponge titanium added to 40 grams of the base flash powder formulation.

b) Spark travel distance is the approximate maximum radial distance traveled by the sparks, rounded to the nearest 5 feet.

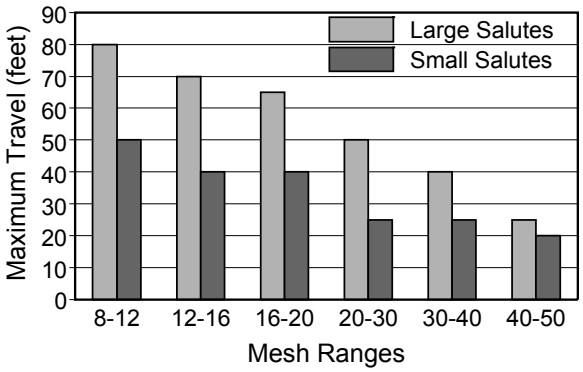

Figure 2. Bar chart displaying the titanium particle spark range data.

While it cannot be said that this brief series of tests has provided any surprises, it does help to document and quantify what was already widely known by practicing pyrotechnists through experience.

Acknowledgement

The authors are grateful to L. Weinman for commenting on an earlier version of this article.

An earlier version appeared in: *Fireworks Business*, No. 269, 2006.

Further Testing of NFPA Safety Shelters

K. L. and B. J. Kosanke

Introduction

Before describing this work it should be mentioned that the purpose was not to find fault with the requirement of the National Fire Protection Association (NFPA) in its *Code for the Display of Fireworks* for a safety shelter on manned electrically fired displays on barges.[1] Rather, it is to determine the level of protection actually provided by a shelter meeting the minimum NFPA requirement as it is most often applied, to share that information with the industry, and to offer suggestions to those that might wish a higher level of protection.

Probably the most extreme test of NFPA's required barge safety shelter construction is the direct impact of an aerial shell fired from the minimum distance allowed.[1] To begin this investigation, last fall some initial testing was conducted and the results were reported.[2] In summary, when a typical 3-inch shell was fired directly at the plywood (i.e., perpendicular to its front surface) from a distance of 8 feet, the 3-inch shell was found to be capable of penetrating ¾-inch AC exterior plywood backed with 2×4 dimensional lumber on 2-foot centers. Following this somewhat surprising result, thought was given to relatively easy and inexpensive ways that the shelter's resistance to shell penetration might be improved. During further trials, it was eventually found that relatively simple and inexpensive modifications could be made that provided substantially improved penetration resistance, ranging to at least 6-inch shells. Descriptions of many of the trials and their results are presented below.

Further Penetration Trials

A summary of the preliminary test results is presented in Table 1 and is discussed below. However, it must be acknowledged that often only a single test was conducted of each configuration. Thus the results cannot be taken as representing what would happen every time had repeat firings and a variety of other aerial shells been used.

An early attempt to improve penetration resistance was simply to use two thicknesses of ¾-inch plywood in contact with each other, without gluing or securing the two pieces of plywood together as a unit. This arrangement successfully protected from a direct impact of a 3-inch shell,

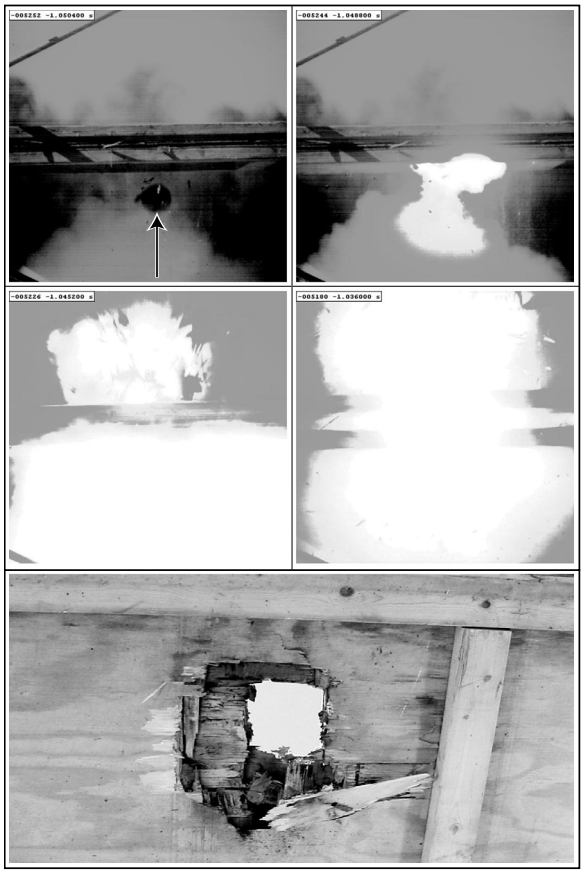

Figure 1. A series of four image (spanning approximately 0.015 second) of the impact of a 4-inch shell into two sheets of 3/4-inch plywood, plus a still photograph (bottom) of the hole through the plywood sheets.

but a 4-inch shell was able to penetrate the double-thickness of plywood. Figure 1 is a series of high frame-rate video images (spanning approximately 0.15 second) recorded during a test of a 4-inch shell impacting a double thickness of ¾-inch plywood that had been reinforced with 2×4 dimensional lumber. In the upper-left image the shell, which had been fired vertically, can be seen emerging ahead of the smoke of the shell firing and a few inches below the horizontally placed sheets of plywood. In the upper-right image the shell has struck the plywood and the contents of the shell have started to ignite. In the middle-left image both sheets of plywood have been penetrated and fire is starting to appear above the second sheet. In the middle-right image substantial fire is seen to have been produced above the pair of plywood sheets. (Because of the great changes in light intensity between the various images, the quality of the images has suffered significantly.) The lower image is a still photograph taken after the trial looking upward at the hole through the two sheets of ¾-inch plywood.

In subsequent testing, it was found that if an aerial shell impacted a single sheet of plywood at an approximate 45º angle, a similar level of protection was achieved as when using two sheets of ¾-inch plywood with an impact angle of 90°. Specifically, it was found that a single sheet of ¾-inch plywood at a 45º angle to the trajectory of the impacting aerial shell survived the impact of a 3-inch shell; however, a 4-inch shell could still penetrate that single-thickness of plywood at a 45° angle. Two possible shelter configurations that present a front wall at an ap-

Table 1. Summary of the Preliminary Penetration Testing of ¾-inch Plywood.

Firing Distance (ft)	Firing Angle (º)	Other Conditions	Shell Size (in.)	Results
8	90	Single-thickness ¾-inch plywood	3	Full penetration
8	90	Double-thickness ¾-inch plywood (loose contact, no gap between)[a]	3	No penetration
			4	Full penetration
8	45	Single-thickness ¾-inch plywood	3	No penetration
			4	Partial penetration
8	45	Double-thickness ¾-inch plywood (loose contact, no gap between)[a]	4	No penetration
			5	Full penetration
8	90	Double-thickness ¾-inch plywood (clamped, with 3-inch gap)[b]	4	Penetration of first thickness only
			5	Full penetration
8	90	Double-thickness ¾-inch plywood (clamped, with 3-inch gap)[b]	6	Not tested[c]
12	90	Single-thickness ¾-inch plywood with sheet metal on impact side[d]	5	No penetration
			6	Not tested, but likely penetration[e]
12	45	Single-thickness ¾-inch plywood with sheet metal on impact side[d]	6	No penetration[f]

a) In these trials the second sheet of plywood was laying loose on top of the first sheet of plywood.

b) In these trials the two sheets of plywood were held together using a series of C-clamps.

c) It would have been interesting to have tested a combined, double-thickness of plywood (with a 3-inch gap) with an impact angle of 45°. Unfortunately, this was not considered at the time of the testing.

d) The sheet metal was 24 gauge (0.024 inch) galvanized steel of the type commonly used for heating ducts.

e) While not tested, based on the results from the 5-inch shell impact, it seemed likely that a 6-inch shell impact at 90° would have penetrated the test panel.

f) This test was repeated four times with four different brands of aerial shells.

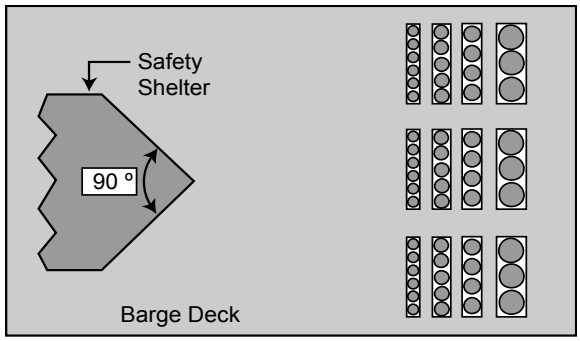

Ship Bow Configuration (overhead view)

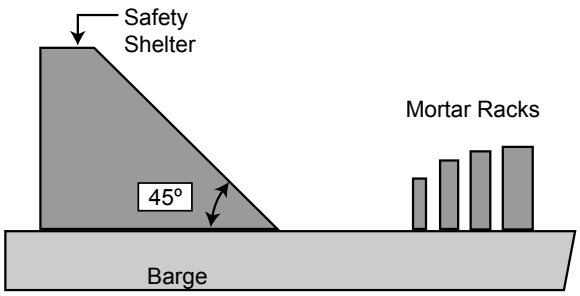

Sloping Front Configuration (side view)

Figure 2. Illustrations of two basic configurations presenting a front wall at an approximate 45° degree angle to mortars that might become repositioned in the discharge area.

proximate 45° angle to the mortar area are shown in Figure 2. One has a front shelter wall appearing somewhat like the bow of a ship; the other is a sloping front shelter wall.

By combining the use of both a double-thickness of ¾-inch plywood (loose contact with no separation between the sheets) and a 45° impact angle, it was found that a further increase in penetration resistance was achieved. This combination was successful in stopping a 4-inch aerial shell, but allowed the penetration of a 5-inch shell.

Another attempt to improve penetration resistance at 90° was to allow a 3-inch gap between two sheets of ¾-inch plywood and to secure the two sheets together as a single unit. The rational for this trial was the hope that the impacting aerial shell would be sufficiently damaged in the process of penetrating the first layer of plywood that the shell (and fragments from the first layer of plywood) would be sufficiently spread-out that they would not be able to penetrate the second layer of plywood. This improved performance was found to be the case for a 4-inch shell, which did penetrate the first sheet of plywood; however, that shell left the second sheet of plywood intact. When this approach was tried again with a 5-inch aerial shell, the impacting shell fully penetrated both sheets of plywood.

It would have been interesting to have tested the combination of a double-thickness of plywood (with a 3-inch gap) and an impact angle of 45°. Unfortunately, this was not considered at the time of the testing, and no further testing is planned at this time.

Next the penetration resistance of a single sheet of ¾-inch plywood combined with a piece of thin (24 gauge, 0.024 in.) sheet metal (galvanized heating duct material) on its front surface was tested. In the first trial of sheet metal plus plywood, a 5-inch aerial shell did not penetrate when fired at a 90° angle to the test panel. However, the damage was sufficient that it seemed likely that a 6-inch shell might penetrate a panel of this type, and a test with a 6-inch shell was not performed. Instead, the angle was changed to 45° prior to a trial with a 6-inch shell. In this trial, the 6-inch shell did not penetrate the test panel. To gain some increased confidence in the result of this successful trial, three additional 6-inch shells were fired into the same test panel. An attempt was made to have the three additional shells impact the panel at slightly different points. However, two of those additional shells impacted the panel within approximately one foot of the first shell. Despite this, none of the three additional shells penetrated the test panel. The upper part of Figure 3 is a series of four images (spanning 0.006 second) from the first of four impact trials. In the upper-left image, the shell (traveling to the left) is about to impact the test panel at a 45° angle. In the upper-right image, the shell has struck the panel and has already significantly collapsed. In the middle-left image, the shell has nearly completely collapsed. In the middle-right image, the collapsed shell has begun to slide upward along the test panel. (Typically in these tests the contents of the shell do visibly ignite but not until they are out of the field of view of the camera.) The lower left still photograph was taken after the impact of the first of the four 6-inch shells had impacted the test panel. The lower right still photograph documents the result of all four 6-inch shell im-

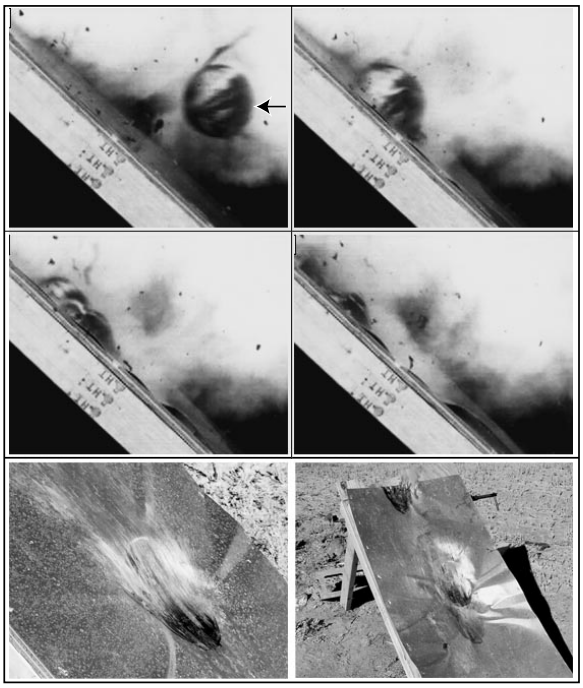

Figure 3. A series of four images (spanning 0.006 second) of a 6-inch aerial shell impacting a sheet metal augmented test panel at a 45° angle, plus two still photographs of the test panel after having been struck by one (left) and four (right) 6-inch shells.

pacts on the panel. By the end of the testing, the plywood backing the sheet metal had been significantly damaged from the four impacts; however, none of the shells or their contents had torn the sheet metal or penetrated the test panel.

Another Safety Strategy

While not tested, it would seem that the layout of mortars in front of a safety shelter has the potential to provide an improved level of protection to occupants of a safety shelter. If the smaller mortars are placed closest to the shelter, it would seem likely that any repositioned larger mortars (those more distant than the smaller mortars) are somewhat unlikely to be able to directly strike the front wall of the shelter. This is illustrated in Figure 4, where it is suggested that any repositioned mortars beyond the first row of racks are likely to either pass over the safety shelter or will first impact those mortars closer to the shelter thus reducing (or eliminating) their potential to penetrate the front wall of the safety shelter. (In addition, the mere fact that the larger mortars are at a greater distance from the shelter, results in a reduced probability that a shell fired from one of those larger repositioned mortars would strike the shelter, because the shelter becomes in effect a smaller target.)

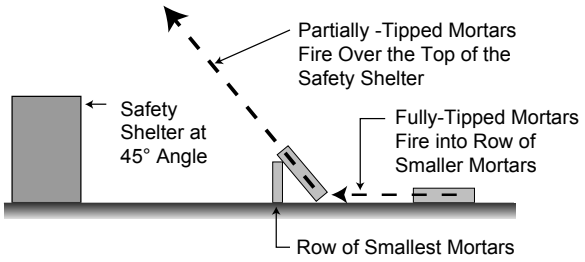

Figure 4. An illustration of how some mortar layouts might be used to reduce the possibility of large caliber aerial shells impacting the front wall of a safety shelter.

Conclusion

Given the modest increase in cost and weight of a front wall made of ¾-inch plywood augmented with sheet metal (24 gauge galvanized steel) as contrasted with bare ¾-inch plywood, it would seem that this is an approach worth considering to improve the penetration resistance of a safety shelter. Further, if the front wall of the shelter is at a 45° angle to the likely trajectory of an impacting aerial shell and if the layout of mortars is chosen to provide some additional protection, it seems likely that the firing crew inside the shelter will have a relatively high degree of safety from direct shell impacts. An example of such a simple safety shelter design (erected as a demonstration) is shown in Figure 5.

In conclusion regarding this testing, it must be acknowledged that:

- The amount of testing performed in this brief study was very limited.
- There may be other problems and consequences not fully considered by the authors.
- Reinforcing the front wall of the shelter offers essentially no added protection from falling dud shells.

Figure 5. An example of a safety shelter design with a sloping sheet-metal covered front wall.

- There certainly may be other reasonably simple configurations that provide equal of greater penetration resistance.

Acknowledgements

The authors gratefully acknowledge L. Weinman for commenting on an earlier draft of this article and especially for suggesting the use of thin sheet metal to aid in the resistance of plywood to aerial shell penetration. The authors are also grateful to L. Hill (and Pyro Shows personnel) for providing the manpower and location for some of the testing reported in this article.

References

1) *Code for Fireworks Display*, NFPA-1123, 2006, paragraphs 4.2.3, 4.3.2 and 4.4.1.

2) K. L. and B. J. Kosanke, "Initial Tests of Barge Safety Shelter Resistance to Penetration by Aerial Shells", *Fireworks Business*, No. 262, 2005; *Selected Pyrotechnic Publications of K. L. and B. J. Kosanke, Part 8 (2005 through 2007),* Journal of Pyrotechnics, 2009.

An earlier version appeared in: *Fireworks Business*, No. 274, 2006.

Convenient Couplers for Lightning Thermo Tube™

K. L. and B. J. Kosanke

An earlier article[1] addressed the characteristics and methods for the use of Lightning Thermo-Tube™[2] (LTT). At about that time, some inexpensive plastic components that can be used to facilitate the coupling and branching of LTT were supplied for evaluation.[3] This article reports on a brief study of the effectiveness and utility of those components.

The plastic components consisted of rigid tubing tees and soft plastic caps, as shown Figure 1. The new tubing tees,[4] unlike those evaluated previously, are of sufficient internal diameter that the LTT fits snugly inside the ends of the tee, see the lower photograph in Figure 2. This direct coupling to the tee eliminates the need to use the three short lengths of rubber tubing, see upper photograph in Figure 2.

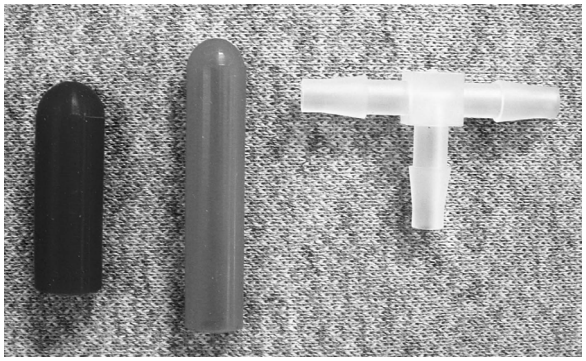

Figure 1. Photograph of the plastic components being evaluated for use with LTT.

Although there were only three trials using this direct coupling tee, all were successful. (It is possible to use these same tubing tees to couple LTT to visco or other pyrotechnic fuses; however, because the diameter of these fuses are typically smaller than LTT and the ID of the new tubing tee, the connection may not be sufficiently secure without taping or using some other means of securing the fuse into the tubing tee.)

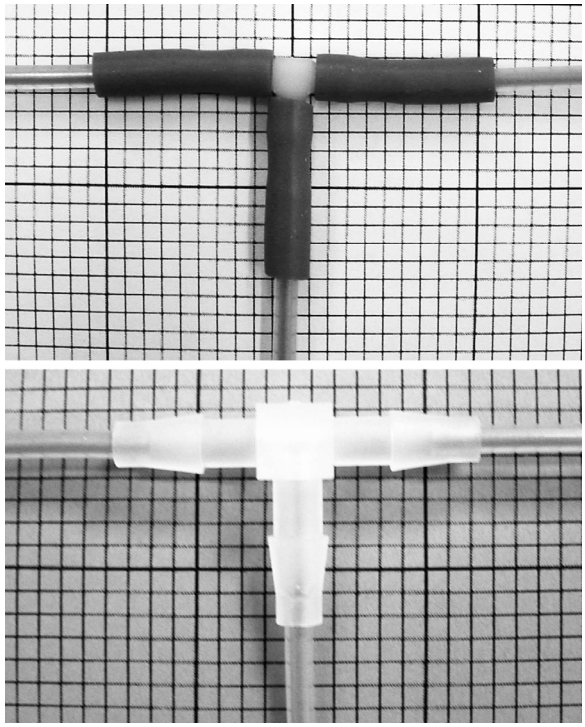

Figure 2. A comparison of the use of the previous (upper) and current (lower) tubing tees to branch LTT using tubing tees.
[Each square is 0.10 inch.]

The two sizes of soft plastic caps[5] shown in Figure 1, were also used to branch LTT. In these trials, four or five lengths of LTT were coupled (branched) by simply inserting the ends of the LTT a short distance into the two sizes of plastic caps, see Figure 3. While a somewhat similar method of branching LTT was evaluated previously, branching using these soft plastic caps can be accomplished much more quickly and with significantly less effort. Although there were only three trials using each of the two types of caps, using 4 and 5 LTT lines, all were successful.

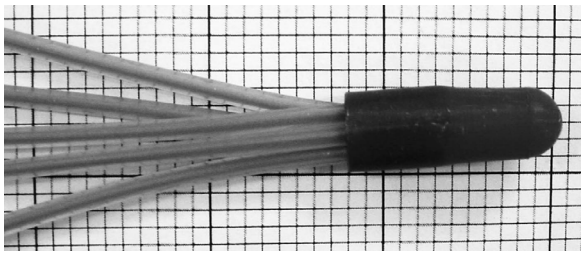

Figure 3. A simplified method for coupling (branching) larger numbers of LTT using soft plastic caps. [Each square is 0.10 inch.]

The coupling and branching methods reported on previously were quite successful and reasonably simple. The methods reported on in this article seem to be equally effective, but are even simpler and easier to use.

References / Notes

1) "An evaluation of Lightning Thermo Tube™ as a Pyrotechnic Ignition System", K. L. and B. J. Kosanke, *Journal of Pyrotechnics*, No. 24, 2006; *Selected Pyrotechnic Publications of K. L. and B. J. Kosanke, Part 8 (2005 through 2007),* Journal of Pyrotechnics, 2009.

2) Lightning Thermo Tube, 12707 N. Freeway, Suite 330, Houston, TX 77060.

3) Mike Kroeger, Next Evolution Pyrotechnics, 323 Lonnie Dr., Muscle Shoals, AL, 35661; phone: 256-381-3123.

4) Ark-Plas Products, P.O. Box 340, Flippin, AR 72634.

5) Harman Corporation, P.O. Box 80665, Rochester, MI 48307.

An earlier version appeared in: *Journal of Pyrotechnics*, No. 24, 2006.

An Evaluation of Lightning Thermo Tube™ As a Pyrotechnic Ignition System

K. L. and B. J. Kosanke
PyroLabs, Inc., Whitewater, CO USA

ABSTRACT

Lightning Thermo Tube (LTT) is a recently introduced type of shock tube with characteristics that make it suitable for use with common pyrotechnics. LTT is reliably initiated by reasonably energetic electric matches and reliably ignites most pyrotechnic compositions. LTT is physically strong, easily spliced and branched, and is highly weather resistant. LTT produces a moderately bright flash of light upon functioning, which may be a useful effect in itself. This paper presents the results of a series of tests performed to determine some of the more important capabilities and characteristics of LTT as it relates to use with pyrotechnics in general and fireworks in particular.

Introduction

Lightning Thermo Tube™[1,2] has recently been introduced to the US firework trade. The product is very similar in appearance to conventional shock tube.[3–5] However, because of the pyrotechnic used in its manufacture, it does not require the flame-to-shock and shock-to-flame converters that regular shock tube needs when used with typical pyrotechnics.[6] This makes it more convenient and cost effective to use with pyrotechnics than conventional shock tube. Fortunately, Lightning Thermo Tube (LTT) retains the safety characteristics, and the ease of splicing and branching of conventional shock tube.

This article reports on an initial brief evaluation of LTT for use with pyrotechnics, specifically fireworks and proximate audience pyrotechnics. However, because of the limited scope of this study, for the most part reliability issues are not thoroughly addressed. For example, LTT was definitely found to have the capability of being initiated with commonly used electric matches and with small exploding charges. A reasonably high level of reliability was found in ignition trials with one type of electric match, where 35 of 35 attempts were successful. However, because only a limited number of trials were run, it is not possible to state with confidence how reliably such initiation can be accomplished. In many other cases, because even fewer trials were conducted, the results are not statistically significant. Finally, all trials were conducted under moderate environmental conditions (i.e., at a temperature of approximately 15 °C (60 °F) and a relative humidity of less than 40%); therefore, it is possible that the performance of LTT under more extreme conditions may be different.

The Product

A small coil of Lightning Thermo Tube (LTT) is shown in Figure 1. It is a thick-walled and strong (high tensile strength) plastic tube, approximately 3 mm (1/8 in.) in outside diameter and approximately 1.2 mm (0.05 in.) in inside diameter. The inside of the tubing has been coated with a thin layer of pyrotechnic composition, which propagates an energetic chemical reaction at a high speed and can ignite various other pyrotechnic materials. Also shown in Figure 1 are three short lengths of rubber tubing and a small plastic tee that can be used to couple and branch the LTT.

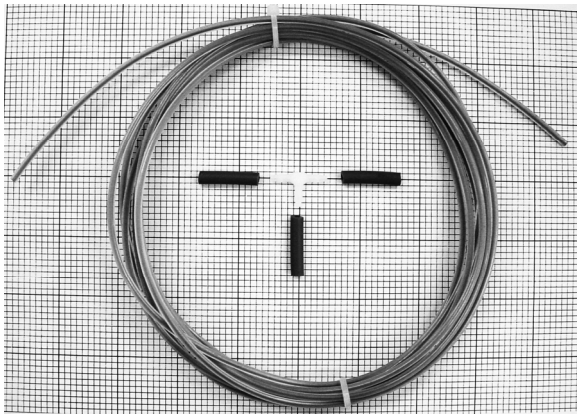

Figure 1. A photograph of a small coil of Lightning Thermo Tube (LTT) and items used in coupling and splitting LTT. [Each small square is 2.5 mm (0.1 in.)].

The stable propagation rate of LTT was measured and found to be approximately 1100 m/s (3600 ft/s), which is reasonably consistent with its reported propagation rate of 1200 m/s.[7] This measurement was accomplished by video recording the propagation of a length LTT at the rate of 20,000 frames per second (see Figure 2).[8] (In Figure 2 and other figures of reacting LTT, the intensity of the light produced by the propagating LTT reaction in relation to the video camera settings was so intense as to give the false appearance that the diameter of the flash reaction greatly exceeds the actual diameter of the LTT tube.) Using these same video images, it was also determined that approximately 0.2 ms and approximately the first 200 mm (8 in.) of propagation in the LTT were required before the propagation rate stabilized and the full intensity of the propagation was established when initiated with an electric match (Martinez Specialties' E-Max electric match[9]) using an 8 J capacitive discharge firing set. It is likely that the initiation method may affect the run-up distance but almost certainly not the steady state propagation rate.

Figure 3 is an electron micrograph of the end of a piece of LTT cut at an angle to better expose its interior for imaging. (Unfortunately in this two-dimensional image, the thin coating on the inside wall of the tubing somewhat gives the erroneous appearance that the inner bore of the tube is completely filled with composition.) The Material Safety Data Sheet for LTT[10] lists as its

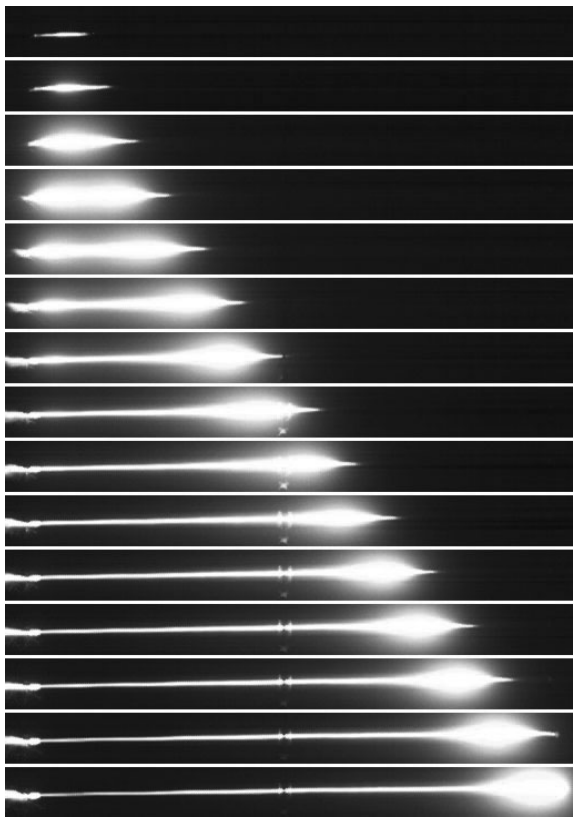

Figure 2. A collection of 15 images of the propagation of LTT after initiation with an electric match. The elapsed time between images is 0.00005 second. (The image width is approximately 800 mm, 32 inches.)

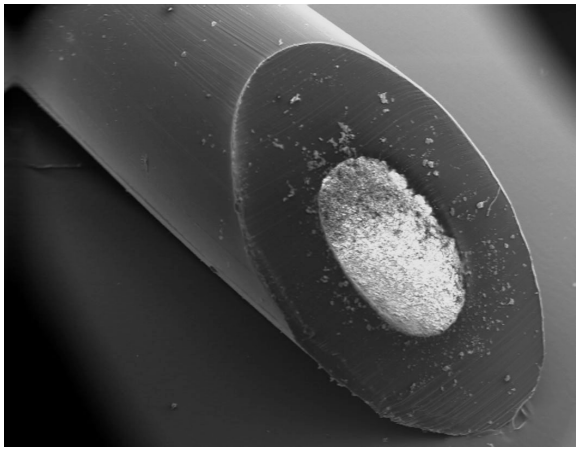

Figure 3. An electron micrograph of a small segment of LTT cut at an angle of approximately 45° to better expose the powder coating on the interior wall of the tube.

hazardous ingredients, potassium perchlorate and aluminum. The X-ray energy dispersive spectrum (above an energy of 0.5 keV) of a sample of the powder coating (see Figure 4) also includes substantial peaks for iron. In comparing this information, the measured propagation rate for the LTT of approximately 1100 m/s (3600 ft/s), and information from the US Patent upon which the LTT is apparently based,[2] suggests that the pyrotechnic composition of the interior wall coating is that given in Table 1.

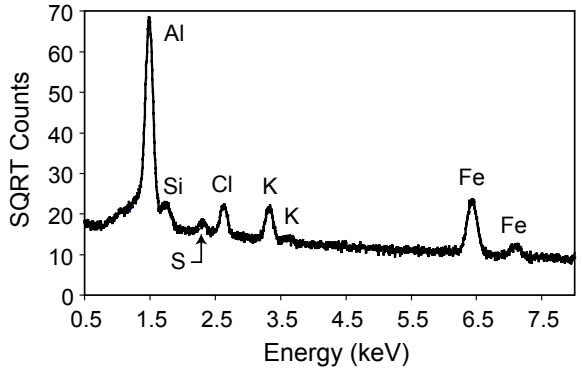

Figure 4. The X-ray energy dispersive spectrum of a sample of LTT's interior powder coating. (SQRT Counts is the square root of the number of counts per energy channel.)

Table 1. Apparent Chemical Formulation of the Internal Powder Coating Used in LTT.

Ingredient	Percentage
Aluminum	50
Iron(II-III) oxide	24.5
Potassium perchlorate	24.5
Talc	1

Because the reported amount of pyrotechnic content is so low (8 mg/m [10]) Lightning Thermo Tube is classed by the US Department of Transportation as "not regulated as an explosive" and can be shipped as non-hazardous material,[11] which is the same classification as for the plastic tubing without the pyrotechnic coating on its interior wall. Nonetheless, the US Bureau of Alcohol, Tobacco, Firearms and Explosives is requiring that LTT only be sold to licensees and that it be stored as a regulated material, including a requirement for magazine storage and record keeping.[7]

Figure 5 is one frame from a standard (NTSC) frame-rate video that demonstrates the projection of fire and sparks emanating from the end of LTT as it functions. The functioning thermo tube is seen as the narrow bright band at the extreme left in the image. The fire output from the LTT is seen to expand to a diameter of approximately 25 mm (1 in.) and to extend to approximately 100 mm (4 in.) to the right. The spray of sparks from the LTT, although not clearly visible in Figure 5, also projects to distance of at least 200 mm (8 in.) from the end of the thermo tube.

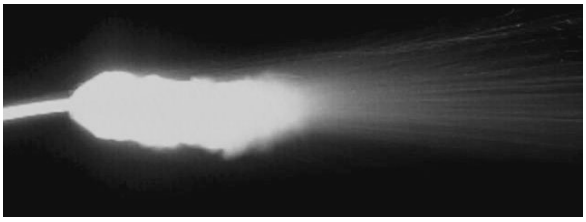

Figure 5. A standard frame-rate video image (NTSC) of functioning LTT, where the total width of the image is approximately 250 mm (10 in.).

When conventional shock tube (charged with explosive composition) functions, the pressure developed within the tube will occasionally cause the tube to burst. This is apparently because of some migration and accumulation of powder within the shock tube. (Conventional shock tube will fairly reliably burst the tube when two nearly simultaneous shock waves are propagated from both ends of the shock tube to collide along its length.) This type of tube bursting was not observed for LTT during the trials that were conducted, even when opposing shocks were caused to collide within the tubing. (However, based on the limited testing being reported, it should not be assumed that LTT will never burst its tube.)

Similar to shock tube, the functioning of LTT can produce moderately loud sound. The sound pressure level (SPL) produced by the emerging shock front is approximately 145 dB (free field – peak – linear) measured at 1.2 m (4 ft) directly in line with the end of the LTT (i.e., at 0° to the axis of the LTT). Under the same conditions, except measured at 90° to the end of the LTT,

the SPL was reduced to approximately 135 dB. The output (blast) from the end of the LTT is the primary source of the sound, as opposed to the sound radiating outward through the walls of the tube. Thus, when the ends of the LTT were sealed (or well muffled) the SPL did not exceed the background sound level in the laboratory at the time (i.e., approximately 90 dB).

Initiation Trials

A series of trials were conducted to determine what common stimuli tend to be capable of initiating Lightning Thermo Tube. In many cases only a limited number of individual trials were performed; thus one should not infer much about the reliability of the various methods. See Table 2 for a summary of the LTT initiation tests that were performed. (The order of the information in Table 2 is not the same as the order in which the trials were conducted.) Table 2 begins with three methods that were unsuccessful in producing initiations of LTT on every attempt, then two methods that worked with less than complete reliability, and finishes with a number of methods that were successful on every attempt.

Table 2. Lightning Thermo Tube Initiation Test Results.

Test Conditions[a]	Initiations / Trials
Fall-hammer impact (5 kg hammer from a height of 1 m, 39.4 in.)	0 / 10
Propane torch flame applied for five seconds (flame temperature was approximately 1900 ºC)	0 / 3
Fire spit from visco fuse coupled using inert tubing [b]	0 / 5
LTT installed into the wall of a discharging consumer fireworks mortar	2 / 4
Luna Tech BGZD electric match[12] coupled using tubing[c]	30 / 35[d]
Martinez Specialties E-Max electric match[9] coupled using tubing[c]	35 / 35
Spark gap using an 8 J capacitive discharge firing unit	30 / 30
Martinez Specialties E-Max electric match coupled using a Martinez Specialties Quick Fire VF Clip[13][c]	3 / 3
Martinez Specialties Exploding-Bridge-Wire initiator coupled using its attached inert tube and an 8 J capacitive discharge firing unit	3 / 3
Bare electric match tip (without any pyrotechnic composition) using an 8 J capacitive discharge firing unit	3 / 3
CCI #209M shot shell primer in a shock tube firing apparatus[e]	3 / 3
Functioning shock tube coupled using tubing	2 / 2
Approximately 50 mg of flash powder in coupling tube, ignited with visco fuse	3 / 3

a) Trials were conducted at a temperature of approximately 15 °C (60 °F) and a relative humidity of less than 40%.

b) Visco fuse is a thread wrapped Black Powder fuse approximately 2.5 mm (3/32 in.) in diameter and is also called hobby, cannon and firework safety fuse.

c) The electric match was fired using either an 8 J capacitive discharge firing set or one using a 5 V power supply.

d) The first 25 trials with these electric matches produced 25 successful initiations of the LTT. However, the last 10 trials only produced 5 successful initiations. At this time it is not known what the reason for this was (e.g., statistics, or some difference in the matches or the LTT). However, the Luna Tech electric matches are noticeably more mild in their functioning than the Martinez Specialties matches that were used with greater success.

e) The US distributor of LTT reports that this is the manufacturer's recommend method of initiation for LTT.

The trials using fall-hammer impacts (0 initiations in 10 trials), the flame from a propane torch (0 initiations in 3 trials) and the fire spit from visco fuse (0 initiations in 5 trials) were all unsuccessful in initiating the LTT. The setup used to determine the capacity for initiation of LTT using visco fuse, approximately 18 mm (¾ in.) of 3 mm (1/8 in.) ID inert tubing was used to connect the initiation source to the LTT. The initiation source and the LTT were inserted into opposite ends of the tubing until contact was made between them. (See the upper illustration in Figure 6.)

The next stronger impetus tried was to mount the end of LTT through the side of a consumer firework mortar and to fire a small aerial shell from the mortar. The combined flame and modest pressure effect that was produced, worked occasionally (2 initiations in 4 trials), but only when the aerial shell was propelled with significant force.

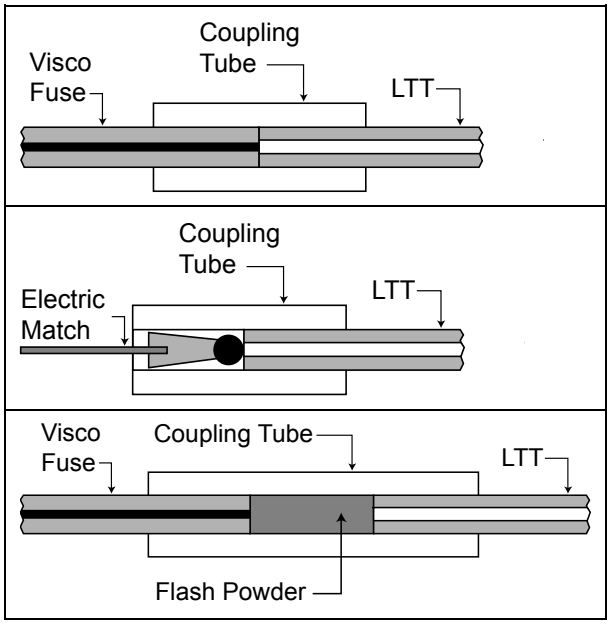

Figure 6. An illustration of some of the methods used in trials for initiating LTT. Top, visco fuse coupled to LTT. Middle, electric match coupled to LTT. Bottom, visco fuse coupled to flash powder that is then coupled to LTT.

The next stronger impetus tried was to use a fairly mildly functioning electric match (Luna Tech's BGZD electric matches).[12] The first 25 trials using these electric matches produced 25 successful initiations of the LTT. However, the last 10 trials only produced 5 successful initiations. At this time it is not known what the reason for this was (e.g., statistical chance, or some difference in the electric matches or in the LTT). The setup used to determine the capacity for initiation of LTT using electric matches was the same as for visco fuse. (See middle illustration in Figure 6.)

The trials using various stronger initiation sources were all successful. These methods included the use of a more powerfully functioning electric match (Martinez Specialties E-Max electric match[9]) (35 initiations in 35 trials); capacitive discharge spark gaps[14] using an 8 J capacitive discharge firing set (30 initiations in 30 trials); an E-Max electric match coupled to the LTT using a Martinez Specialties Quick-Fire VF clip[13] (3 initiations in 3 trials); commercial exploding bridgewire initiators (Martinez Specialties) using an 8 J capacitive discharge firing set (3 initiations in 3 trials); hand-made exploding bridgewire initiators (a bare electric match tip, without any pyrotechnic composition) using an 8 J capacitive discharge firing set (3 initiations in 3 trials), CCI #209M shot shell primer using a commercial shock tube firing appliance (3 initiations in 3 trials) and functioning commercial shock tube (2 initiations in 2 trials). In all cases, the setup in these initiation trials was as described above.

In the case where the initiation source was visco fuse augmented with a small flash powder charge, the coupling method was similar to that used for visco fuse. However the length of tubing was extended to approximately 32 mm (1-1/4 in.) in length and a small amount (approximately 50 mg) of flash powder was added to the tubing between the initiation source and the LTT. (See the lower illustration in Figure 6.) The flash powder used in these trials was 70:30 potassium perchlorate and dark pyro aluminum (–400 mesh).

LTT Coupling Methods

One of the standard (and effective) methods used to couple lengths of shock tube is to insert the ends to be joined together into a short length of inert tubing. (This coupling method is demonstrated in the top photograph of Figure 7.) Providing the two ends of tubing are reasonably close together inside the coupling tube, communication of the shock reaction seems assured. However, because the coupling tube is inert, there is a limited gap length between the two shock tube ends that will still provide reasonably assured communication of the shock reaction.[15] The testing of LTT took two forms: 1) to verify that LTT can be effectively coupled using the same general end-to-end method that is effective for conventional shock tube, and 2) to establish the approximate maximum gap that will provide reasonably assured propagation of LTT's pyro-

technic reaction. A summary of the test results is presented in Table 3. In each case, the length of LTT before the coupling was approximately 300 mm (12 in.), to allow for the full development of LTT's propagating reaction.

In the coupling trials with the ends of two lengths of LTT in direct contact inside a short length of slightly larger inert tubing (upper photograph in Figure 7) a total of at least 30 trials were attempted and all successfully propagated the LTT reaction.

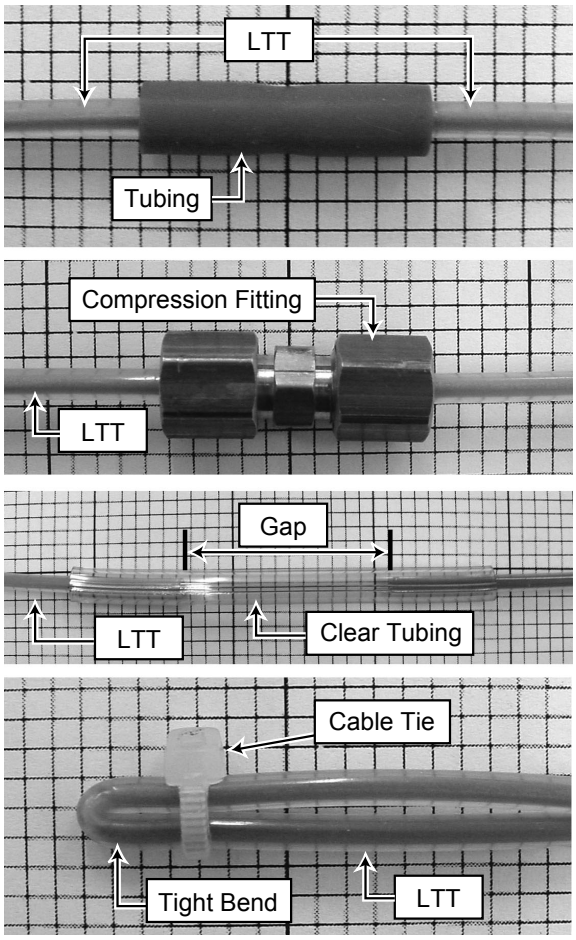

Figure 7. A photograph demonstrating the LTT "direct contact" in inert tubing (top), "compression fitting" (upper middle), and "gap" (lower middle) coupling methods. Also shown is the "very tight bend"(bottom) used in a propagation test. [0.1 in. per division.]

In addition to the coupling trials using inert tubing, trials were also conducted using metal compression fittings (upper middle photograph in Figure 7) and reusable plastic compression fittings (not shown). By design, these fittings operate with a short gap between the ends of the tubing being coupled. In the metal fitting the gap was approximately 5 mm (0.2 in.) and in the plastic fitting the gap was approximately 12 mm (0.5 in.). While the fittings could have been drilled out to allow the end of the LTT to be in close end-to-end contact, this would have been an inconvenience and was anticipated to be unnecessary. This is because LTT should be capable of successfully propagating through a short length of an inert coupler. In a limited number of trials (1 using a metal fitting and 5 using plastic fittings), all trials were successful.

Table 3. A Summary of the Results from the Testing of LTT Coupling Methods.

Test Conditions[a]	Successes / Trials
Direct contact, end to end coupling using inert tubing[b]	30 / 30
Coupled using metal compression fittings[c]	1 / 1
Coupled using plastic compression fittings	5 / 5
Coupled through ≈ 18-mm (3/4-in.) inert tubing gap[d,e]	2 / 2
Coupled through ≈ 38 mm (1-1/2-in.) inert tubing gap[d,f]	10 / 10
Coupled through ≈ 51-mm (2-in.) inert tubing gap[d]	3 / 7
Coupled through ≈ 76 mm (3-in.) inert tubing gap[d]	0 / 3
Propagating through very tight bend[g]	2 / 4

a) Unless otherwise stated, to allow for the full development of LTT's propagating reaction, approximately 300 mm (12 in.) of LTT was included before attachment to a coupling tube. This allowed for the full strength of the LTT propagation reaction to be fully established. Trials were conducted at a temperature of approximately 15 °C (60 °F) and a relative humidity of less than 40%.

b) See the upper photograph in Figure 7 for an illustration of the "direct contact" coupling method used.

c) See the upper middle photograph in Figure 7 for an illustration of the "compression fitting" coupling method used.

d) See the lower middle photograph in Figure 7 for an illustration of the "gap" coupling method used.

e) See Figure 8 for a composite series of photographs of the propagation the LTT reaction through an approximately 18-mm (3/4-in.) gap.

f) See Figure 9 for a composite series of photographs of the propagation the LTT reaction through an approximately 38-mm (1-1/2-in.) gap.

g) See the lower photograph in Figure 7 for just how tight a bend was attempted.

Next a series of trials were conducted to determine the approximate maximum gap that would provide reasonably reliable propagation of the LTT reaction. In these trials, the ends of two lengths of LTT were inserted into a length of inert tubing with an inside diameter the same as the outside diameter of the LTT (see the lower middle photograph in Figure 7). The two ends of the LTT were left separated within the larger diameter tubing by distances of approximately 18, 38, 51 and 76 mm (3/4, 1-1/2, 2 and 3 in.). All of the trials using the approximately 18 and 38 mm (3/4 and 1-1/2 in.) gaps were successful in propagating the LTT reaction. However, in viewing the propagation using high frame-rate video[16] it seemed apparent that the approximately 38 mm (1-1/2 in.) gap was near the maximum gap that could be tolerated. This can be seen by comparing Figures 8 and 9, high frame rate video of the propagation through approximately 18 and 38 mm (3/4 and 1-1/2 in.) gaps, respectively. For the approximately 18 mm (3/4 in.) gap (Figure 8) there is only a single image (0.0001 s) in the sequence of images before the propagation of the LTT reaction was reasonably fully reestablished after reaching the gap. To the contrary, for the approximately 38 mm (1-1/2 in.) gap (Figure 9) eight images lapsed before the propagation is reasonably fully reestablished after reaching the gap. Note in Table 3 that when the gap was increased to approximately 51 mm (2 in.), propagation was only successful in three of seven trials, and when the gap was further increased to approximately 76 mm (3 in.), none of three trials were successful.

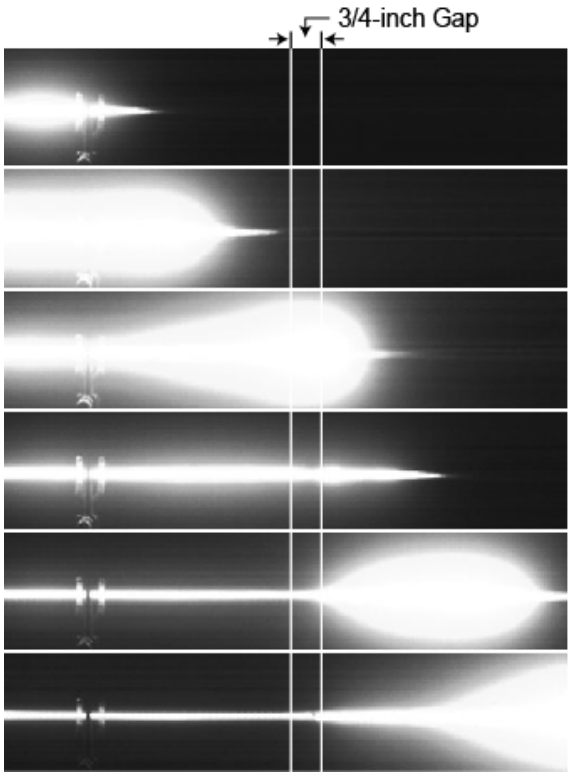

Figure 8. A collection of 6 images of the propagation of LTT through an approximately 18 mm (3/4 in.) gap. The elapsed time between images is 0.0001 second.[16]

Tight Bend Propagation Test

The ability of LTT to propagate through an extremely tight bend was briefly investigated. The tightness of the bend is documented in the bottom photograph of Figure 7, and it approximates the very tightest bend imaginable for LTT. It was found that two of four trials were successful; however, the number of tests was so small as not to be definitive.

LTT Branching Methods

A series of trials were performed to help establish the ability of LTT line to successfully branch (split) into two or more LTT lines. The results are summarized in Table 4 and discussed in more detail below.

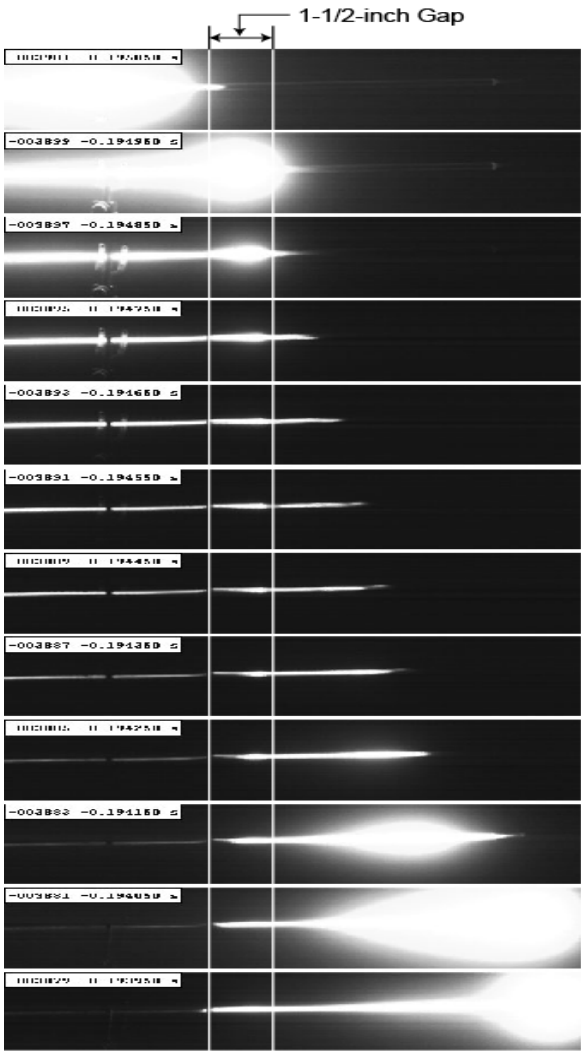

Figure 9. A collection of 12 images of the propagation of LTT through an approximately 38 mm (1-1/2 in.) gap. The elapsed time between images is 0.0001 second.[16]

Table 4. A Summary of the Results from the Testing of LTT Branching Methods.

Test Conditions[a]	Ignitions / Trials
Into the mid-branch of a single tubing-tee[b,c]	10 / 10
Into a side-branch of a single tubing-tee[b,d]	4 / 4
Through a tubing-tee into two additional tubing-tees[b,e]	10 / 10
Through a tubing-tee with only ≈ 76 mm (3 in.) of LTT leading to two additional tees[b,e]	
Through a tubing-tee directly (no LTT) into two additional tubing-tees[b]	0 / 4
Through a reusable plastic compression fitting tee[f]	3 / 3
Through a single-use metal compression fitting tee	1 / 1
Propagating through a notched LTT[g]	8 / 8
Split into three lines by coupling a pair of notches[h]	2 / 2
Split into seven lines by coupling inside inert tubing[i]	2 / 2

a) Unless otherwise stated, to allow for the full development of LTT's propagating reaction, approximately 300 mm (12 in.) of LTT was allowed before attachment to a tee or the first notch. This allowed the full strength of the LTT reaction to be established before branching. Trials were conducted at a temperature of approximately 15 °C (60 °F) and a relative humidity of less than 40%.

b) See the upper photograph in Figure 10 for an example of LTT branching through a tubing tee.

c) See the upper illustration in Figure 11 for the orientation of the tubing tee in these trials.

d) See the lower illustration in Figure 11 for the orientation of the tubing tee in these trials.

e) This arrangement is illustrated in Figure 12.

f) See the middle photograph in Figure 10 for an example of LTT branching through a compression fitting tee.

g) See the lower photograph in Figure 10 for an example of a notch made into LTT and the lower photograph in Figure 13 for the fire output from notches in a LTT line being fired.

h) See Figure 14 for photographs of this LTT splitting method.

i) See Figure 15 for a photograph of this LTT splitting method.

The first branching method tried used standard tubing tees coupled as shown in the upper photograph of Figure 10. The attachment of LTT to the tubing tees was accomplished using short lengths of inert tubing. In the first trials, the LTT propagating reaction entered the middle branch

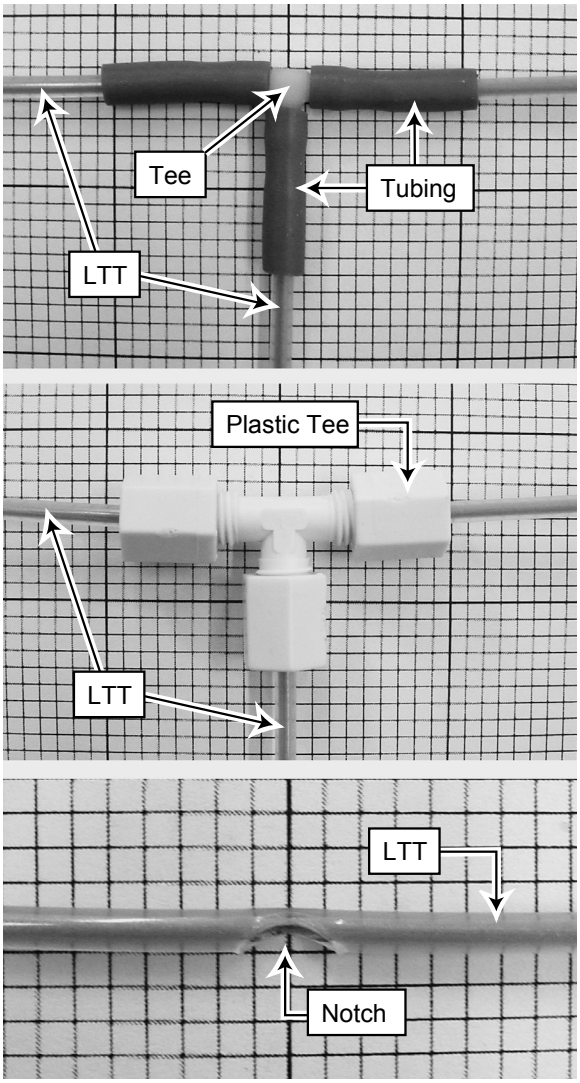

Figure 10. Photographs demonstrating three of the LTT branching methods used in this study. [2.5 mm (0.1 in.) per division.].

of the tee, after traversing a total gap length of approximately 24 mm (0.95 in.) of inert tubing tee plus having negotiated a 90° bend (see the upper drawing in Figure 11). Ten of ten trials of this branching method successfully propagated the LTT reaction. Further testing was performed using a slight modification of this tubing tee method, where the LTT propagation reaction entered one of the side-branches of the tee (see the lower drawing of Figure 11). Four of four trials of this branching method were successful in propagating the reaction.

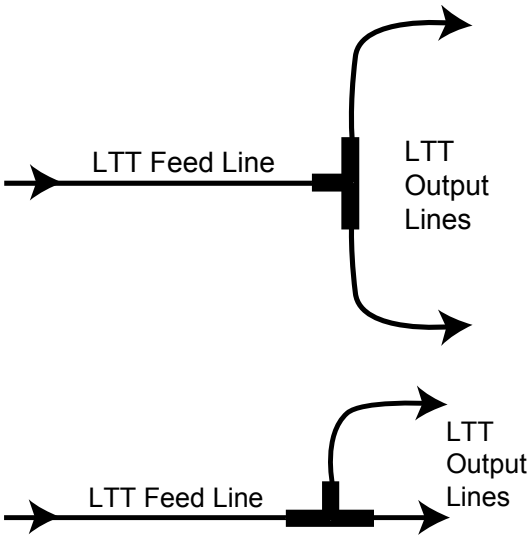

Figure 11. Illustrations of the configurations used for the testing through a single tee: upper, LTT reaction enters through middle-branch of the tee; lower, LTT reaction enters through one side branch of the tee.

In the next series of trials, the pair of outputs from the one tee were sent into two additional tees for additional branching into a total of four LTT lines (see Figure 12). When the LTT lines between the first and the additional tees was approximately a full 300 mm (12 in.), ten of ten trials successfully propagated the LTT reaction. However, when the length of LTT between the tees was reduced to approximately 76 mm (3 in.), only nine of ten trials were successful. When the three tees were coupled directly together with no LTT between the tees, none of four trials were successful. Note that this is consistent with the gap testing, where it was found that the maximum gap providing relatively reliable propagation of the LTT reaction was approximately 76 mm (1.5 in.). The use of additional tees coupled directly to the first tee requires the LTT reaction to traverse approximately 48 mm (1.9 in.) plus negotiate two 90° bends.

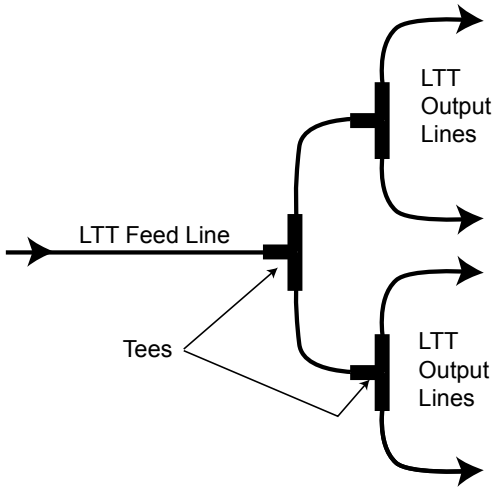

Figure 12. An illustration of the configuration used for the testing through multiple tees.

The next series of trials involved only a very slight modification of the tubing tee trials, in these tests compression tees were used (see middle photograph of Figure 10). In trials with plastic compression tees, three of three were successful. A single trial with a metal compression tee was also successful.

Another branching method tried consisted of simply cutting a series of notches into lengths of LTT using a standard hand-held paper punch. A typically produced notch is shown as the bottom photograph in Figure 10. (Even though it is thought to be highly unlikely that punching notches in the LTT would cause its initiation, it is appropriate to employ all of the ordinary precautions that one would use in cutting any type of fuse.) Figure 13 consists of two images taken from a standard frame-rate video recording, demonstrating the basis for trying this method of branching. The upper image shows a length of LTT with a series of 5 paper punch notches prior to firing the LTT. The lower image shows the fire-spit from the five notches as the LTT fires. In eight of eight trials, LTT successfully propagated through a series of notches separated by 100 mm (4 in.) producing significant fire spit at each notch. While the arrangement shown in Figure 13 is of essentially no use in itself, it can be useful in: a) branching to additional LTT lines, and b) igniting pyrotechnic compositions if a charge of powder is positioned in the immediate area of each notch.

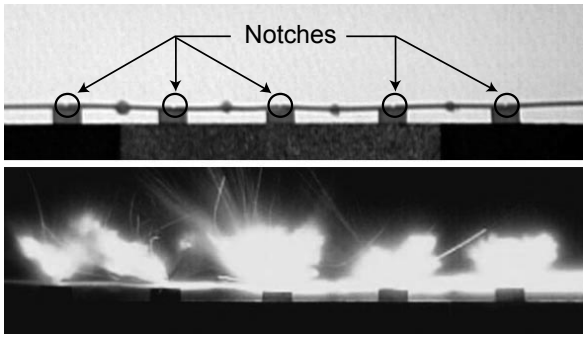

Figure 13. Two images demonstrating the basis for trying the notch method of branching and fire spit produced from a series of 5 notches approximately 100 mm (4 in.) apart in a length of LTT. The upper image is of the LTT hot melt glued to a support with pieces of tape below marking the location of each notch. The lower image documents the fire spit from the notches when the LTT was fired.

Using the notch method for branching is demonstrated in Figure 14. In this method, a notch was first cut into two LTT lines using a paper punch. The two notches were placed over each other (notch to notch) and held on a small piece of tape. The two LTT lines were further secured using a second piece of tape. Only two trials using this method were attempted and both were successful. While easy to accomplish, this notch splitting method divides one LTT input line into three output lines.

Another method for branching was attempted in which the input LTT line was split into seven output lines (see Figure 15). This method used a short length of inert tubing with an internal diameter just large enough to accommodate the seven output LTT lines, which were inserted a short distance into the coupling tube. The input LTT line was fit through a sleeve that was large enough to fit securely into the larger diameter inert tubing. The input and output LTT lines were separated by approximately 5 mm (0.2 in.) inside the coupling tube. Again only two trials were attempted using this method and again both were successful.

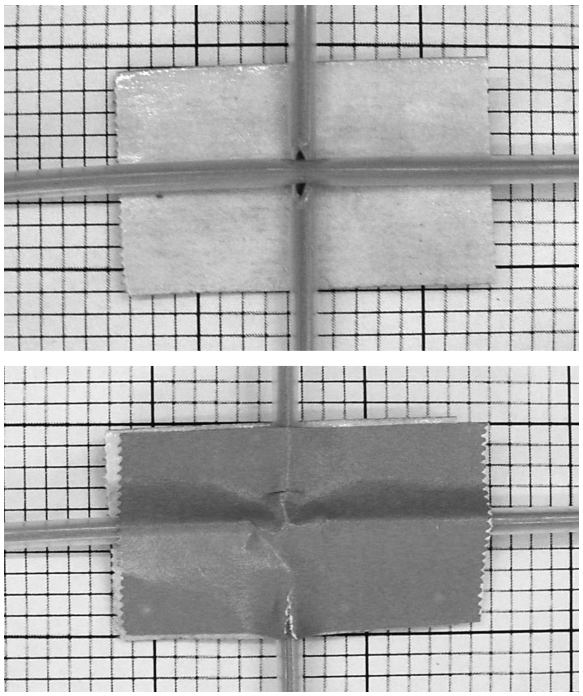

Figure 14. Photographs demonstrating a possible LTT branching method using the "notch" method. [2.5 mm (0.1 in.) per division.]

LTT Ignition Capabilities

One of the attractive characteristics of LTT is its ability to ignite typical pyrotechnic compositions directly (i.e., without using the shock-to-flame converters needed with conventional shock tube). The results from the ignition trials are summarized in Tables 5 and 6 and are discussed further below.

The first series of trials was conducted to determine the ability of LTT to ignite various pyrotechnic fuses. When the fuses were of approximately the same diameter as the LTT, both the LTT and fuse were inserted a short distance into a length of 3 mm (1/8 in.) internal diameter (ID) inert tubing. This is illustrated in Figure 16 for coupling to visco fuse (also called hobby, cannon or fireworks safety fuse). This method was tried using a medium quality visco fuse (10 trials), fast burning visco-like fuse such as used on reloadable consumer firework aerial shells (4 trials), and both Thermolite (4 trials) and Mantidor (10 trials) igniter cords. In each case, all trials were successful in igniting the various fuse types.

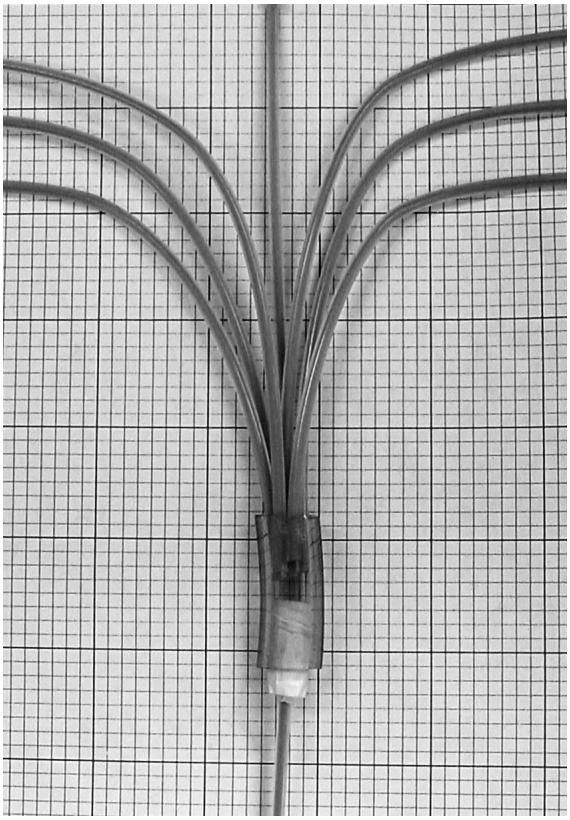

Figure 15. A Photograph demonstrating one possible multiple branching method using a coupling tube. [2.5 mm (0.1 in.) per division.]

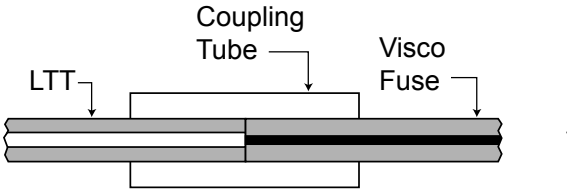

Figure 16. An illustration of the inert tube coupling method used to ignite the visco fuse and other small diameter pyrotechnic fuse types.

The inert coupling tube method was also tried using a reasonably high quality firework time fuse. However, in this case, because of the larger diameter of the time fuse, a 6 mm (1/4 in.) ID inert coupling tube was used. For the LTT to be reasonably well secured into the larger diameter coupling tube, the end of the LTT was first fitted into a very short length of a spacer tube to enlarge its effective outside diameter

Table 5. Results of Testing LTT's Ability to Directly Ignite Various Types of Pyrotechnic Fuse.

Test Conditions[a]	Ignitions / Trials
Coupled to medium quality visco fuse[b]	10 / 10
Coupled to fast burning visco-like fuse such as used on reloadable consumer firework shells[b]	4 / 4
Coupled to fast Thermolite™ igniter cord[b]	4 / 4
Coupled to Mantidor™ plastic igniter cord[b]	10 / 10
Coupled to firework time fuse[b,c]	3 / 3
Coupled to medium quality visco fuse using a notch[d]	4 / 4
Coupled to quick match shell leader (Jumping Jack brand) using a notch[d]	5 / 5
Inserted into quick match shell leader[e]	14 / 14

a) To allow for the full development of LTT's propagating reaction, in each trial an approximately 300 mm (12-in.) length of LTT was provided before its attachment to a pyrotechnic fuse. Trials were conducted at a temperature of approximately 15 °C (60 °F) and a relative humidity of less than 40%.

b) In each case the LTT was coupled to the fuse using a short length of 3 mm (1/8 in.) ID inert tubing, for example see Figure 16. The ends of the LTT and fuse were in contact or near contact within the coupling tube.

c) In the case of coupling LTT to firework time fuse, a 6 mm (1/4 in.) ID inert coupling tube was used and the LTT was fit into a sleeve to increase its OD to fit securely into the coupling tube.

d) This notch method is demonstrated in Figure 17.

e) In these trials, the LTT was either inserted into the end of a length of the quick match or through a small slit made in the match pipe, such that the LTT was immediately alongside of the black match. Shell leaders from three manufacturers (Sunny, Thunderbird and Jumping Jack) were used in these trials.

from 3 to 6 mm (1/8 to 1/4 in.). Three of three trials produced successful ignitions.

One potential drawback of the coupling tube method described above (as in Figure 16) is that it terminates the LTT line, which is then not available to produce more than the single ignition. Thus a variation of the notch branching method was tried. This method employed a notch cut into the side of the LTT using a paper punch. The end of the fuse to be ignited was positioned against the notch and then held in place using tape. In the first of these trials visco fuse was used, as shown in the upper pair of photographs of Figure 17. In these trials, four of four fuse ignitions were successful. The lower pair of photographs in Figure 17 is a similar notch coupling method this time using quick match with a short length of black match exposed. After the notch was made in the LTT, the black match was laid into the notch, folded back over the LTT and secured with 50-mm (2-in.) wide plastic packaging tape. In these trials, five of five fuse ignitions were successful.

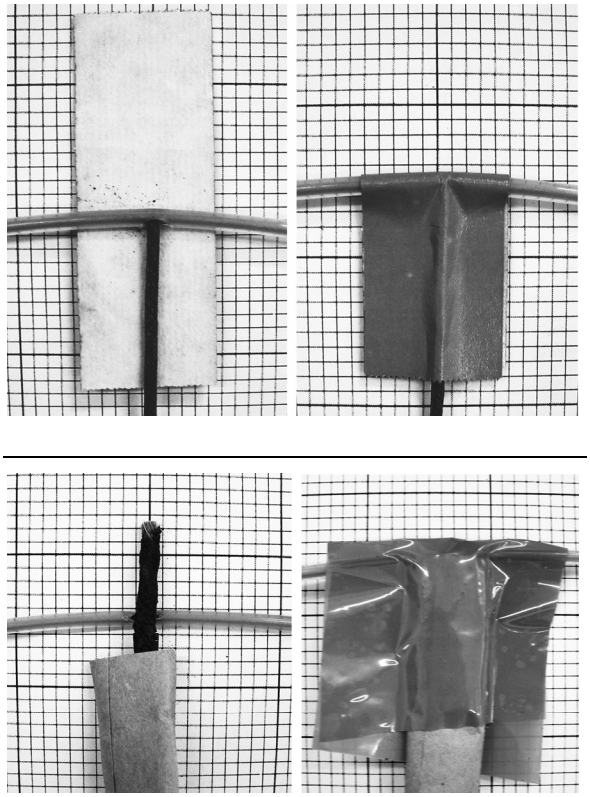

Figure 17. Photographs demonstrating the notch method of coupling fuse to LTT. The upper pair of photographs used visco fuse and the lower pair used a short length of black match from a shell leader. [2.5 mm (0.1 in.) per division.]

A final series of fuse ignition trials was attempted in which the end of the LTT was simply inserted into quick match either into the end of a length of quick match or through a small hole made in the match pipe somewhere along the length of quick match. Using either method, care was taken to assure that the end of the LTT was immediately alongside the black match in the shell leader. Shell leaders from three manufacturers (Thunderbird, Jumping Jack and Sunny) were used in these trials, where 14 of 14 attempts to ignite quick match were successful.

Having completed the trials of fuse ignition, LTT's ability to directly ignite a variety of pyrotechnic compositions was investigated. The results of these trials are presented in Table 6. In those trials, the powders, whether loose or granulated, were placed in a small container and the end of the LTT was introduced a short distance into the powder charge, as shown in Figure 18. The first powder type to be investigated was Black Powder. These trials used 3Fg, 4FA, 2FA commercially manufactured powder, loose fine-grained hand-made Black Powder, and Black Canyon™ powder (a commercial Black Powder substitute based on ascorbic acid as the primary fuel). In these trials, all 42 of 42 attempts produced successful ignitions of the powders.

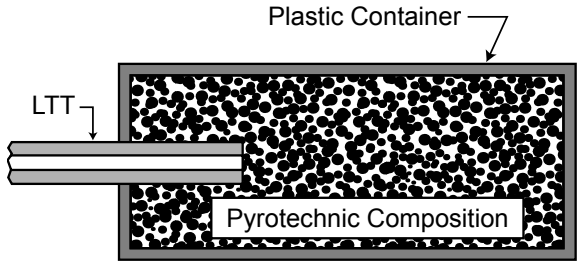

Figure 18. An illustration of the test method used in the trials of LTT ignition of loose pyrotechnic powders.

One potential drawback of the direct insertion method described above (as in Figure 18) is that it terminates the LTT line, which is then not available to produce additional ignitions. Thus a variation to the direct insertion method was tried. In one trial of the ignition of small charges of Black Powder, a series of four small mortar tubes were mounted over a single length of LTT

Table 6. Results of Testing LTT's Ability To Ignite Various Pyrotechnic Powders Directly.

Test Conditions[a]	Ignitions / Trials
3Fg Black Powder[b]	4 / 4
4FA Black Powder[b]	14 / 14
2FA Black Powder[b]	10 / 10
Unconsolidated (loose) hand-made Black Powder[b,c]	4 / 4
Black Canyon™ 2Fg powder (a Black Powder substitute)[b]	10 / 10
4FA Black Powder[d]	4 / 4
7:3 flash powder (potassium perchlorate and dark aluminum)[b,c]	3 / 3
4:2:1 flash powder (barium nitrate, dark aluminum and sulfur)[b,c]	3 / 3
IMR 7828 smokeless powder[b,e]	4 / 10
Pyropack 2-second titanium whistles[f]	3 / 3

a) To allow for the full development of LTT's propagating reaction, in each trial an approximately 300 mm (12-in.) length of LTT was provided before its attachment to a pyrotechnic powder. Trials were conducted at a temperature of approximately 15 °C (60 °F) and a relative humidity of less than 40%.

b) In the trials to ignite loose pyrotechnic powders, a small container, typically 12 by 50 mm (0.5 by 2 in.) was filled with the test powder. The LTT entered into the container through a hole, with the end of the LTT positioned a short distance into the powder charge. (See Figure 18.)

c) This powder was sufficiently fine grained that a small amount of powder might possibly have entered into the end of the LTT. In the event that such powder infusion needs to be avoided, the US distributor of LTT[1] suggests that the end of the LTT can first have a thin coat of nitrocellulose lacquer applied over the hole in the end of the LTT.

d) In this trial all four charges of Black Powder were simultaneously ignited using 4 notches cut into a single length of LTT (discussed further in the text).

e) This type of smokeless powder was chosen only because it was immediately available in the laboratory. It is a rather coarse powder and is somewhat unlikely to be chosen for most entertainment pyrotechnic uses. It is quite possible that a finer grained powder would be more readily ignited by LTT.

f) In this case the end of the LTT was inserted into the end of the whistle tube with the end of the LTT in near contact with the whistle composition and temporarily held in place with a small wad of tissue paper.

(see Figure 19). At the location of each tube, a notch had been cut in the LTT with a hand-held paper punch. The distance between notches was approximately 100 mm (4 in.). A small charge of 4FA Black Powder and a projectile were added to each of the four small mortar tubes. Upon firing the single LTT line, all four Black Powder charges were simultaneously ignited and successfully fired the four small projectiles into the air.

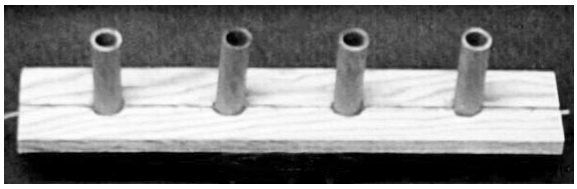

Figure 19. A photograph of the test configuration for simultaneously firing four small mortars from a single LTT line running under the mortars in a grove cut into the mounting board.

Next, two types of flash powder were used in the ignition trials. Both flash powders were of standard formulations. One was a mixture of potassium perchlorate (70%) and dark-pyro aluminum (30%), and the other flash powder was a mixture of barium nitrate (58%), dark-pyro aluminum (28%), and sulfur (14%). Again the end of the LTT was placed into a small charge of the powder (see Figure 18). In these trials, all six of six attempts produced successful ignitions.

One type of smokeless powder (IMR 7828) was used in the ignition trials. This type of smokeless powder was chosen only because it was immediately available in the laboratory. It is a rather coarse powder and is somewhat unlikely to be chosen for most entertainment pyrotechnic uses. Only four of ten attempts with this powder were successful. As a result, if it were desired to reliably ignite such fairly large particle size smokeless powders (and perhaps others as well) it is likely that the output of the LTT would need to be augmented, such as perhaps by first igniting a small charge of Black Powder.

As a final trial, the ignition of three small whistles (Pyropak, manufactured by Luna Tech, Inc.[12]) was attempted. In these attempts, the end of the LTT was simply inserted into the end of the whistle tube, such that the end of the LTT was in near contact with the compacted whistle composition. The LTT was temporarily held in place within the whistle using a small plug made of wadded-up tissue paper. All three whistle ignition trials were successful.

Conclusion

While the number of trials reported in this paper give some indication of the capabilities of Lightning Thermo Tube (LTT), often the number of individual trials was not statistically significant. This not withstanding, it seems reasonably certain that LTT is a useful product and will find a number of uses in fireworks and proximate audience pyrotechnics. Probably the most desirable features of Lightning Thermo Tube (LTT) are:

- Its ability to be reliably initiated using reasonably energetic electric matches (without having to use flame-to-shock converters).
- Its ability to reliably ignite typical pyrotechnic fuses and powders (without having to use shock-to-flame converters).
- Its ability to produce a bright flash of light (with or without a fairly loud explosive sound).
- Its resistance to accidental ignition due to strong impact and high temperature flame.
- Its ability to be coupled and branched using the same methods commonly used for shock tube.
- Its non-hazardous classification for transportation.

In considering the results reported in this paper, it is important to note that all trials were conducted at a temperature of approximately 15 °C (60 °F) and a relative humidity of less than 40%. Certainly, it is possible that the performance of LTT under more extreme conditions may be different. Thus further testing under more adverse conditions would be appropriate.

While there undoubtedly are many potential uses for LTT in fireworks and proximate audience performances, and while this paper may

have put readers in mind of some applications, it was not the purpose of this paper to suggest or recommend any specific applications for LTT.

Acknowledgments

The authors are grateful to R. Webb for supplying some patent and background information about thermo-tube, to R. Gilbert for supplying samples of LTT for evaluation, and to E. Contestabile and L. Weinman for commenting on an earlier draft of this paper.

Notes and References

1) Trade marked and distributed in the US by Lightning Thermo Tube, 12707 N. Freeway, Suite 330, Houston, TX, 77060, USA.

2) "Process for the Production of a Thermal Shock Tube", M. A. Falquete, US Patent Number 205/0109230 A1.

3) "Low Energy Fuse for Transmission or Generation of Detonation", P. A. Persson, Swedish patent 333 321, July 20, 1968.

4) "Wherl Element", P. A. Persson and G. Lithner, US patent 3-817-181, Jan. 5, 1972, granted Jan. 18, 1974.

5) *A New Non-Electric Blasting System – NONEL*, E. Contestabile, Energy Mines and Resources Canada, MRL/75-20, 1975.

6) In the 1990s in the US a product called No Match™ and intended for the firework trade, was introduced. No Match was based on conventional shock tube as used in the blasting industry. However, to facilitate its use in fireworks, it required flame-to-shock initiators for use with pyrotechnic fuse or electric matches, and shock-to-flame converters for reliable ignition of pyrotechnic materials.

7) Lightning Thermo Tube, Draft Technical Data Sheet, Sept. 2005.

8) The high frame-rate video camera was provided by Speed Vision, San Diego, CA, USA.

9) Martinez Specialties, Inc., 205 Bossard Rd., Groton, NY 13073, USA.

10) Material Safety Data Sheet, IBQ Industrias, Quimicas, Ltda, Quatro Barras, PR, Brasil.

11) "Classification of Explosives", US Department of Transportation, Tracking Number 2005030367, 2005.

12) Luna Tech, Inc., Owens Cross Road, USA.

13) "Evaluation of 'Quick-Fire' Clips", K. L. and B. J. Kosanke, *Fireworks Business*, No. 263, 2005; *Selected Pyrotechnic Publications of K. L. and B. J. Kosanke, Part 8 (2005 through 2007),* Journal of Pyrotechnics, 2009.

14) "Electric Shock Tube Firing Systems", K. L. Kosanke, *American Fireworks News*, 156, 1994; also in *Best of AFN III*, American Fireworks News, 1995; *Selected Pyrotechnic Publications of K. L. and B. J. Kosanke, Part 3 (1993 and 1994),* Journal of Pyrotechnics, 1996.

15) In one study of the ability for conventional shock tube to propagate its reaction through various lengths of inert tubing, it was found capable of spanning a length of nearly 200 mm (8 in.).[5]

16) The collections of photographs in Figures 8 and 9 were produced using a frame-rate of 20,000 fps; however, only every other photograph is included in the two figures. This was done to limit the size of the figures for publication.

An earlier version appeared in: *Fireworks Business*, No. 277, 2007.

Probabilities of Dying from Various Causes

K. L. and B. J. Kosanke

In the August 2006 issue of the *National Geographic*, S. Roth published a comparison of probabilities of Americans dying from various causes, based on 2003 data from the National Safety Council. The data provides some interesting information that helps to keep things in perspective when attempting to evaluate some of the risks associated with life. Table 1 below presents some of these data, comparing the number of fatalities from various causes to those from the use of fireworks. In Table 1 the relative numbers of fatalities have been normalized to 1 for firework fatalities. This was done to simplify making comparisons.

Table 1. A Comparison of the Annual Numbers of Fatalities for Various Occurrences.

Activity or Event	Relative Number of Fatalities
Fireworks Discharge	1
Lightning Strike	4
Legal Execution	5
Accidental Electrocution	34
Accidental Firearm Discharge	67
Bicycling Accident	68
Motorcycle Accident	340
Drowning	340
Pedestrian Accident	540
Firearm Assault	1000
Falling	1600
Suicide	2800
Motor Vehicle Accident	4100

According to these figures, 5 times as many people are legally executed than are being accidentally killed as a result of discharging fireworks. Similarly, 1000 times more people are murdered with a firearm than are killed as a result of discharging fireworks.

All this not withstanding, there are a number of ways for fireworks (especially consumer fireworks) to be made safer to use. Although the firework industry (especially through the American Fireworks Safety Laboratory) has done much to improve consumer firework safety in recent decades, there is more that can and should be done to further improve safety. In addition to being the right thing to do out of a sense of duty to the consumer, doing so also has the economic advantage of encouraging the continued expansion in the use of consumer fireworks.

An earlier version appeared in: *Pyrotechnics Guild International Bulletin*, No. 154, 2007.

A Study Evaluating the Potential for Various Aluminum Metal Powders To Make Exploding Fireworks

K. L. and B. J. Kosanke

Scope

This investigation was commissioned[1] to evaluate a range of various aluminum metal powders for their potential use in compounding flash powders for use in powerfully exploding devices such as so-called M-80s and devices of similar construction.

Introduction

Flash powders are used in fireworks to produce a bright flash of light and the loud sound of an explosion.[2] There is a general understanding among both pyrotechnic chemists and firework manufacturers of approximately what pyrotechnic compositions constitute being a flash powder. For example, to produce the bright flash of light, all flash powders must be capable of producing a high temperature as well as refractory reaction products.[3] Both of these results can be accomplished using some types of small particle-size aluminum metal powders.[4,5]

However, it needs to be understood that there are a wide variety of aluminum metal-containing pyrotechnic compositions, many of which are used for purposes other than to produce a bright flash of light and the loud sound of an explosion.[6,7] For those reasons, the question of exactly which pyrotechnic compositions are and which are not flash powders can be difficult to answer, especially for those compositions falling in the middle of the range of light and sound producing properties.[8]

The question, regarding exactly what is and what is not a flash powder, is further complicated by the fact that flash powder has never been quantified for regulatory purposes, [9] rather it has only been specified by the intended use of the composition, as in "intended to produce an audible report and a flash of light". Because of the lack of quantitative guidance from either science or regulation, it must be concluded that "flash powder" is a term of art. Accordingly, this study focuses more narrowly on the central issue at hand, i.e., which aluminum metal powders are reasonably suitable for the production of flash powders as used in relatively small salutes[10] (so called M-80s and other similarly-sized exploding items) as they are typically constructed by individuals (hobbyists).

There are two paramount requirements for the flash powders used in such salutes, and these two requirements form the basis for quantifying the flash powder performance of the range of aluminum metal powders being evaluated. The first requirement is that the potential flash powder be reasonably capable of ignition and subsequent propagation using a common firework safety fuse.[11,12] The second requirement for the aluminum metal powder is that it is capable of producing a flash powder that will explode relatively powerfully when confined inside a paper tube, as is typically used for so called M-80s and other similarly-sized exploding items as they are commonly constructed by individuals.[13]

Power is defined as the time rate of energy production or release. Thus, powerful explosions result when much energy is released and that energy is released very quickly. For pyrotechnic chemical reactions, the first of the two principal characteristics that determines its ability to produce powerful explosions is the amount of energy that is released in the pyrotechnic chemical reaction. For flash powders, the amount of energy produced is directly related to the choice of ingredients, with the combination of potassium perchlorate and aluminum producing more energy than any other commonly available chemicals.[5] The second characteristic relating to the power of explosions is the rate of the pyrotechnic chemical reaction that occurs upon its igni-

tion. For flash powders, the rate of the chemical reaction is most directly related to the surface-to-mass ratio of the individual aluminum metal particles, which in turn relates directly to its particle size and form (e.g., flakes versus spheroids[14]).[15]

Test Conditions

Over the period of the last 50 years, the most commonly used flash powder is one composed of an intimate mixture of 70% potassium perchlorate and 30% aluminum metal powder. While other formulations are occasionally used to manufacture exploding fireworks, an earlier study of the explosive power of a range of flash powders under modest confinement found that none of the other formulations investigated were more powerful than the 70:30 composition.[16] For this reason, and because this is the most commonly used formulation in the US, only the 70:30 flash powder formulation was used in this study.

In addition to a number of aluminum powders available in this laboratory, additional aluminum metal powder samples were provided by two suppliers of small quantity chemicals to the firework trade (Skylighter, Inc. and Firefox, Inc.). Appendix A lists information regarding the aluminum metal powders being evaluated.

Examples of the test salutes prepared for use in this study are shown in Figure 1, which consists of a photograph (showing both side and end views of a test salute) and a cross sectional drawing. The test units consisted of a spiral-wound paper tube with the following dimensions: outside diameter, 5/8 inch; wall thickness, 1/16 inch; and length, 1-1/2 inch.[17] The amount of powder encased in each of the tubes in preparation for testing was 1.00 gram.[18] The end plugs were 0.04 inch thick and were inserted to a total depth of approximately 0.5 inch into the ends of the tubes. The ignition fuse was a length of standard firework safety fuse, 3/32 inch in diameter visco fuse with an ample core of Black Powder.[19] The end plugs and fuse were glued in place using common white carpenter's glue, and the glue was allowed to dry for a day before the salutes were test fired.

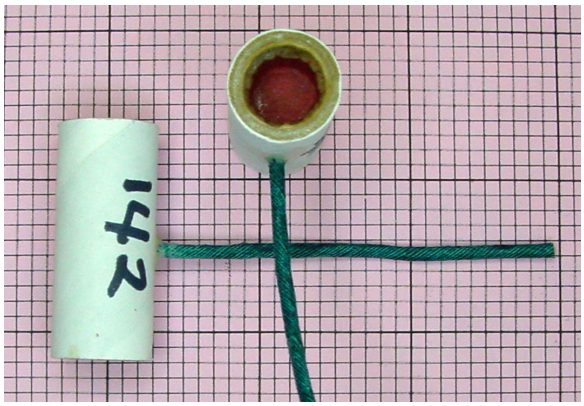

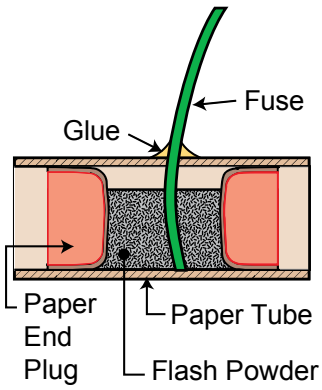

Figure 1. A photograph and cross sectional drawing of the test salutes used in this study.

Potential flash powder compositions were made using each of the various aluminum metal powders (see Appendix A) in the standard flash powder formulation (70% potassium perchlorate and 30% aluminum metal powder). The potassium perchlorate was –200 mesh technical grade of the type generally available for use in making pyrotechnic compositions.[20] The compositions were mixed using a combination of sieving and rotary tumbling. In preparation for testing, each of the potential flash powders was used to construct a group of 5 test salutes (as described and shown above). One at a time, a test salute was positioned at the top of a thin metal rod at a height of 4 feet above the ground. A pair of instruments[21] was used to measure the explosive sound output (blast pressure) of each test salute. This was accomplished by recording sound pressure levels at a distance of 10 feet from the test salute and at the same height above the ground as the test salute. One instrument was set to record peak sound pressure levels with linear frequency weighting (Linear-Peak). These settings

were selected because they would allow a direct conversion to the peak air blast pressure of the explosion (in pounds per square inch),[22] which can then be used to establish the power of the explosion.[23] The other instrument was set to record the maximum impulse sound pressure level using A-weighting of the frequency spectrum (A-weighted-Impulse).[24] The fuse of the test salute was ignited and the functioning (or lack of functioning) of the test salute was visually monitored. On many occasions, the test salute failed to explode (i.e., the flash powder failed to be ignited or did not appreciably propagate a chemical reaction). On those occasions when the test salute did explode, the resulting sound pressure levels were recorded.

Test Results

The full set of individual results from this series of explosive output measurements are presented in Appendix B of this report. Table 1 presents the average relative sound power results for each set of five test salutes for each aluminum metal powder evaluated. The results are listed in decreasing order of sound power.

Table 1. Explosive Output Measured for the Test Salutes.

Aluminum Metal Powder Type[a]	Relative Explosive Output [b] (%)
S-CH0100, ≈ 5 µ Atomized	100
S-CH0140, ≈ 50 µ Flake	69
Valimet-H2, 2.5 µ Atomized	67
US Alum-809, ≈ 40 µ Flake	64
ATA-2000, 36 µ Flake	59
US Alum-807, 11 µ Flake	53
S-CH0152, ≈ 8 µ Flake	50
Reynods-400, 4.5 µ Atomized	44
FF-C103GD, ≈ 15 µ Flake	43
S-CH0144, ≈ 3 µ Flake	39
US Bronze-913, ≈ 20 µ Flake	38
FF-C099B5M, ≈ 3 µ Atomized	36
FF-C099B2M, 1.5 µ Atomized	34
FF-C100, 36 µ Flake	22
S-CH0142, ≈ 40 µ Flake	21
FF- C102, ≈ 60 µ Flake	16
KSI 100 Mesh, ≈ 80 µ Flake	11
FF-C099C, ≈ 60 µ Flake	7
S-CH0155, 40–325 mesh Flitter	0 [c]
S-CH0148, –20 Flitter	0 [c]
S-CH0141, 16–325 mesh Flitter	0 [c]
S-CH0150, 10–12 mesh Flitter	0 [c]
Reynolds-S10, ≈ 12 µ Atomized	0 [c]
FF-C099B71, 13 µ Atomized	0 [c]
S-CH0105, ≈ 20µ Atomized	0 [c]
S-CH0103, ≈ 20µ Atomized	0 [c]
FF-C099BND, 21 µ Atomized	0 [c]
FF-C099B, 24 µ Atomized	0 [c]
FF-C099B14, 36 µ Atomized	0 [c]
S-CH0120, 80–325 mesh Atom.	0 [c]
FF-C099AFF, 40–270 m G. Flk.	0 [c]
FF-C099A150, 50–150 m Gran.	0 [c]
FF-C099M100, 100 mesh Gran.	0 [c]
FF-C099ES, Granular Chips	0 [c]

a) Average particle sizes are given in microns, abbreviated with the symbol µ for particle sizes up to 100 microns. For information on why this was done and a definition of micron, see note "b" to Appendix B.

b) Sound power is proportional to the square of the peak air blast pressure. Thus the measured average sound pressures from the table in Appendix A were squared, normalized to the greatest average sound pressure observed for any aluminum metal powder, and reported a percentage.

c) The test salutes made with these aluminum metal powders failed to explode; thus their explosive power was zero.

Conclusions

A. It was established that there are two requirements that qualify an aluminum metal powder as having a reasonable potential for use in making exploding items such as so-called M-80s and similarly constructed items. The first requirement is that the flash powder made from the aluminum metal powder must be reasonably readily ignited by the thermal action of a burning firework safety fuse (i.e., common visco fuse) and that the pyrotechnic reaction then propagates explosively under the expected confinement conditions. From the detailed data reported in the table in Appendix B and listed as having zero sound power in Table 1, it can be

seen that 16 of the aluminum metal powders tested failed to meet the ignition and propagation requirement for an aluminum metal powder to be suitable for making a flash powder.

B. The second requirement established for an aluminum metal powder to be useful in making a flash powder is that the flash powder made with the aluminum metal powder produces a relatively powerful explosion. Deciding just how powerful an explosion qualifies as a relatively powerful explosion is a subjective decision. It is not readily amenable to being answered scientifically, and so it is left to others to decide. However, if the threshold were set at 50% in Table 1, then another 11 of the aluminum metal powders would be eliminated as being reasonably suitable flash powder aluminums for salutes of the size and construction as used in these tests. If the explosion power threshold were set at 30 %, then only an additional 5 aluminum metal powders would be eliminated as reasonably suitable flash powder aluminums.

C. It is generally true that aluminum metal powders with a small average-particle size tend to be suitable for making flash powders,[25] and those with a large average-particle size are not suitable for making flash powders.[26] However, for those aluminum metal powders with an average-particle size in a broad mid-range, considering particle size alone will not allow one to assuredly determine their usefulness to make flash powders.[27] Because the performance of individual types of aluminum metal powder of a given particle size may vary widely, the only way to be assured of properly quantifying their performance in flash powders is to test them under the expected conditions of use. This not withstanding, it is possible to separate aluminum metal powders into three generalized categories regarding their potential to qualify as suitable for making flash powders for use in small salutes (such as so-called M-80s and other similarly sized and constructed items). Based on the results of this study and consistent with prior experience in this laboratory, the conclusions are summarized in the Table 2.

Table 2. The Suitability of Various Aluminum Metal Powders for Making Flash Powders.

Powder Type	Particle Size Range		
	Suitable	Questionable	Unsuitable
Atomized	Less than 6 microns	6 to 10 microns	Greater than 10 microns (a)
Flake	Less than 40 microns	40 to 75 microns	Greater than 75 microns (b)

a) This would correspond to a mesh size of approximately 1000, if such a sieve existed.

b) This corresponds to a mesh size of approximately 200.

Acknowledgment

The authors gratefully acknowledge the suggestions of L. Weinman, H. Gilliam, J. Steinberg and T. Handel on an earlier draft of this article.

Notes and Literature References

1) Because of the authors' long term research interest in the subject of the chemistry and characteristics of flash powder, combined with an agreement that this laboratory was free to publish and use any or all of the results produced in the current study, the authors funded the major portion of the current study. Some additional funding was provided by the Pyrotechnics Guild International, Inc.; the Fireworks Foundation, Inc.; and Skylighter, Inc.

2) *The Illustrated Dictionary of Pyrotechnics*, K. L. and B. J. Kosanke, et al., Journal of Pyrotechnics, 1996.

3) "From a Technical Standpoint, What is Flash Powder?", K. L. Kosanke and L. Weinman, *Fireworks Business*, No. 246, 2004; *Selected Pyrotechnic Publications of K. L. and B. J. Kosanke, Part 7 (2003 and 2004),* 2006.

4) In this investigation, only aluminum metal powders were investigated for use in making flash powder. The reasons for this are two fold. 1) Thermodynamic free energy

minimization calculations reveal that aluminum produces the greatest amount of energy in pyrotechnic reactions, in contrast with other potentially usable metal powder candidates. [5] 2) In the US, aluminum metal powder is by far the most commonly used fuel in making exploding fireworks.

5) Thermodynamic calculations were performed using the ICT (Institute for Chemical Technology) and the NASA (National Aerodynamics and Space Administration) thermodynamic modeling codes.

6) These other common uses probably account for roughly 80 to 90 percent of the aluminum metal powder used in pyrotechnic compositions. Some examples of other common uses for small particle size aluminum metal powders are: 1) in common hand-held sparklers, 2) as a flame brightening agent for colored flame effects, 3) as the active ingredient in both glitter and flitter comet effects, and 4) as an agent used to modify the burn rate of pyrolants.

7) **"**Aluminum Metal Powders Used in Pyrotechnics", K. L. and B. J. Kosanke, *Pyrotechnics Guild International Bulletin*, 85, 1993; *FPAG*, Vol. 6, No. 7, 1997; *Selected Pyrotechnic Publications of K. L. and B. J. Kosanke, Part 3 (1993 – 1994),* 1996.

8) The burning of essentially any firework composition – by its very nature as a pyrotechnic material – is capable of a self-contained and self-sustained chemical reaction that releases energy,[2]**Error! Bookmark not defined.** will produce some light and, if sufficiently well confined, will have the potential for producing the sound of an explosion.

9) "As Defined in Regulation, What is Fireworks Flash Powder?", K. L. Kosanke and L. Weinman, *Fireworks Business*, No. 244, 2004; *Selected Pyrotechnic Publications of K. L. and B. J. Kosanke, Part 7 (2003 – 2004),* 2006.

10) A salute is the descriptive term for a firework that is principally designed to explode violently so as to produce a loud sound. [2]

11) Fireworks safety fuse is also known as visco fuse, hobby fuse and cannon fuse. It is composed of an ample core of fine-grained Black Powder and is relatively heavily wrapped with two layers of cotton thread.[2]

12) If the potential flash powder can not be ignited or does not propagate reasonably completely, then it cannot produce a bright flash of light and the sound of an explosion as are required for a flash powder.

13) If the aluminum metal powder to be used in a potential flash powder does not produce a reasonably powerful explosion, then there is little if any reason for someone to devote the time, expense and effort to acquire all of the needed chemicals and materials, to make the flash powder and then to construct the salute.

14) Flake aluminum metal powders are typically produced in a milling process wherein larger particles are in effect hammered into thin flakes. However, to keep the flakes from sticking together and being hammered back into larger particles, it is necessary to use a lubricant such as stearin to coat the individual particles during the milling process.[7] Spheroidal aluminum metal powders are produced in an atomizing process wherein molten aluminum is sprayed into a more or less inert atmosphere. When the atmosphere has modest oxygen content, an oxide coating quickly forms on the particles, which results in their freezing-out as distorted spheroids (grossly out-of-round particles). If the atmosphere is more nearly inert, the atomized aluminum particles take comparatively well-rounded shapes (more nearly spherical) before they solidify. Below are three photo-micrographs, demonstrating the typical appearance of aluminum metal powder as flakes, and so called spheroidal and spherical atomized particles of aluminum metal powder.

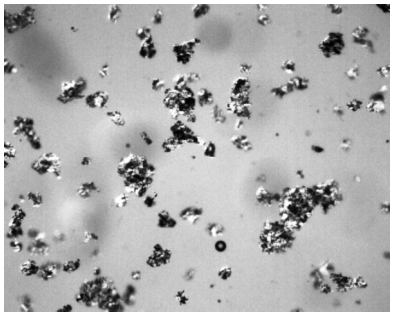

Eckart, SDF 4-591, flake

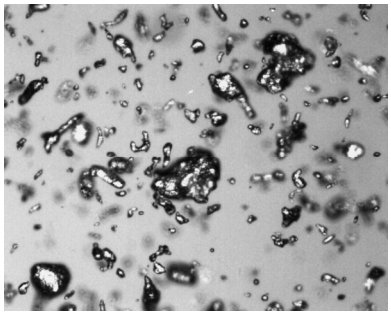

Toyal, ATA-101, spheroidal

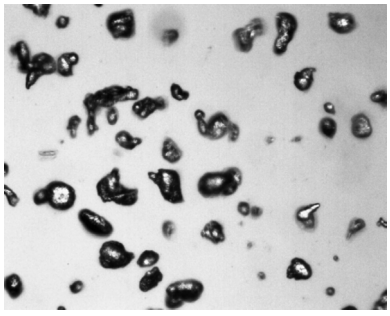

Valimet, H-30, spherical

15) *Pyrotechnic Chemistry*, Chapter 5, "Control of Pyrotechnic Burn Rate", K. L. and B. J. Kosanke, et al., Journal of Pyrotechnics, 2005.

16) "Flash Powder Output Testing: Weak Confinement", K. L. and B. J. Kosanke, *Journal of Pyrotechnics*, No. 4, 1996; *Selected Pyrotechnic Publications of K. L. and B. J. Kosanke, Part 4 (1995 through 1997),* 1999.

17) Historically, this is the approximate size of a typical consumer M-80 or Silver Salute.

18) This amount of flash powder is 20 times the maximum powder content allowed in consumer firecrackers and is approximately the same powder content of currently available pest and predator control devices. (Pest and predator control devices are relatively small exploding items most typically used by individuals and various agencies to disperse wildlife from crops, fishing nets, airport runways, etc. These items tend to be quite similar in physical construction to the test salutes used in this study.)

19) This is also the type of fuse almost universally used to make this type of exploding firework as well as that used to manufacture pest and predator control devices.

20) It had been confirmed in earlier studies that the explosive power of flash powders are relatively independent of the exact nature of the potassium perchlorate used in their manufacture.[16]

21) These instruments were Quest Technologies models 1800 and 2700, set to record "Linear-Peak" and "Maximum A-Weighted Impulse" sound pressure levels, respectively.

22) Calculated as described in *Van Nostrand's Scientific Encyclopedia*, 5th ed., Van Nostrand Reinhold, 1976, p 25.

23) "Correspondence: Flash Powder Output Testing: Weak Confinement", K. L. and B. J. Kosanke, *Journal of Pyrotechnics*, No. 5, 1997.

24) Standards for the permissible exposure to impulse sounds (e.g., the sounds of explosions) are typically based on measurements made with instrument settings of A-weighted Impulse sound pressure levels.

25) It would be a mistake to assume that the only reasonable or practical use for small particle size aluminum metal powders is to make flash powders. (See again references 6 and 7 for more information.)

26) In properly formulated flash powders, small particle size aluminum metal powders are relatively easily ignited, and once ignited the aluminum particles participate vigorously and fully in the energy producing chemical reactions to produce a powerful explosion. To the contrary, large particle size aluminum metal powders used in flash powders will be difficult or impossible to ignite, and if ignited, they generally will not propagate throughout the composition. Even if ignition and propagation of larger particle size aluminum particles were somehow achieved, only a portion of the energy producing potential for the aluminum will be realized. This is because a significant amount of the energy is produced after the explosion (if there is one) as the still burning aluminum particles (seen as sparks) radiate outward.

27) For example, for flake powders, it is more nearly the thickness of the individual flakes

that is the determinant factor (in whether an aluminum metal powder will be useful in making flash powders), rather than the other linear dimensions (size) of the flakes. The nature of the distribution of particle size about the average will also affect the aluminum metal powder's performance in flash powder. Further, the lubricant coating on the flakes, such as almost always necessitated in the small flake manufacturing process, also generally limits the effectiveness of the flake aluminum in making flash powders. Beyond this, the thickness of the oxide coating that is allowed to form on the flakes affects the aluminum metal powder's usefulness in making flash powders. There are similar factors that affect the performance of atomized aluminum metal powders. However, atomized particles (being spheroids) are substantially thicker than flakes of the same particle size. The result is that only very much smaller particle size atomized aluminum metal powders, in comparison with flake powders, are useful in making flash powders.

Appendix A: Information Regarding Aluminum Metal Powders Used in This Study.

Designation [a]	Manufacturer and Product Number	Product Type	Average Particle Size and Other Information [b]
S-CH0144	Unknown, Indian GD	Flake	≈ 3 microns [c]
Obron GD	Obron Atlantic, 5413	Flake	≈ 5 microns [c]
S-CH0152	Eckart, 5413-H Super	Flake	≈ 8 microns [c]
USA-807	US Aluminum, 807	Flake	11 microns, coated [d]
FF-C103GD	Eckart, 10980	Flake	≈ 15 microns [b]
USB-913-S	US Bronze, 913-S	Flake	≈ 20 microns [c]
ATA-2000	Alcan-Toyo America, 2000	Flake	36 microns, coated [d]
FF-C100	Alcan-Toyo America, 2500	Flake	36 microns, coated [d]
S-CH0142	Eckart, SDF 4-591	Flake	≈ 40 microns [c]
USA-809	US Aluminum, 809	Flake	≈ 45 microns [c]
S-CH0140	US Aluminum, 808	Flake	≈ 50 microns [c]
FF-C099C	Eckart, U2	Flake	≈ 60 microns [c]
FF-C102	Eckart, HL/NE	Flake	≈ 60 microns [c]
KSI-100	Unknown	Flake	≈ 80 microns [c]
S-CH0155	Transmet, unknown	Flitter [e]	40-325 mesh [f]
S-CH0148	Eckart, 41813/G	Flitter [e]	–20 mesh [f]
S-CH0141	US Aluminum, 812	Flitter [e]	16–325 mesh [f]
S-CH0150	Transmet, K-102	Flitter [e]	10–12 mesh [f]
FF-C099B2M	Alcan-Toyo America, ATA 5621	Atomized	1.5 microns [d]
Val-H2	Valimet, H2	Atomized	2.5 microns, spherical [d]
RA-400	Reynolds Aluminum, 400	Atomized	4.5 microns, spheroidal [d]
S-CH0100	Unknown	Atomized	≈ 5 microns, spherical [c]
FF-C099B5M	Alcan-Toyo America, ATA105	Atomized	5.5 microns spherical [d] [g]
RA-S10	Reynolds Aluminum, S10	Atomized	≈ 12 microns, spherical [c]
FF-C099B71	Alcan, XC-71	Atomized	13 microns, spherical [d]
S-CH0105	Unknown	Atomized	≈ 20 microns, spheroidal [c]
S-CH0103	Unknown	Atomized	≈ 20 microns, spherical [c]
FF-C099BND	Alcoa, 1641/L	Atomized	21 micron spherical, coated [d]
FF-C099B	Valimet, H-30	Atomized	24 microns, spherical [d]
FF-C099B14	Toyal America, ATA101SS	Atomized	36 microns, spheroidal [d]
S-CH0120	Unknown	Atomized	80–325 mesh, spheroidal [f]
FF-C099AFF	Unknown	G. Flk. [h]	40–270 mesh [f]
FF-C099A150	Unknown	Granular	50–150 mesh [f]
FF-C099M100	Unknown	Granular	≈ 100 mesh [c]
FF-C099ES	Unknown	Gran. Ch.	Fine chips [f]

a) This is how the aluminum metal powders are identified in the table of results in this report. The aluminum powders starting with "S" were from Skylighter and those starting with "FF" were from Firefox.

b) For consistency and convenience in this study, most aluminum metal particle sizes are stated as averages given in microns. Only the very largest particles list a mesh range. For comparison, a 325-mesh standard sieve has openings that are 34 microns, and a 100 mesh standard sieve has openings that are 150 microns.)

c) This is the approximate average particle size estimated using photo micrographs of the aluminum powders.

d) This is the average particle size as taken from the manufacturer's specification for the product.

e) Flitters are a type of relatively large, thick flakes, usable almost exclusively for spark effects in comets.

f) This is the particle size as stated by the pyro-chemical supplier.

g) Based on photo micrographs, the average particle size appears to be approximately 3 microns, rather than the 5.5 microns as reported in the manufacturer's product specifications.

h) Described by the supplier as "ground flake".

Appendix B: Explosive Output Measured for the Test Salutes

Powder Type	Explosive Output (a) Peak Air Blast Pressure (psi) / A-Weighted Impulse) (dB)					
	Test 1	Test 2	Test 3	Test 4	Test 5	Averages
S-CH0100, ≈ 5µ Atomized	0.32/130	0.32/131	0.46/132	0.32/131	0.32/131	0.348/131.0
S-CH0140, ≈ 50µ Flake	0.32/131	0.29/131	0.26/131	0.29/130	0.29/130	0.290/130.6
Valimet-H2, 2.5µ Atomized	0.29/129	0.26/129	0.29/130	0.29/130	0.29/130	0.284/129.6
US Alum-809, ≈ 40µ Flake	0.26/127	0.29/129	0.29/130	0.26/129	0.29/130	0.278/129.0
ATA-2000, 36µ Flake	0.26/129	0.29/129	0.18/127	0.32/131	0.29/130	0.268/129.2
US Alum-807, 11µ Flake	0.26/128	0.26/129	0.23/127	0.29/130	0.23/130	0.254/128.8
S-CH0152, ≈ 8µ Flake	0.32/130	0.23/128	0.16/128	0.23/130	0.29/130	0.246/129.2
Reynods-400, 4.5µ Atom.	0.29/128	0.16/129	0.16/126	0.29/130	0.26/129	0.232/128.4
FF-C103GD, ≈ 15µ Flake	0.23/131	0.16/131	0.23/130	0.26/130	0.26/131	0.228/130.6
S-CH0144, ≈ 3µ Flake	0.16/130	0.23/130	0.23/130	0.23/130	0.23/130	0.216/130.0
US Bronze-913, ≈ 20µ Flake	0.29/130	0.07/122*	0.13/126*	0.29/130	0.29/131	0.214/127.8
FF-C099B5M, ≈ 3 µ Atom.	0.18/130	0.23/131	0.23/131	0.23/131	0.18/130	0.210/130.6
FF-C099B2M, 1.5 µ Atom.	0.20/131	0.23/131	0.20/130	0.20/130	0.18/130	0.202/130.4
FF-C100, 36 µ Flake	0.14/127*	0.29/130	0.16/129	0.08/124*	0.14/127	0.162/127.4
S-CH0142, ≈ 40µ Flake	0.16/124	0.06/118*	0.02/107*	0.26/128	0.29/130	0.158/121.4
FF- C102, ≈ 60 µ Flake	0.09/126*	0.08/124*	0.26/130	0.11/126	0.16/128	0.140/126.8
KSI 100 Mesh, ≈ 80 µ Flake	0.08/124	0.04/120*	0.16/130	0.23/129	0.08/124*	0.118/125.4
FF-C099C, ≈ 60 µ Flake	0.06/121*	0.10/125*	0.13/126*	0.11/125*	0.06/123*	0.092/124.0
S-CH0155, 40-325 M Flitter	ftp	ftp	ftp	ftp	ftp	ftp
S-CH0148, –20 Flitter	ftp	ftp	ftp	ftp	ftp	ftp
S-CH0141, 16–325 M Flitter	ftp	ftp	ftp	ftp	ftp	ftp
S-CH0150, 10–12 M Flitter	ftp	ftp	ftp	ftp	ftp	ftp
Reynolds-S10, ≈ 12 µ Atom.	ftp	ftp	ftp	ftp	ftp	ftp
FF-C099B71, 13 µ Atom.	dne	dne	ftp	dne	ftp	ftp/dne
S-CH0105, ≈ 20µ Atomized	ftp	ftp	ftp	ftp	ftp	ftp

Powder Type	Explosive Output (a) Peak Air Blast Pressure (psi) / A-Weighted Impulse) (dB)					
	Test 1	Test 2	Test 3	Test 4	Test 5	Averages
S-CH0103, ≈ 20µ Atomized	ftp	ftp	ftp	ftp	ftp	ftp
FF-C099BND, 21 µ Atom.	ftp	ftp	ftp	ftp	ftp	ftp
FF-C099B, 24 µ Atomized	ftp	ftp	ftp	ftp	ftp	ftp
FF-C099B14, 36 µ Atomized	ftp	ftp	ftp	ftp	ftp	ftp
S-CH0120, 80–325 M Atom.	ftp	ftp	ftp	ftp	ftp	ftp
FF-C099AFF, 40–270 M Gr.	ftp	ftp	ftp	ftp	ftp	ftp
FF-C099A150, 50–150 M. G.	ftp	ftp	ftp	ftp	ftp	ftp
FF-C099M100, 100 M. Gran.	ftp	ftp	ftp	ftp	ftp	ftp
FF-C099ES, Granular Chips	ftp	ftp	ftp	ftp	ftp	ftp

a) Peak air blast pressures (P) in units of pounds per square inch are derived from Linear-Peak decibel values (dBLP) using the definition of decibel (dBLP = 170.8 - 20 log P). In this study, the individual measurements and the averages are reported to two and three decimal places, respectively. The individual measurements and the averages of the A-Weighted Impulse sound pressure levels are reported to the nearest dB and to one decimal place, respectively.

* means that the tube itself did not explode, but rather blew-out one or both end plug(s).

"ftp" means that there was a "Failure to propagate". There was no reaction and the test salute did not explode. In essence the potential flash powder did not ignite (but it may have produced a few sparks out of the fuse hole as long as the fuse was still burning within the test salute).

"dne" means that the test salute "Did not explode", but the flash powder did burn somewhat with a brief jet of flame and sparks from the fuse hole.

An earlier version appeared in: *The Proceedings of the10th International Symposium on Fireworks*, 2007.

Forensic Accident Investigation Using Pyrotechnic Reaction Residue Particle Analysis

K. L. Kosanke[*], R. C. Dujay[†] and B. J. Kosanke[**]

[*] PyroLabs, Inc., 1775 Blair Rd, Whitewater, CO 81527, USA email: ken@jpyro.com

[†] Mesa State College, Electron Microscopy Facility, Grand Junction, CO 81501, USA

[**] Journal of Pyrotechnics, Inc., 1775 Blair Rd, Whitewater, CO 81527, USA email: bonnie@jpyro.com

ABSTRACT

Pyrotechnic reaction residue particle (PRRP) production, sampling and their basic analyses are similar to that for primer gunshot residue (PGSR). Both types of particles originate from energetic chemical reactions that generate products that are initially melted and/or vaporized. These chemical reaction products are dispersed by the temporary and permanent gases from the chemical reaction. Then the reaction products solidify and are deposited as tiny spheroidal particles on objects in the area. Sampling is accomplished using conductive carbon adhesive dots. Analysis is performed using scanning electron microscopy to locate potential PRRPs and energy dispersive X-ray spectroscopy is used to characterize the signature of each suspect particle's constituent chemical elements.

Often, standard micro-analytical chemistry performed on pyrotechnic residues cannot be expected to provide sufficient information for an investigation of the cause and course of an accident. On those occasions, PRRP analysis generally provides important information that is not otherwise available. For example, there are times when standard micro-analytical chemistry will fail to discriminate sufficiently between materials of pyrotechnic origin and other unrelated substances also present on the items being sampled. In addition, there are times when PRRP analysis can help identify details concerning the cause and course of events that are simply beyond the capability of micro-analytical chemistry.

Introduction

In the course of pyrotechnic reactions, residues (reaction products) are generated. This is true whether the reaction is occurring in the primer of an small arms ammunition cartridge, in a pipe bomb or in a firework device. A large portion of the reaction products from nearly all pyrotechnic compositions are solids at room temperature. As such these reaction products are potentially available for collection and analysis using a methodology similar to that used for primer gunshot residues (PGSR). In many cases, pyrotechnic reaction residue particle (PRRP) analysis is a useful adjunct to conventional micro-analytical chemistry since it can provide forensic information not otherwise provided (or not provided with a high confidence level).

Much of the current interest in pyrotechnic reaction residue particle (PRRP) analysis[1–4] originated with articles expressing concern that some fireworks might be capable of producing residue particles meeting the forensic criteria for PGSR.[5–7] PRRP production, sampling and their basic analysis are similar to that of PGSR. Both types of residue originate from energetic chemical reactions that generate products that are initially melted and/or vaporized. These chemical reaction products are dispersed by the temporary and permanent gases produced by the reaction. Then the reaction products solidify as tiny spheroidal particles deposited on objects in the area.

Residue sampling is generally accomplished using conductive carbon adhesive dots or tape. Then the preferred method of analysis of those residues is to use scanning electron microscopy

(SEM) to locate suspect pyrotechnic reaction residue particles. Those suspect particles are then analyzed in the SEM using X-ray energy dispersive spectroscopy (EDS) to develop the suspect particle's signature of constituent chemical elements.

As an example of when and to what extent PRRP analysis can be helpful, consider the following. Standard micro-analytical chemistry may fail to discriminate sufficiently between pyrotechnic residues and other unrelated substances also present on items sampled after an accident. These unrelated substances may predate the pyrotechnic incident, they may be contributed during the course of the event but are not from the pyrotechnic composition, they may be deposited post-event, or they may result from any combination of these three possibilities.

When unrelated materials are known to be present, sometimes they can be successfully accounted for with standard micro-analytical chemical analyses, although this will require additional or more complex analyses. However, when unrelated material is not known to exist or if it shares chemical species in common with the pyrotechnic composition, erroneous information is likely to result. In such cases, these unrelated residues could be incorrectly identified as being part of the pyrotechnic residue, or those species in common could be missed because of having been attributed to a non-pyrotechnic source. In this case the morphologic specificity of PRRP (spheroidal particles that range from about 0.5 to 20 micrometers) will generally allow the successful differentiation between PRRP and non-PRRP (background) materials. This plus an analysis of the chemical elements present in the particles, provide highly reliable identification of PRRP and the characteristics of the pyrotechnic material that produced them.

Another example of the special capabilities of PRRP analysis is that it can be used to differentiate between pyrotechnic residues present on the same item, but contributed by different pyrotechnic sources, possibly at different times. With such information, insight can often be gained into the cause and course of an incident that could never have been possible using standard analytical methods. This is because standard micro-analytical chemistry produces a single set of results representing the combined total of the various different pyrotechnic residues present on a sampled item, whereas PRRP analysis can generally differentiate between the different pyrotechnic residue sources.

The special capabilities of PRRP analyses are demonstrated later in this paper by reviewing three specific examples.

SEM/EDS Basics

In its simplest terms, the operation of a SEM can be described as follows. An electron gun produces high-energy electrons that are focused and precisely directed toward a target specimen in a vacuum (Figure 1). As a result of this bombardment, among other things, low energy secondary electrons are produced through interactions between the beam electrons and the atoms in the specimen. In one commonly-used SEM mode, these secondary electrons are collected and used to generate an electronic signal, where the amplitude of the signal is dependent on the nature and spacial features of the portion of the specimen being bombarded at any given time. The impinging electron beam can be systematically moved over the specimen in a rasterized pattern of scans (Figure 2). The resulting secondary electron signal can then be used to create an overall (television-like) image of that portion of the specimen being scanned. Because the inci-

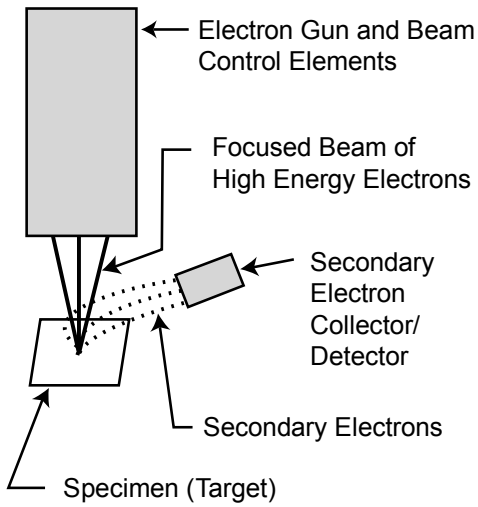

Figure 1. An illustration of some aspects of production and collection of secondary electrons in a SEM.

dent beam of electrons is highly focused and because the pattern of scans across the specimen can be precisely (microscopically) controlled, the image produced is of high spatial resolution and can be highly magnified (easily to 20,000 times).

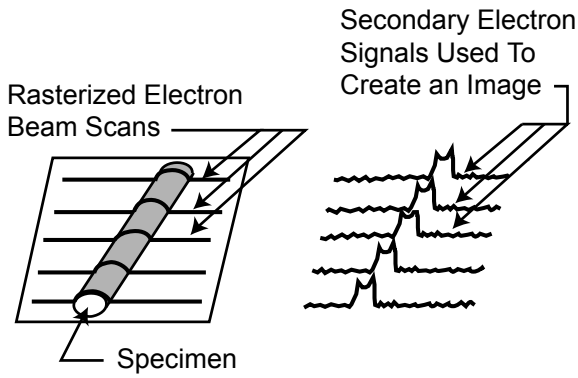

Figure 2. An illustration of some aspects of the production and collection of secondary rasterized SEM scanning to produce an electron in a SEM image.

In addition to the production of secondary electrons, another result of the interaction of the electron beam with the target specimen is the production of X-rays. These X-rays are uniquely characteristic of the atoms that produced them. By detecting and analyzing the energies of the X-rays that are generated, the identity of the chemical elements in the target specimen can be uniquely determined.

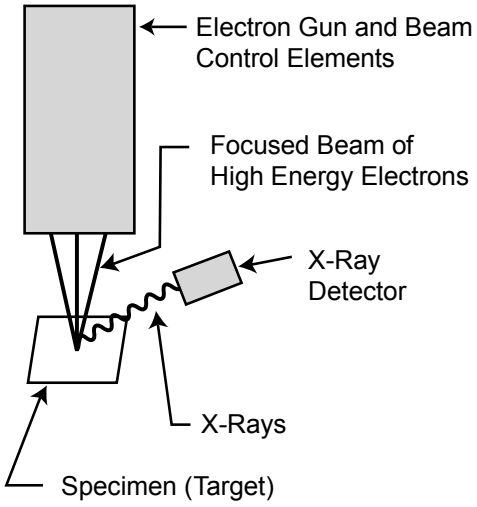

Figure 3. Illustration of some aspects of the production and detection of X-rays in a SEM.

The most common method for analyzing the X-rays produced by the specimen is described as energy dispersive spectroscopy (EDS) using a solid state X-ray detector as shown in Figure 3. The output of this detector consists of electronic pulses that are proportional to the X-ray energies being deposited in the detector. Using a multichannel analyzer (MCA), the pulses are sorted according to voltage (i.e., X-ray energy) and the results (Figure 4) are then stored for subsequent interpretation (i.e., the identification of the atomic elements present).

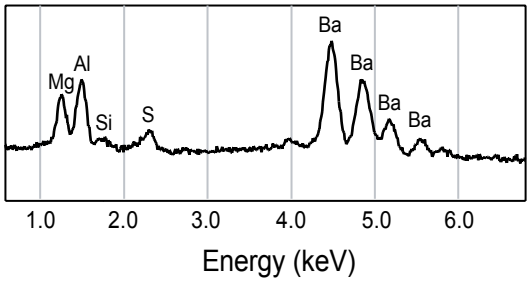

Figure 4. Illustration of an X-ray energy spectrum produced using EDS in a SEM.

Accordingly, the combination of SEM/EDS allows (with some limitations) the microscopic imaging of specimens and the determination of the chemical elements present in the individual particles in those specimens. This is a powerful combination of capabilities that allows for the rapid identification and characterization of PRRP.

Particle Morphology

Most often there are easily discernable differences between PRRP morphologies and those of geologic soil particles. As shown in Figure 5 the vast majority of PRRP are spherical or at least spheroidal in shape, with a substantial fraction of those particles falling in the range of 0.5 to 20 micrometers in diameter. By comparison, most soil (dirt) particles in this same size range have angular features as shown in Figure 6. However, this difference cannot be absolutely

relied upon. Some geologic particles can be spheroidal as the result of their having been mobile in the environment for a long time, during which time abrasive action tends to remove their sharp angular features. Also some organic particles (e.g., grass pollen) are roughly spheroidal in shape and are in the size range of PRRP. Even though morphology alone does not provide absolute certitude with regard to identifying PRRP, using morphology allows one to eliminate the vast majority of non-PRRP from consideration. Then using EDS, the remaining non-PRRP can readily be eliminated from consideration.

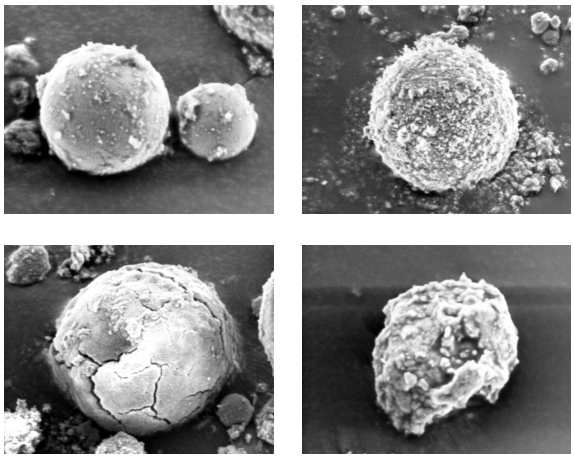

Figure 5. Examples of 10 to 20 micrometer spheroidal pyrotechnic reaction residue particles (PRRP).

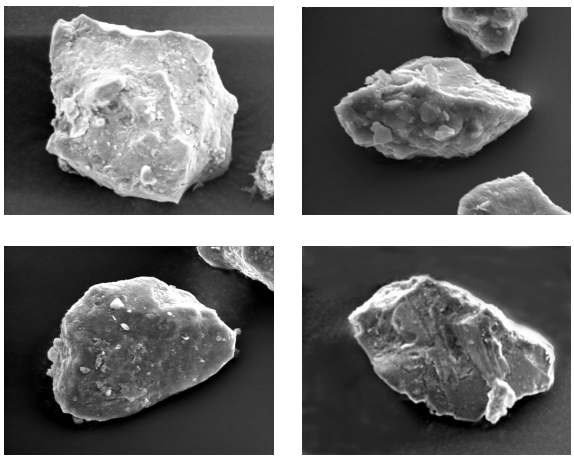

Figure 6. Four examples of typical 10 to20 micrometer particles of geologic origin (soil).

Basic PRRP Methodology

The basic methodology of PRRP analysis has much in common with standard forensic trace analysis using an SEM with EDS capability. First samples are collected, generally from objects in the immediate area of a pyrotechnic event and also from persons and their clothing when that is available. In many cases the residues on objects near the seat of the event will be visible as a whitish, grayish or blackish haze on the surface of the objects. Residue samples are collected using conductive carbon adhesive dots (often 13 mm in diameter) such as commonly used for SEM work.

Except when attempting to produce relatively high quality images, the residue samples are generally not carbon or sputter coated prior to analysis. This is because the PRRP and other particles collected are generally sufficiently conductive that they do not cause serious problems with charging from the electron beam. Also, because atomic number discrimination, based on back scatter contrast differences, is rarely if ever useful in identifying PRRP, the SEM is typically operated in the secondary electron mode. Accordingly minor problems with excessive contrast can generally be tolerated.

In the search for and characterization of PRRP on an object thought to have been exposed to a pyrotechnic event, primary attention is paid to those particles of the correct morphology, as discussed above. These suspect particles are then analyzed using X-ray EDS and the information is archived. During this particle search process, usually a moderate number of non-PRRP are also investigated using EDS. This helps to establish the components present in the background particles on that specific item. (It is possible that this background material may be different than that on other items and in bulk background samples taken from the area in general.) Analysis of the background components on individual items may thus be useful to increase ones confidence in the identification and characterization of PRRP in some cases.

Having found and characterized a sufficient quantity of PRRP, it will always be possible to conclude something definitive about the nature of the pyrotechnic material involved. However, it is often necessary for the analyst to have a

thorough knowledge of the pyrotechnic chemistry of both the materials used and their reaction products under the conditions of the event. This may be more complicated than might at first be appreciated, and it is sometimes necessary to use thermo-chemical modeling to correctly account for the reaction products. (While most interesting, because of its length, a proper discussion of this subject must be delayed for a subsequent paper.)

As a brief example, consider the X-ray spectra shown in Figure 7. These were produced as part of the investigation of an accident where an individual received burns when a firework allegedly exploded and sent burning pieces of pyrotechnic composition in his direction. Uppermost is the gross spectrum of the unreacted firework composition taken from the type of firework alleged to have been responsible for the injury. In the middle is a spectrum that is typical of a PRRP produced by burning this same pyrotechnic composition under laboratory conditions. Lowermost is a spectrum that is typical of PRRPs taken from the clothing of the burn victim. In comparing the two lower spectra, note that the spectrum of PRRPs from the victim is consistent with having been produced by the suspect firework. (Note that "consistent with" is not the same as "produced by". It is certainly possible that a number of other similar pyrotechnic devices could have been the source of the residue.)

During another investigation, one involving a night club fire, a quite different conclusion was reached. In that case, when a similar set of comparisons to those in Figure 7 was performed, it was shown that the residues from the pyrotechnic material could not have been produced by the product that was alleged. (In this case the results were found to be consistent with another product that was available to the band's pyrotechnician.)

Applied PRRP Methodology

Three examples of PRRP analyses are presented to demonstrate in greater detail the unique capabilities of the method.

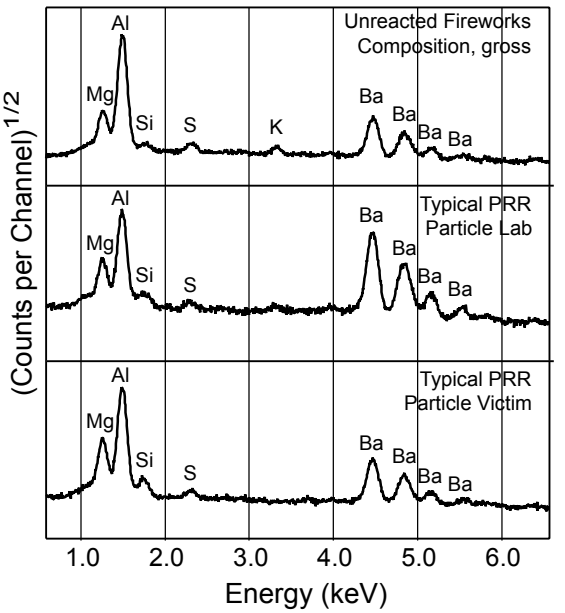

Figure .7– Three X-ray spectra produced during an accident investigation.

Example 1: Background Discrimination

When a pyrotechnic device explodes on the ground, the force of the explosion will mobilize a substantial amount of soil material, some of which will be deposited on remnants of the device and other objects in the area. This process, however, does not result in the mixing of the soil and pyrotechnic components within the individual particles being deposited. The magnitude of the temperature and duration of the explosion event is generally not sufficient to vaporize or even melt the soil particles. As a result, intimate co-mingling of soil and pyrotechnic components does not occur. In addition, because they have not melted, soil particles tend to maintain their generally non-spheroidal morphology. Accordingly, the normal PRRP methodology works well to differentiate successfully between PRRP and soil material. There can, however, be a complication wherein some pyrotechnic reaction products may tend to collect on the surface of the mobilized soil particles that are within the gas cloud of the explosion. This tends to occur when there is a large difference between the high temperature of an explosion fireball and the much lower condensation temperatures of some of the reaction products. The example that follows is one case where this occurred. (While this

Figure 8. Setup for background discrimination demonstration, showing a collection surface attached to a heavy metal support and a 35-mm film canister containing fireworks flash powder.

is discussed briefly below, a more complete discussion must be deferred to a future paper.)

Because of the large degree of commonality between the chemical elements present in inorganic soil components and pyrotechnic compositions,[2] combined with a somewhat similar range of solubility and reactivity, conventional micro-analytical chemistry may fail to differentiate sufficiently between the two sources. Further, even a direct comparison between the samples collected from the immediate area of the explosion and PRRP-free soil may fail to produce fully definitive analytical chemical results regarding the nature of the pyrotechnic residues present. In part this difficulty results from the fact that the PRRP present on sampled items after an explosion on the ground can be overwhelmed by the larger amounts of soil collecting on those items. In that case the components present as PRRP may not be detected.

A demonstration was conducted using a small polyethylene container, a common 35-mm film canister, filled with approximately 28 g of a typical fireworks flash powder (70% potassium perchlorate and 30% aluminum powder). The container was placed directly on the ground and caused to explode using an electric match that had been installed in the device (Figure 8). Following the event, residues were collected from the previously cleaned surfaces of objects placed in the immediate area of the explosion. One collecting surface, as seen in Figure 8, was positioned approximately 150 mm from the explosive charge. The collecting surface was a small piece of 3-mm thick tileboard with a hard, thick and tightly laminated surface. Figure 9 presents a series of three EDS spectra, two produced by the residues on the test surfaces plus one from a sample of unaffected dirt (labeled "Pristine Dirt").

The top spectrum of Figure 9, labeled "1) "Dirt" plus PRRP" is a composite of gross EDS spectra, taken at low magnification and scanning over relatively large portions of the post explosion residue sample. This gross EDS spectrum integrates the results of a very large number of individual particles in the sample. In the spectrum the major peaks are from aluminum, sili-

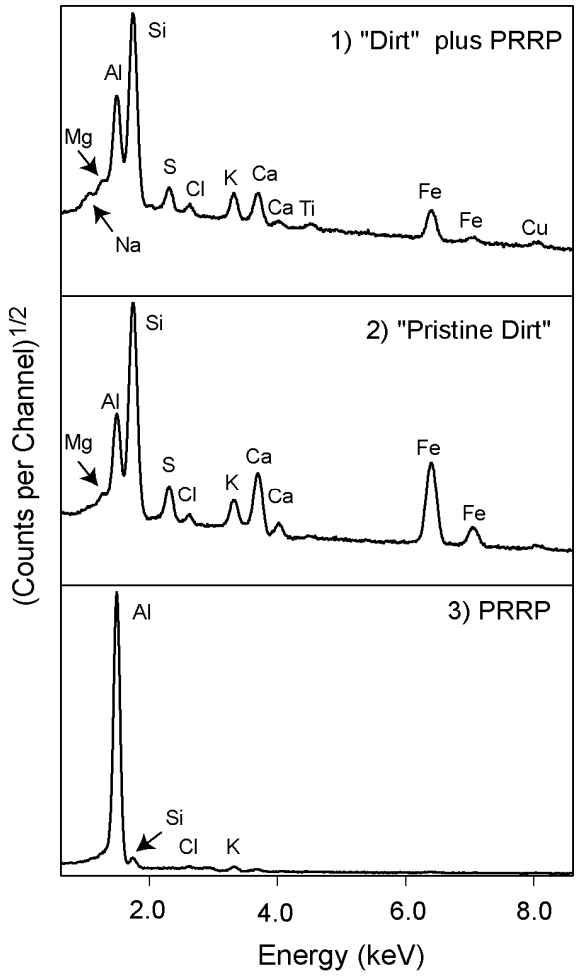

Figure 9. Collection of three composite spectra taken from samples of pyrotechnic residues co-mingled with soil.

con, sulfur, potassium, calcium and iron. When examined more closely, minor peaks from sodium, magnesium, chlorine, titanium and copper can be seen to be present as well. The second spectrum labeled as "2) Pristine Dirt" is a composite of the spectra from 16 individual soil component grains. Based on the different assemblages of the constituent elements present, the individual soil particles fell into four reasonably distinct and recognizable geologic categories that were consistent with the clay-based soil. However, this is a composite (i.e., average) spectrum of the four types of soil particles.

The results embodied in spectra 1 and 2 are similar to what would be expected if conventional micro-analytical chemistry were performed on these two samples, with the exception that chemical species (ions) and not just the elements present might be determined (depending on the analytical method chosen). These two spectra are quite similar to each other especially considering that any two samples of pristine dirt (both without the presence of PRRP) would be expected to have slight differences in the quantities of the elements present because of the naturally variable mixture of its four primary soil components. Accordingly, while it is likely that standard micro-analytical chemistry would reveal the presence of some unreacted and slightly soluble perchlorate ion from the flash powder in this sample, it is unlikely that a statistically significant excess presence of aluminum would be found. To the contrary, by using the morphological criteria for PRRP, the presence of aluminum in the PRRP is unambiguous. This is presented as the third spectrum labeled "3) PRRP", which is a composite spectrum of 16 pyrotechnic reaction residue particles.

Another potential problem for results from micro-analytical chemistry is that trace quantities of other species might be found that are unrelated to the explosion event, but which might be incorrectly interpreted as originating from the pyrotechnic composition. For example, chlorate ions could originate from weed-killer, and nitrate, sulfate, ammonium and potassium ions could originate from fertilizer.

In this case, only an aluminum peak (from aluminum oxide, Al_2O_3) from the flash powder reaction products is readily seen in the PRRP spectra. Substantial potassium and chlorine peaks (from the potassium chloride [KCl] reaction product) are essentially missing in the composite spectrum, but are weakly present in some of the individual particle spectra. In this case, the virtual absence of the potassium and chlorine peaks is a result of the condensation temperature of potassium chloride being moderate (1478 °C[8]) compared with the high temperature of the fireball and the condensation temperature of aluminum oxide (3528 °C[8]). The result is that the potassium chloride tends preferentially to condense onto the surface of the relatively cool dirt particles that were mobilized as a result of the explosion. As mentioned above, a thorough discussion of this phenomenon is beyond the scope of this paper, but this does help to make the point that knowledge of the expected products of pyrotechnic reactions, and the physical and chemical properties of those products, can be important in correctly interpreting PRRP results.

Note that in this example, neither micro-analytical chemistry nor PRRP analysis alone would be likely to yield completely definitive results about the nature of the pyrotechnic composition involved. Rather it is the combination of information produced by both techniques that can be expected to produce fairly unambiguous results.

Example 2: Use History

An accident was thought to have been caused when a reusable performance appliance was loaded with an inappropriately powerful explosive charge. The appliance was made using an approximately 300-mm (12-inch) length of 102-mm (4-inch) diameter steel tubing having a 6-mm (1/4-inch) wall, welded to a thick steel base plate for stability, as illustrated in Figure 10. This type of appliance can be used to produce both an audible and visual effect by exploding an appropriately sized and constructed pyrotechnic charge within it. Following the incident in question, the appliance was held as evidence and after several months the inside surface of the device was sampled and analyzed for PRRP. The result was that approximately equal numbers of two fairly distinct types of PRRP were found to be present. Their EDS spectra (composites from 8 particles of each type) are shown in Figure 11. One type of PRRP is differentiated by its having an abundance of strontium present

with relatively little titanium and aluminum, while the other type had no strontium and an abundance of titanium and aluminum.

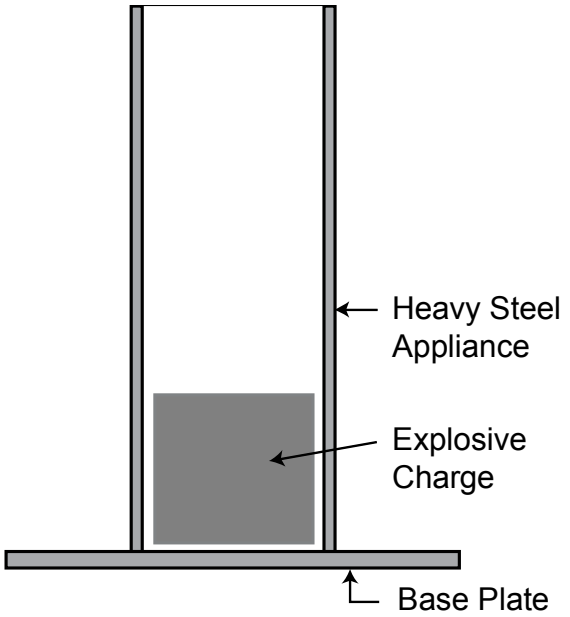

Figure 10. Sketch of the basic construction of a reusable performance appliance used to produce visual and audible effects.

Based on witness accounts and post-incident photography, it had been theorized that the performance appliance had been loaded with an inappropriately powerful explosive charge rather than what had normally been used. The identification of two distinctively different PRRP supported the theory that there had been a fairly recent change in the type of pyrotechnic composition used in the appliance. Had a single type of pyrotechnic charge been used, one principally producing both titanium rich and strontium-rich residues (in addition to the magnesium and aluminum), then the PRRP would have all been somewhat similar in composition, with the vast majority of PRRP containing substantial and approximately equal quantities of the elements. To the contrary in this case, less than 10% of the PRRP were found to contain approximately comparable quantities of the two sets of characteristic PRRP elements.

Armed with definitive information about the use history of the performance appliance, pyrotechnic crew members acknowledged that both

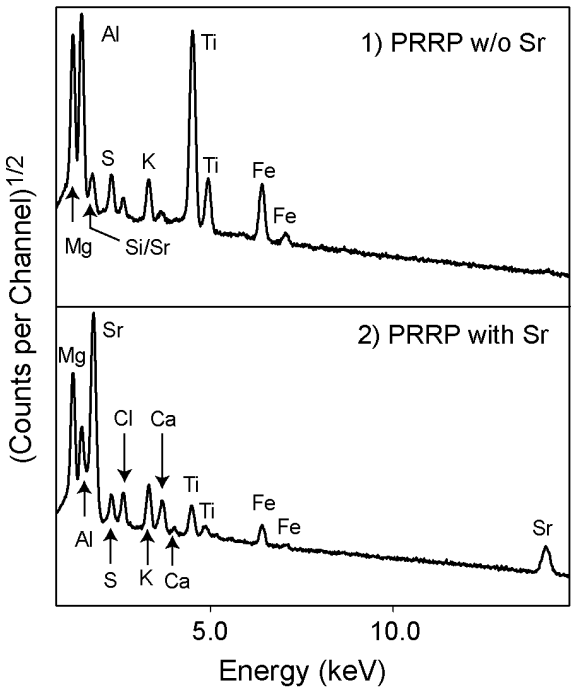

Figure 11. Two composite spectra taken from a performance appliance whose misuse was thought to have resulted in an accident.

red color producing (strontium containing) devices and much more powerfully explosive titanium flash powder devices had been exploded within the device.

In this case, PRRP analysis produced results that would not have been possible with conventional analytical chemical methods. Had the samples from the appliance been analyzed using conventional micro-analytical chemistry, only a single combined set of results would have been produced.

Example 3: Incident Chronology

When an explosion occurs, if the blast or thermal output is sufficient and there are other explosive devices in the immediate area, it is possible for the first explosion to initiate secondary explosions. This occurred in a firework display accident, wherein it was important to identify which of two events occurred first. To simulate such an event on a small scale, a demonstration was staged wherein two relatively small pyrotechnic charges were exploded within 0.2 s of one another. One of the two explosive charges is seen in the upper photograph of Fig-

ure 12, and the pair of charges can be seen in the lower photograph at opposite ends of the setup. Each of the charges contained approximately 28 g of composition. One charge was a standard fireworks flash powder (70% potassium perchlorate and 30% aluminum powder) while the other was a common theatrical concussion powder, a type of fuel-rich flash powder (50% strontium nitrate and 50% magnesium). The distance between the two charges was approximately 0.5 m (20 inches). The demonstration was conducted in a research bay approximately 4 by 4 by 4 m (12 by 12 by 12 feet) and configured such that one wall was completely removed and open to the outside environment.

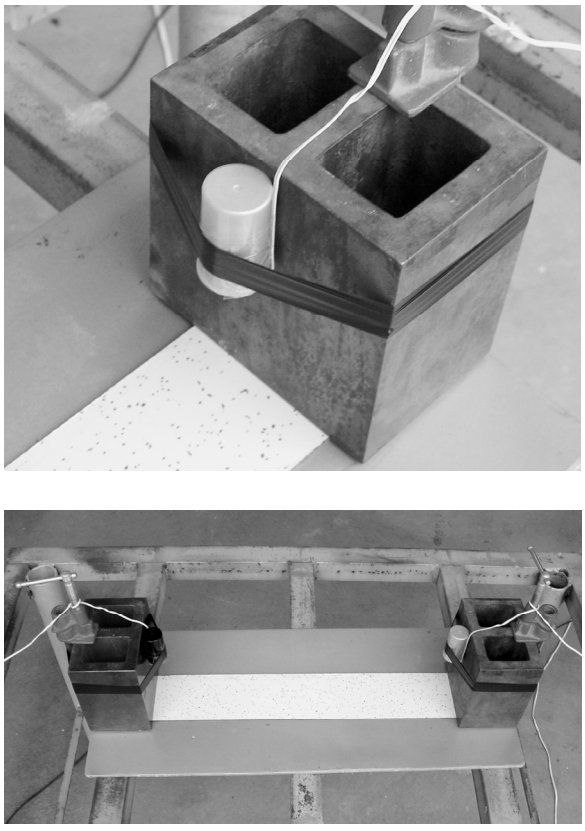

Figure 12. Photographs showing the setup for a demonstration in which PRRP is used to discover details of the course of an explosion event.

After exploding the two charges, the room was cleared of smoke using a large exhaust fan. Once the air had cleared, fragments of the containment vessels (two 35 mm-film canisters, one made from black polyethylene and the other made from uncolored polyethylene) were collected and mounted for PRRP analysis. A total of four specimens were made; each using three small pieces of the same type (color) plastic. Two were made with black plastic, one specimen had the fragments mounted in an orientation such that the inside surface of plastic canister was in an upward orientation, and one specimen with the fragments mounted in an outside-up orientation. (The inside versus outside orientation of the fragments was determined by their direction of curvature.) A similarly-prepared pair of specimens was assembled with the uncolored plastic fragments. In addition a sample was obtained from the midpoint of the light-colored collecting surface, seen in Figure 12, extending between the two steel blocks to which the explosive charges had been attached. (The mostly white strip of collecting material was 3-mm thick tileboard that had been cleaned prior to the test. The pattern of small random spots seen in the upper photo of Figure 12, were permanently imprinted within the surface coating by the tileboard's manufacturer.) This midpoint PRRP specimen was prepared by contact using an adhesive carbon dot as described above.

Based on an initial brief analysis of the PRRP on the sampled items, it was quickly obvious that two chemically different pyrotechnic explosives were involved. Thus, following somewhat the same scheme as in the "Use History" example above, PRRP spectra were divided into different categories. These composite spectra are presented in Figure 13 and are representative of the four categories: "1) Pure Firework Flash", "2) Mostly Firework Flash", "3) Mostly Theatrical Concussion", and "4) Pure Theatrical Concussion". In this demonstration, 25 PRRP from each of 5 samples were analyzed. Table 1 is a summary of the number of PRRP in each category found on each type specimen.

Note that the PRRP found in the inner surfaces of the two containment vessels were radically different. Of the PRRP on the inside surface of the black plastic fragments, approximately 85% were Category 4, having only the components of the theatrical concussion powder. Of the PRRP on the inside surface of the clear plastic fragments, 70% were Category 1, having only the components of the firework flash powder. Accordingly, it is obvious that the black

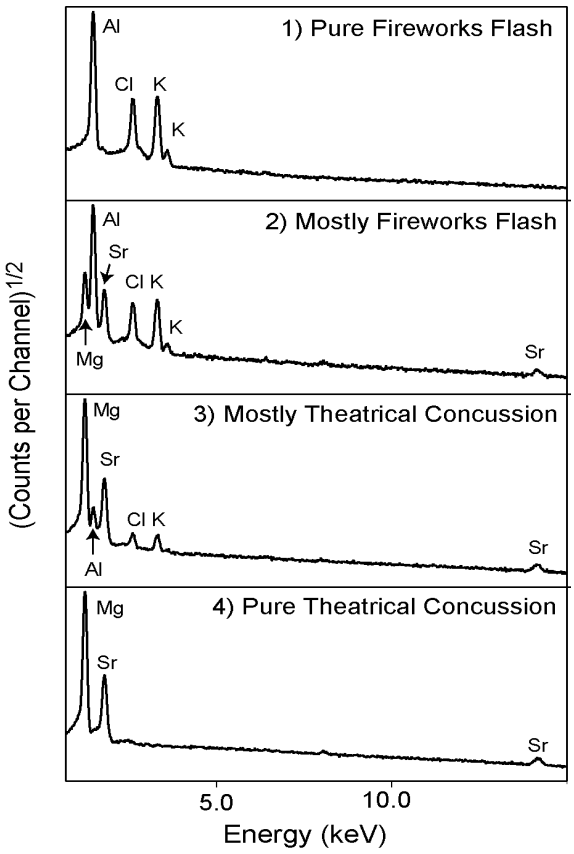

Figure 13. A series of four composite spectra representing the four categories of PRRP found in this analysis.

film canister must have contained the theatrical concussion powder while the clear film canister must have contained the firework flash powder. Had both pyrotechnic compositions been a single mixture of all of the ingredients, the PRRP on the inside surfaces of both containers would have been essentially the same and the vast majority would have been a mixture of all the individual components.

Given the geometry of the demonstration setup, it must be expected that there will be a tendency for each exploding charge to project its PRRP outward toward the initial location of the other charge. However, note that the PRRP found on the outside surfaces of both containers were mostly Category 1, having only the components of firework flash powder. Note further that 40% of the PRRP on the outside surface of the black container (that had contained theatrical concussion powder) were also Category 1 (from the firework flash powder). To the contrary, the outside surface of the clear container (that had contained firework flash powder) had no PRRP of Category 4 (pure concussion powder components). This is consistent with the flash powder charge having exploded first, because if the flash powder charge exploded first, its container would no longer be present in the immediate area to collect PRRP from the concussion powder charge when it explodes, even if that second explosion occurred only a small fraction of a second later.

In Table 1, the column labeled "Surface Total" is the total of the PRRP particles collected on the exterior surfaces of the two containment vessels plus those from the midpoint of the collecting surface. Approximately 40% of the PRRP fell into the two "Mixed" categories (Categories 2 and 3). This is an indication of the timing of the two explosions, specifically that there was only a slight delay between the two explosions. (Recall that in this demonstration the two explosions were made to occur within approximately 0.2 s.) From other demonstrations using the same charges and setup, it has been observed that:

- Had the two explosions occurred at the same instant, there would have been more complete mixing of their respective fireballs, and roughly 70% of the PRRP would

Table 1. Number of Each of the Four Types of PRRP on the Items Sampled.

	Black Plastic		Clear Plastic		Surface	Surface
PRRP Category	Outside	Inside	Outside	Inside	Midpoint	Total
1) Pure Firework Flash	10	2	15	18	3	28
2) Mostly Firework Flash	7	1	6	5	2	15
3) Mostly Theatrical Concussion	4	1	4	2	7	15
4) Pure Theatrical Concussion	4	21	0	0	13	17

have contained a significant mixture of the components of both of the pyrotechnic explosives.

- Had the two explosions been more widely separated in time (with as little as 2 s between explosions), there would have been no mixing of the fireballs and only a little mixing in the PRRP. This relatively minor mixing is the result of the remobilization of some of the previously deposited PRRP and would result in roughly 10% of the PRRP containing a mixture of the components of both of the pyrotechnic compositions.

In this example, a thorough analysis of the PRRP reveals that two different types of explosive charges were involved, that two separate explosions took place, that the flash powder charge exploded first, and that the two explosions were only slightly separated in time. There is simply no way in which standard micro-analytical chemical analysis could have produced these results.

Conclusion

PRRP analysis will not supplant micro-analytical chemistry as an important analytical tool in the forensic analysis of pyrotechnic incidents. However, at the very least, PRRP analysis provides information that is a useful adjunct to normal micro-analytical chemistry, and there are many occasions when PRRP analysis provides information that is simply beyond the ability of standard micro-analytical chemistry.

References

1) S. A. Phillips, "Analysis of Pyrotechnic Residues—Detection and Analysis of Characteristic Particles by SEM / EDS", Proceedings of the 2nd European Academy of Forensic Science Meeting, Sept. 2000. Also appearing in *Science and Justice*, Vol. 41, pp 73–80, 2001.

2) K. L. & B. J. Kosanke and R. C. Dujay, "Pyrotechnic Reaction Residue Particle Identification by SEM / EDS", *Journal of Pyrotechnics*, No. 13, pp 40–53, 2001; *Selected Pyrotechnic Publications of K. L. and B. J. Kosanke, Part 6 (2001 and 2002),* 2006.

3) K. L. Kosanke, R. C. Dujay, and B. J. Kosanke, "Characterization of Pyrotechnic Reaction Residue Particles by SEM/EDS", *Journal of Forensic Science*, Vol. 48, No. 3, pp 531–537, 2003; *Selected Pyrotechnic Publications of K. L. and B. J. Kosanke, Part 7 (2003 and 2004),* 2006.

4) K. L. Kosanke, R. C. Dujay, and B. J. Kosanke, "Pyrotechnic Reaction Residue Particle Analysis", *Journal of Forensic Science*, Vol. 51, No. 2, pp 296– 302, 2006.

5) M. Trimpe, "Analysis of Fireworks for Particles of the Type Found in Primer Residue (GSR), *International Association for MicroAnalysis*", Vol. 4, No. 1, pp 1–8, 2003.

6) P. V. Mosher, M. J. McVicar, E. D. Randall, and E. H. Sild, "Gunshot Residue-Similar Particles by Fireworks", *Canadian Society of Forensic Science Journal*, Vol. 31, No. 2, pp 157–168, 1998.

7) J. R. Giacalone, "Forensic Fireworks Analysis and Their Residue by Scanning Electron Microscopy / Energy-Dispersive Spectroscopy", *Scanning*, Vol. 20, No. 3, pp 172–173, 1998.

8) Institute for Chemical Technology (Thermodynamic-Code) data base.